Conversion of L-Rhamnose to *N*-Acetyl-L-Fucosamine

By

Mathew T. Maust

Submitted in Partial Fulfillment of the Requirements

for the Degree of

Master of Science

in the

Chemistry Program

YOUNGSTOWN STATE UNIVERSITY

August, 2005

Conversion of L-Rhamnose to *N*-Acetyl-L-Fucosamine

Mathew T. Maust

I hereby release this thesis to the public. I understand that this thesis will be made available from the Ohio LINK ETD Center and the Maag Library Circulation Desk for public access. I also authorize the University or other individuals to make copies of this thesis as needed for scholarly research.

Signature: _____ 8/5/05

Mathew T. Maust — Date

Approvals:

_____ 8/5/05

Dr. Peter Norris — Date
Thesis Advisor

_____ 8/5/05

Dr. John Jackson — Date
Committee Member

_____ 8/5/05

Dr. Timothy Wagner — Date
Committee Member

_____ 8/9/05

Dr. Peter J. Kasvinsky — Date
Dean of Graduate Studies

Thesis Abstract

The following work describes an attempted synthesis of *N*-Acetyl-L-fucosamine from L-Rhamnose. Many bacteria, such as *Staphylococcus aureus*, rely on a capsular polysaccharide which contains *N*-acetyl-L-fucosamine to protect themselves from destruction by the host's immune system. Therefore, an efficient synthesis of this rare sugar is required for further experiments in designing small molecule glycomimetics which may inhibit the capsular polysaccharide formation.

Acknowledgements

First and foremost I would like to thank the Youngstown State University Chemistry Department and the School of Graduate Studies for the opportunity to pursue my Master's degree in Chemistry. Also particular thanks to the faculty of the Chemistry Department, especially Dr. John Jackson and Dr. Timothy Wagner for graciously agreeing to be on my committee and for the feedback they've given on my thesis.

I am thankful for the friendship of all of the members of the Norris group, especially Dave and Sara who have become less like colleagues to me and more like good friends. I am most grateful to my research advisor Dr. Peter Norris for his constant guidance, support, and feedback, as well as the almost daily cup of coffee. Without his dedication to research and his students, it would have been much more difficult to complete my Master's work. Thank you Doc.

My special thanks go to my family (Mom and Erin) and my best friend Laura for their love, support, patience, and understanding through not only my two years of graduate school, but in every hobby, goal, or job, or task I've ever undertaken.

Table of Contents

List of Schemes

List of Equations

List of Figures

List of Tables

Introduction

Carbohydrate background

Although the chemistry of carbohydrates has been investigated for well over a century, only over the past three decades has their importance in roles other than the body's simple energy source begun to be understood. Carbohydrates, or sugars, play an important role in a wide variety of biological processes. This is reasonable considering they are the most abundant biological molecules, outnumbering other important biomolecules such as nucleic acids and proteins. Today their chemistry is being explored in the synthesis of new food products such as Splenda® brand artificial sweetener,[1] biodegradable plastics such as EcoPLA,[2] and most importantly in pharmaceuticals such as the anti-tumor agent Daunomycin, or the antibiotic Streptothricin F.[3]

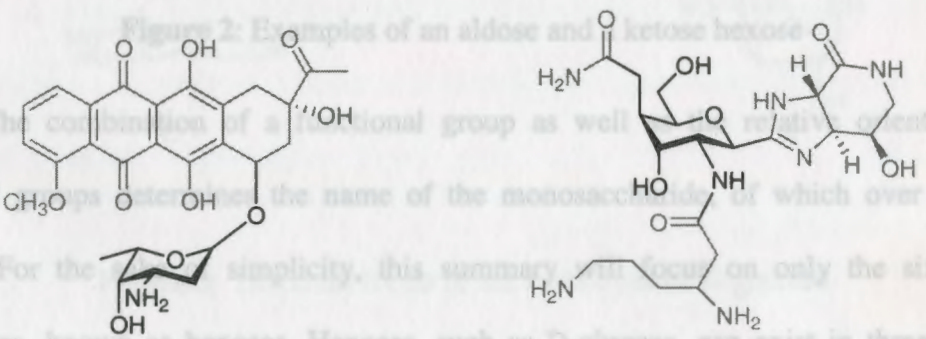

Daunomycin Streptothricin F

Figure 1: Examples of carbohydrate-based pharmaceuticals

Carbohydrates are composed of one or more basic units called monosaccharides. Monosaccharides consist of straight-chain polyhydroxylated alcohols of three to typically no more than six carbon atoms in length. Each monosaccharide also contains either an aldehyde or a ketone. Monosaccharides containing the aldehyde functionality are called aldoses, and those containing the ketone functionality are known as ketoses. D-Glucose

and L-fructose are simple examples of both an aldose and ketose respectively (Figure 2). The notations of D and L in this example refer to the orientation of the hydroxyl group on the bottom-most stereocenter in the Fischer projection. If the hydroxyl group is on the left side of the main chain, it is given the L notation, and if it is positioned on the right side of the chain it is given the D notation.

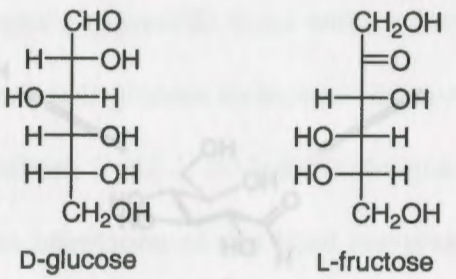

Figure 2: Examples of an aldose and a ketose hexose

The combination of a functional group as well as the relative orientation of hydroxyl groups determines the name of the monosaccharide, of which over 200 are known. For the sake of simplicity, this summary will focus on only the six-carbon derivatives, known as hexoses. Hexoses, such as D-glucose, can exist in three distinct forms. The linear acyclic form, or *aldehydo*, is the least stable of the three forms (Figure 3:**A**). More commonly, a hydroxyl group reacts with the carbonyl of the aldehyde or ketone to form the hemiacetal or hemiketal. This reaction results in either a five-membered ring called a furanose (Figure 3: **D**, **E**), or a more stable six-membered ring that is known as a pyranose (Figure 3: **B**, **C**), the names of which are analogous to the structures of furan and pyran.

Upon ring closing, there are two possible configurations for the resulting hydroxyl group at the carbonyl carbon, or anomeric carbon. If the hydroxyl group is positioned below the plane of the ring, it is given the α designation (Figure 3: **B**, **D**). If it is positioned above the ring, it is designated as the β anomer (Figure 3: **C**, **E**).

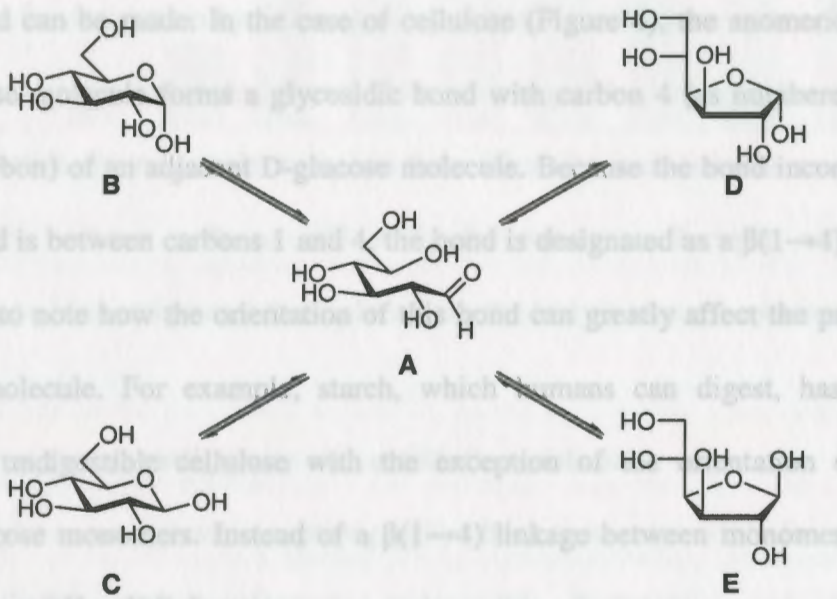

Figure 3: Different forms of the carbohydrate D-glucose

Like cyclohexane, pyranose rings most often assume a chair conformation to minimize strain between each tetrahedrally arranged carbon atom. The predominant chair is the one in which the largest ring substituents are situated in equatorial positions rather than in the sterically crowded axial positions. Incidentally, β-D-glucose is the only sugar that can have all of its hydroxyl groups in equatorial positions simultaneously (Figure 3: **C**), which may explain why it is the most common monosaccharide found in Nature.[4]

Monosaccharides can be linked together to form long chains called polysaccharides (such as the natural polysaccharides starch and cellulose) or they can be

linked to other molecules to take advantage of their functionality (such as the ribose component of ATP). In these cases, the anomeric group can condense with an alcohol to form a glycoside. The bond connecting the anomeric group to the alcohol oxygen is called a glycosidic bond. In the case of a glycosidic bond forming between two monosaccharides, it is important to realize that there are several different alcohols with which a bond can be made. In the case of cellulose (Figure 4), the anomeric carbon of one D-glucose molecule forms a glycosidic bond with carbon 4 (as numbered from the anomeric carbon) of an adjacent D-glucose molecule. Because the bond incorporates the β anomer and is between carbons 1 and 4, the bond is designated as a β(1→4) linkage. It is important to note how the orientation of this bond can greatly affect the properties of the entire molecule. For example, starch, which humans can digest, has the same structure as undigestible cellulose with the exception of the orientation of the link between glucose monomers. Instead of a β(1→4) linkage between monomers, they are connected by an α(1→4) linkage.

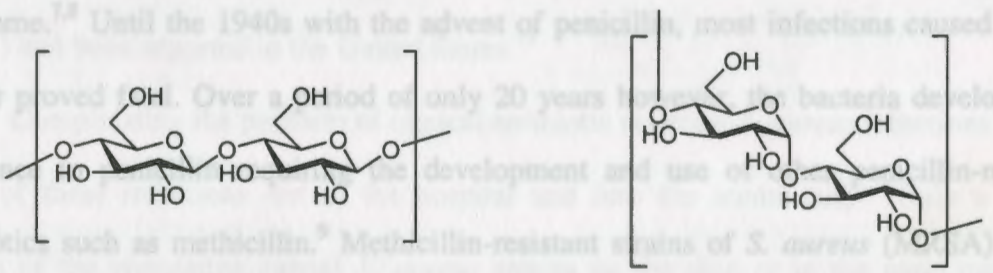

Figure 4: Difference in linkage between glucose monomers in starch and cellulose

Sugars with functionalities other than hydroxyl groups have become a large part of carbohydrate research. This may be due in part to the large number of biological

processes that incorporate carbohydrate analogues. The human body uses carbohydrate-containing molecules as a means of immune system recognition and demarcation. B lymphocytes (a type of white blood cell) contain proteins that contain bound carbohydrate derivatives that can bind to particular antigens. Once bound to the carbohydrate portion, the B lymphocytes can mark the antigen with a carbohydrate "tag," marking them for destruction by different components of the immune system.[5,6]

Bacteria also use carbohydrates to their advantage. The large number of hydrogen bonds that carbohydrates can form makes them ideal for bacterial use as a means of attachment to surfaces such as cell walls for infection. Bacteria can also use carbohydrates to hide and protect themselves from the body's immune system.

***Staphylococcus aureus* malignancy and antibiotic resistance**

Staphylococcus aureus is a gram-positive bacterium responsible for a variety of illnesses, including wound infections, endocarditis, bacteremia, and toxic shock syndrome.[7,8] Until the 1940s with the advent of penicillin, most infections caused by *S. aureus* proved fatal. Over a period of only 20 years however, the bacteria developed a resistance to penicillin requiring the development and use of other penicillin-related antibiotics such as methicillin.[9] Methicillin-resistant strains of *S. aureus* (MRSA) were discovered in the 1960s and the rates of infection by these strains are on a steady increase around the world (Figure 5).[10]

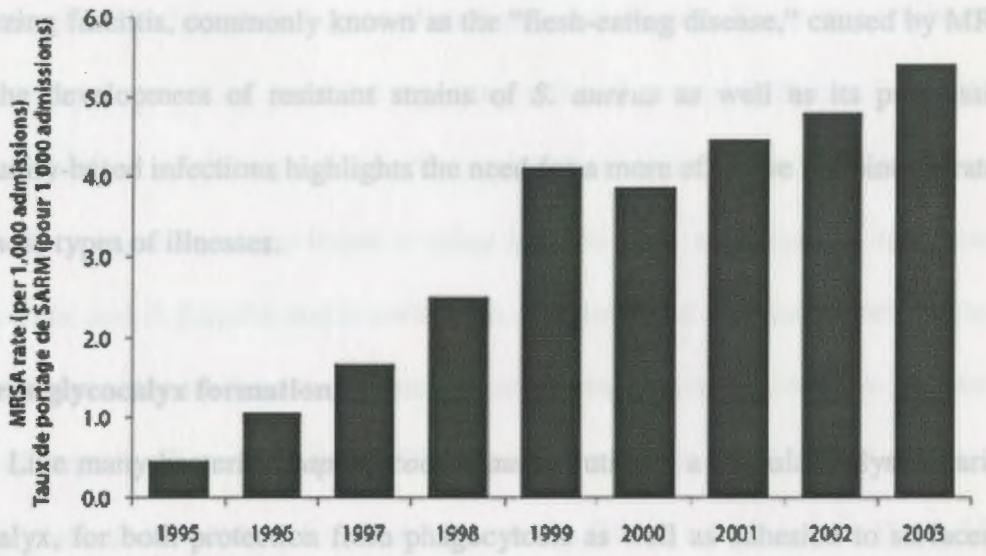

Figure 5: Increase of Canadian clinical MRSA infections from 1995 to 2003[10]

In addition to the prevalence of MRSA, in the past decade these infections have also shown resistance to vancomycin - the antibiotic once though of as a last-resort treatment. Vancomycin-resistant *S. aureus* (VRSA) infections were first reported in Japan in 1996, and as of June 2002 eight patients with vancomycin-intermediate *S. aureus* (VISA) had been reported in the United States.[11]

Complicating the problem of clinical antibiotic resistant *S. aureus* infections is the move of these infections out of the hospital and into the community. While a large portion of the population carries *S. aureus* strains on the skin or in the nasal cavities, these infections are usually innocuous.[12] However, community-associated infections of *S. aureus* have risen from essentially zero a decade ago to between eight to twenty percent in 2003.[13] These infections have appeared in people that not only have had no recent exposure to a hospital or clinic, but also exhibited none of the risk factors common for infection. Of an even greater concern is the emergence of community-associated cases of

necrotizing fasciitis, commonly known as the "flesh-eating disease," caused by MRSA.[14] Both the development of resistant strains of *S. aureus* as well as its progression to community-based infections highlights the need for a more effective antibiotic strategy to fight these types of illnesses.

S. aureus glycocalyx formation

Like many bacteria, *Staphylococcus aureus* utilizes a capsular polysaccharide, or glycocalyx, for both protection from phagocytosis as well as adhesion to surfaces. The glycocalyx of *S. aureus* is composed of repeating trisaccharide units, of which serotypes 5 and 8 are the most common. Together, they compose nearly 80% of all clinical strains of *S. Aureus*.[7] Both serotypes are composed of the same monosaccharide units, differing only by the connections between them (Figure 6).

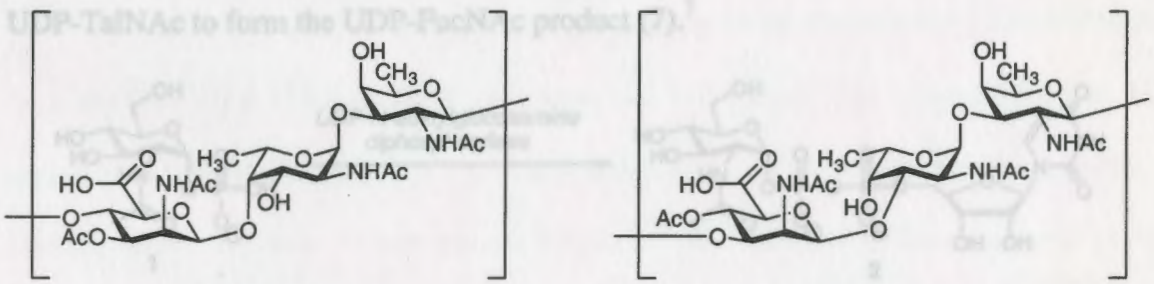

Serotype 5:

(→4)-3-*O*-Ac-β-D-ManNAcA-(1→4)-α-L-FucNAc-(1→3)-β-D-FucNAc-(1→)*n*

Serotype 8:

(→3)-4-*O*-Ac-β-D-ManNAcA-(1→3)-α-L-FucNAc-(1→3)-β-D-FucNAc-(1→)*n*

Figure 6: Serotypes 5 and 8 of *S. aureus*

S. aureus synthesizes each of the individual monomers used in the capsular polysaccharide from the common starting material *N*-acetyl-D-fucosamine-1-phosphate (GlcNAc-1-phosphate). The bacterium then utilizes a series of enzymatic pathways to

synthesize UDP-activated analogues of each monosaccharide. These monomers are then combined by enzymes to form the repeating units of serotypes 5 and 8 found in the glycocalyx.[7] One of the monomers, *N*-acetyl-L-fucosamine (L-FucNAc), is found not only in *S. aureus* but is also found in other bacteria such as *E. coli*, *P. aeruginosa*, *S. pneumoniae*, and *B. fragilis*, and is not known to be involved in human biochemistry.[15]

Experiments by Kneidinger and coworkers support a four-enzyme pathway in 6 chemical steps for the conversion of GlcNAc-1-phosphate to UDP-FucNAc. First, *UDP-N-acetylglucosamine diphosphorylase* converts the GlcNAc-1-phosphate (**1**) to UDP-*N*-acetyl-D-glucosamine (UDP-GluNAc) (**2**). A 4,6-dehydration and a 3,5-epimerization is then catalyzed by the enzyme *Cap5E*, yielding a keto-deoxy-sugar (**5**). This sugar is then reduced at C-4 to UDP-2-acetamido-2,6-dideoxy-L-talose (UDP-TalNAc) (**6**) by the enzyme *Cap5F*. In a final step, the enzyme *Cap5G* inverts the stereochemistry of C-2 in UDP-TalNAc to form the UDP-FucNAc product (**7**).[7]

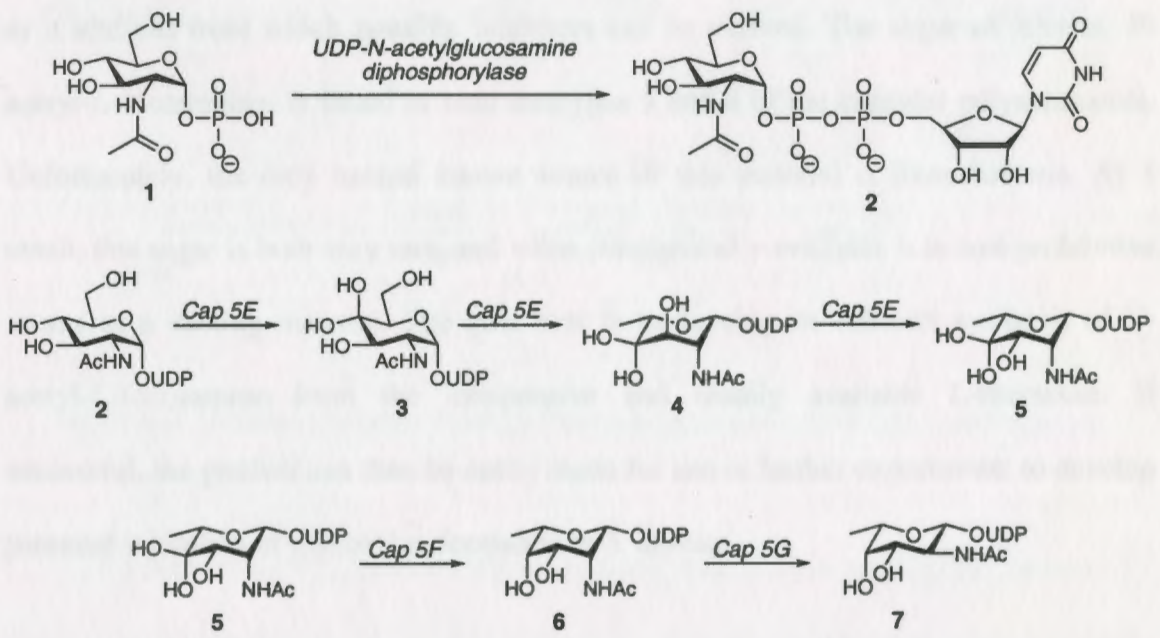

Scheme 1: Ezymatic pathway from GlcNAc-1-phosphate (**1**) to UDP-FucNAc (**7**)

This enzymatic information makes analogues of L-FucNAc a promising area of study for the development and discovery of small, glycomimetic inhibitors. Inhibition of any one of the four enzymes used in the conversion of GlcNAc-1-phosphate to UDP-FucNAc could result in the disruption of not only UDP-FucNAc synthesis, but of the *S. aureus* capsular polysaccharide as well. Antibiotic activity in this manner would also target a different enzymatic pathway than the penicillin-related drugs, which inhibit transpeptidases involved in the formation of the bacterial cell wall.[16] Arguably the most important aspect of this approach is the possibility that a successful inhibitor might also be active against the enzymes that incorporate L-FucNAc in their own capsular polysaccharides.

Statement of Problem

Antibiotic-resistant strains of *S. aureus* have grown in number and malignancy over the past several decades, making treatment of these infections more difficult. While treatment with vancomycin is still effective in most cases, it is only a matter of time before it loses its effectiveness as well. One option for the development of new antibiotics is to shift focus away from the disruption of cell wall formation, as the penicillin-type antibiotics do. A likely target for this strategy is to interrupt the formation of the capsular polysaccharide that the bacteria use to hide from and defend themselves from their host's immune system. Since the bacteria use enzymes to synthesize all of the components of this glycocalyx from a common starting material, interruption of one or more of these enzymes may effectively retard or even stop production of this protective layer, opening the bacteria up to phagocytosis.

Therefore, it is useful to use the sugars that make up the capsular polysaccharide as a scaffold from which possible inhibitors can be derived. The sugar of interest, *N*-acetyl-L-fucosamine, is found in both serotypes 5 and 8 of the capsular polysaccharide. Unfortunately, the only natural known source of this material is from bacteria. As a result, this sugar is both very rare, and when commercially available it is cost-prohibitive to use as a starting material. The goal here is to develop an efficient synthesis of *N*-acetyl-L-fucosamine from the inexpensive and readily available L-rhamnose. If successful, the product can then be easily made for use in further experiments to develop potential inhibitors of glycocalyx formation in *S. aureus*.

Results and Discussion

1. Inversion of the C-4 Stereocenter

The major goal of this project is to develop a synthetic pathway from the cheap and abundant L-rhamnose (**8**) to the rare *N*-acetyl-L-fucosamine for future use in developing small molecule glycomimetics. The main use of these molecules would be as possible inhibitors of the enzymes that create the glycocalyx of *S. aureus*, of which *N*-acetyl-L-fucosamine is a part. The synthetic pathway (Scheme 2) requires the inversion of two stereocenters on L-rhamnose, which can be accomplished through a selective protection strategy to isolate each center, then through an oxidation-reduction sequence. Inversion of the hydroxyl at C-4 was targeted first, since a protection strategy to leave only that oxygen unprotected was already known in the literature.[17, 18, 19]

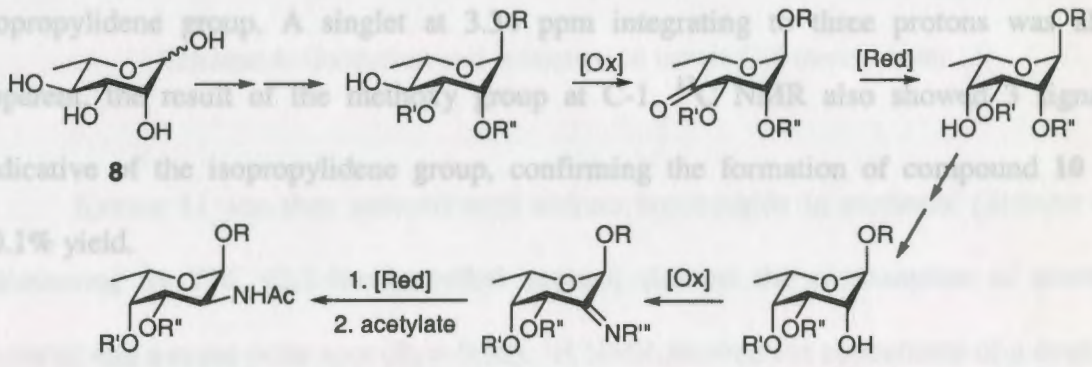

Scheme 2: General synthetic strategy from L-rhamnose to *N*-acetyl-L-fucosamine

An acid-catalyzed glycosylation in methanol was used to protect C-1 (Scheme 3). Monitoring the reaction by TLC (ethyl acetate) revealed the formation of a less polar spot (R_f = 0.48) compared to the more polar L-rhamnose (R_f = 0.12). The lower polarity may

be attributed to replacing the hydroxyl group at C-1 with a methoxy group. Orientation of the group in the α-orientation may be explained by the anomeric effect, in which the σ* antibonding orbital of the C1-OMe bond overlaps with one of the lone pairs of the ring oxygen. This interaction helps to direct the methoxy group to adopt an axial position after attacking the planar heteroatom-stabilized carbocation during glycosylation. This results in the α-anomer as the thermodynamic product of this reversible reaction.

The mixture was then evaporated to a yellow syrup and the crude product **9** was used in the next step; the protection of oxygen atoms at C-2 and C-3 using an isopropylidene group. The reaction was monitored by TLC (2:1 hexanes:ethyl acetate), showing a less polar spot with an R_f value of 0.42, the result of the much less polar acetal group being present. A ^{1}H NMR spectrum of the product showed two singlets at 1.31 and 1.49 ppm integrating to three protons each, representing the six protons of the isopropylidene group. A singlet at 3.34 ppm integrating to three protons was also apparent, the result of the methoxy group at C-1. ^{13}C NMR also showed 3 signals indicative of the isopropylidene group, confirming the formation of compound **10** in 70.1% yield.

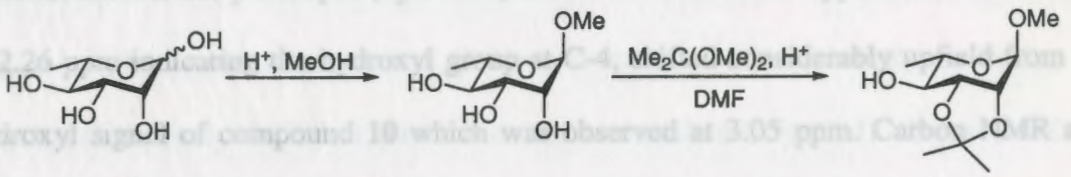

8 **9** **10**

Scheme 3: Protection strategy to isolate C-4

Sugar **10** was then oxidized *via* typical Swern conditions (Scheme 4). Monitoring the reaction with TLC (2:1 hexanes:ethyl acetate) revealed the consumption of starting material and formation of a new, less polar spot with $R_f = 0.58$. The product was column purified (2:1 hexanes:ethyl acetate) to afford a pale yellow syrup of **11** in 60.4% yield. ^{1}H NMR showed a quartet at 4.26 ppm, which couples with a doublet at 1.40 ppm ($J = 6.59$ Hz), indicating that the only neighboring protons to those at C-5 are those at C-6, which agrees with having a carbonyl at C-4. ^{13}C NMR showed a signal at 205 ppm, also indicative of a ketone.

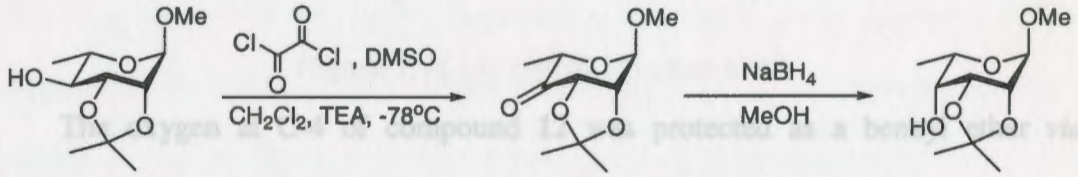

Scheme 4: Oxidation and reduction to invert C-4 stereocenter

Ketone **11** was then reduced with sodium borohydride in methanol (Scheme 4). Monitoring by TLC (2:1 hexanes:ethyl acetate) showed the consumption of starting material and a more polar spot ($R_f = 0.32$). ^{1}H NMR showed the appearance of a doublet at 2.26 ppm indicating the hydroxyl group at C-4, shifted considerably upfield from the hydroxyl signal of compound **10** which was observed at 3.05 ppm. Carbon NMR also showed the disappearance of the ketone signal, showing evidence for reduction to compound **12**. The stereoselectivity of this reaction is due to the large acetal group on the *Re* face of the ketone, as well as the methyl group of C-6. These groups block this face of

the ketone from hydride addition by the borohydride ion, resulting in addition from the *Si* face.

2. Protection of C4 and Removal of Isopropylidene Protecting Group

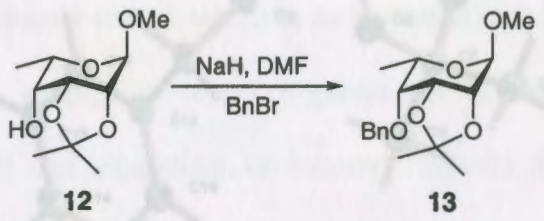

Equation 1: Protection of C-4 as a benzyl ether

The oxygen at C-4 of compound **12** was protected as a benzyl ether *via* a Williamson ether synthesis (Equation 1). Monitoring the reaction with TLC (2:1 hexanes:ethyl acetate) showed a less polar, UV active spot (R_f = 0.58). Column chromatography (2:1 hexanes:ethyl acetate) afforded white crystals in a 64.7% yield. ^{1}H NMR showed two doublets at 4.56 and 4.87 ppm typical of diastereotopic benzyl ether protons as well as a multiplet from 7.28 to 7.40 ppm representative of the phenyl ring. Carbon NMR showed four new signals from 129 to 139 ppm also indicating the aromatic ring. An X-ray crystal structure was obtained from the purified product, confirming not only the formation of **13**, but also the correct stereochemistry of **12**. From the X-ray structure (Figure 7), it is clear to see that the ring shape is not in the usual chair conformation normally seen in a six-membered ring, but is instead in more of a "puckered" conformation. This is due to the tying together of C-2 and C-3 with the isopropylidene group, which pulls the chair into this conformation.

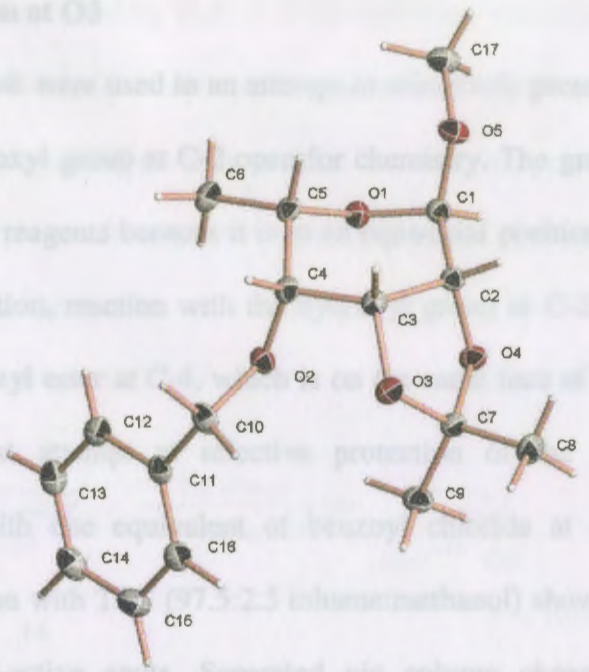

Figure 7: X-ray crystal structure of **13**

The isopropylidene group in **13** was removed with a 60% solution of trifluoroacetic acid in water. The reaction was monitored with TLC (1:1 hexanes:ethyl acetate) and showed the consumption of starting material and the formation of a more polar, UV-active spot ($R_f = 0.33$). Column purification of the mixture (1:1 hexanes:ethyl acetate) resulted in **14** as a yellow syrup in 99% yield. ^{1}H NMR showed the disappearance of the two isopropylidene singlets (1.36 and 1.56 ppm) in the upfield region of the spectrum, indicating cleavage of the acetal group. ^{13}C NMR confirmed this observation, with the disappearance of the isopropylidene group peaks.

3. Selective Protection at O3

Several methods were used in an attempt to selectively protect the oxygen at C-3, thus leaving the hydroxyl group at C-2 open for chemistry. The group at C-3 appears to be more accessible to reagents because it is in an equatorial position, sticking away from the molecule. In addition, reaction with the hydroxyl group at C-2 is likely hindered in part by the bulky benzyl ester at C-4, which is on the same face of the ring. Using these assumptions, the first attempt at selective protection of the C-3 oxygen was a benzoylation of **6** with one equivalent of benzoyl chloride at –10°C (Equation 2). Monitoring the reaction with TLC (97.5:2.5 toluene:methanol) showed the appearance of three less polar UV-active spots. Separated *via* column chromatography (97.5:2.5 toluene:methanol), the least polar, major product (R_f = 0.52) was determined to be the bisprotected product **15**, and the other two products were determined to be the 3-protected (R_f = 0.38) **16** and 2-protected product (R_f = 0.36) **17**.

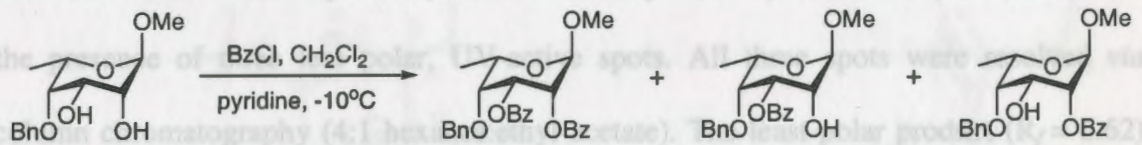

14 **15** **16** **17**

major product

Equation 2: Benzoyl ester protection reaction products

It was hypothesized that if the lack of protective selectivity was related to the size of the protecting group; a larger protecting group may result in greater selectivity. Thus, **14** was mixed with *tert*-butyl diphenyl silyl chloride and imidazole in DMF (Equation 3)

and the reaction was monitored by TLC (1:1 hexanes:ethyl acetate). After two days there was no change by TLC and ^{1}H NMR confirmed no reaction. As a compromise between the medium-sized benzoyl group, which resulted in mostly bis-protected product, and the rather large silyl chloride resulting in no reaction, the use of pivaloyl chloride to form the pivaloyl ester (**19**) was attempted.

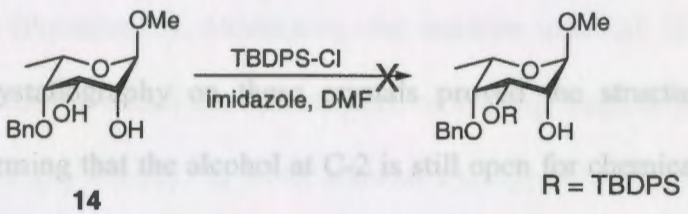

14

Equation 3: Attempted protection with *tert*-butyl diphenylsilyl chloride

One equivalent of pivaloyl chloride was reacted with **14** (Equation 4) and the reaction was monitored by TLC (4:1 hexanes: ethyl acetate). After 2 days, TLC showed the presence of three less polar, UV-active spots. All three spots were resolved *via* column chromatography (4:1 hexanes:ethyl acetate). The least polar product (R_f = 0.62) was determined by ^{1}H NMR to be the bis-protected product (**18**). The middle compound (R_f = 0.44), also the major product at a 58% yield, was found to be the desired O3-protected product (**19**). The least polar spot (R_f = 0.32) was determined to be the O2-protected product (**20**). From the mixture, the desired product **19** was found to crystallize from methanol, aiding in purification.

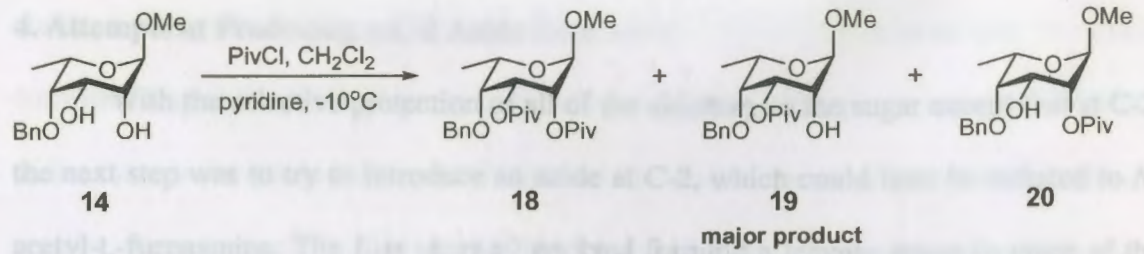

Equation 4: Protection of **14** as a pivaloyl ester

X-Ray crystallography on these crystals proved the structure of the desired product **19**, confirming that the alcohol at C-2 is still open for chemical modification. It is notable that the ring's return to a chair conformation with the removal of the isopropylidene group can clearly be seen. Rotation of the *t*-butyl group is also evident by the elongated ellipsoids labeled as C8-C10 (Figure 8).

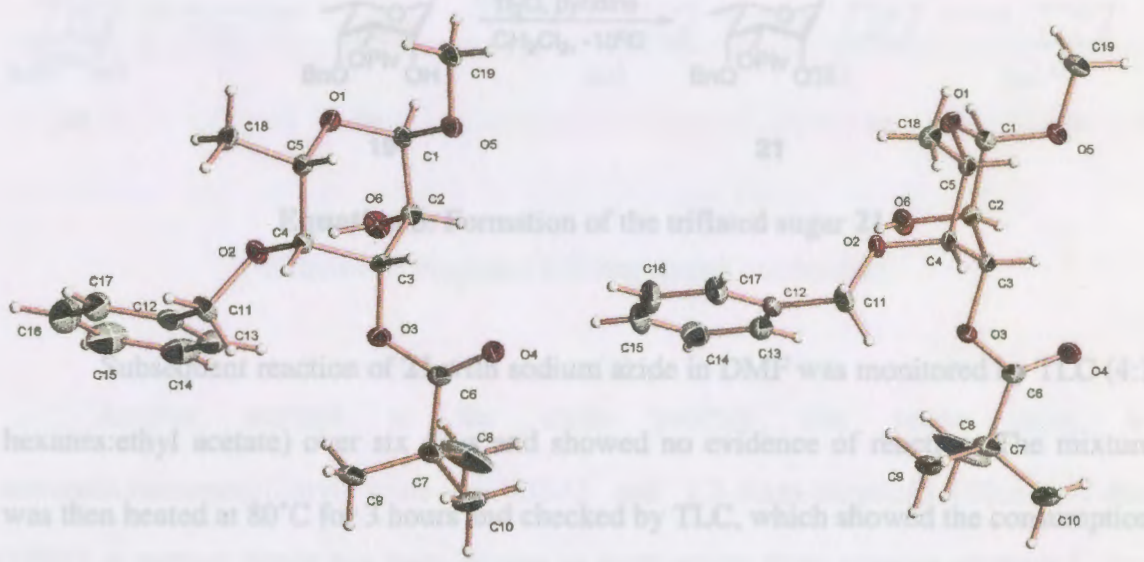

Figure 8: Two perspectives of the X-ray crystal structure of **19**

4. Attempts at Producing a C-2 Azide Derivative

With the selective protection of all of the alcohols on the sugar except that at C-2, the next step was to try to introduce an azide at C-2, which could later be reduced to *N*-acetyl-L-fucosamine. The first attempt involved forming a leaving group in place of the alcohol at C-2, and then an S_N2 reaction with sodium azide to form the azidosugar. The alcohol **19** was reacted with triflic anhydride to form the triflated sugar *via* a nucleophilic acyl substitution (Equation 5). Monitoring the reaction after 24 hours by TLC (4:1 hexanes:ethyl acetate) revealed the consumption of starting material and the appearance of a less polar spot (R_f = 0.43). ^{1}H NMR showed a disappearance of the alcohol proton signal, as well as a downfield shift of the proton at C-2, suggesting the formation of compound **21**.

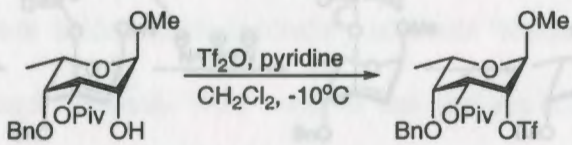

19 **21**

Equation 5: Formation of the triflated sugar **21**

Subsequent reaction of **21** with sodium azide in DMF was monitored by TLC (4:1 hexanes:ethyl acetate) over six days and showed no evidence of reaction. The mixture was then heated at 80°C for 3 hours and checked by TLC, which showed the consumption of starting material and the appearance of two products. The products were isolated by column chromatography (4:1 hexanes:ethyl acetate). ^{1}H NMR of the less polar product (R_f = 0.52) showed the loss of the proton at C-3 and a downfield shift of the signals

corresponding to the protons at C-1 and C-2. ^{13}C NMR also showed that the peaks corresponding to the pivaloyl group were still present, suggesting compound **22**. ^{1}H NMR of the more polar product (R_f = 0.38) showed the loss of the pivaloyl ester peak of nine protons at approximately 1.3 ppm, and carbon NMR showed a peak corresponding to a ketone, which was hypothesized to be compound **24**. Mass spectra confirmed the mass of this structure. Based on these products, it can be inferred that heating did not lead to the S_N2 product but instead encouraged formation of the E2 product **22**. This product likely decomposes into **24** by a nucleophilic acyl substitution, possibly by the azide which is in large excess, resulting in the enol product **23**. This product then tautomerizes to form the ketone product as in the proposed mechanism below (Scheme 5).

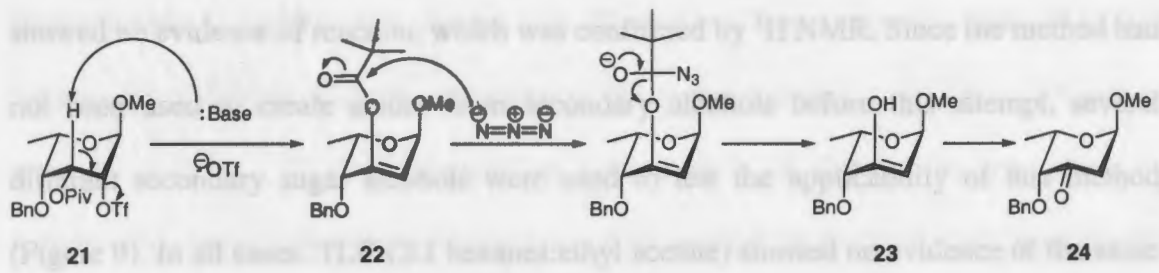

Scheme 5: Proposed E2/deacylation mechanism

Another attempt at the azide product was made using 4-acetamidobenzenesulfonyl azide (*p*-ABSA) and 1,8-diaza-bicyclo[5.4.0]undec-7-ene (DBU), a method which has been proven to yield azides from primary alcohols.[20] The proposed mechanism involves the formation of a sulfonyl ester leaving group *in situ*, which can then be attacked *via* an S_N2 reaction by an azide nucleophile, also formed *in*

situ (Scheme 6). While successful on primary alcohols, this method had not been tested at a secondary carbon.

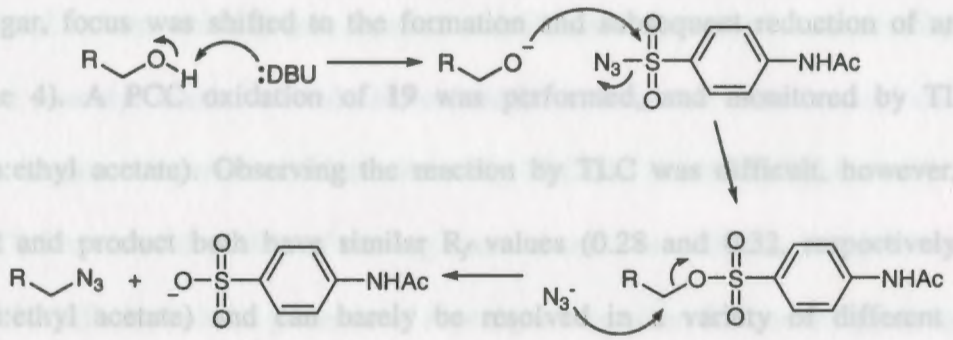

Scheme 6: Proposed *p*-ABSA / DBU azidation mechanism

Monitoring the reaction by TLC (2:1 hexanes: ethyl acetate) over three days showed no evidence of reaction, which was confirmed by ^{1}H NMR. Since the method had not been used to create azides from secondary alcohols before this attempt, several different secondary sugar alcohols were used to test the applicability of this method (Figure 9). In all cases, TLC (2:1 hexanes:ethyl acetate) showed no evidence of the azide products, and this was confirmed by ^{1}H NMR after each reaction was worked up.

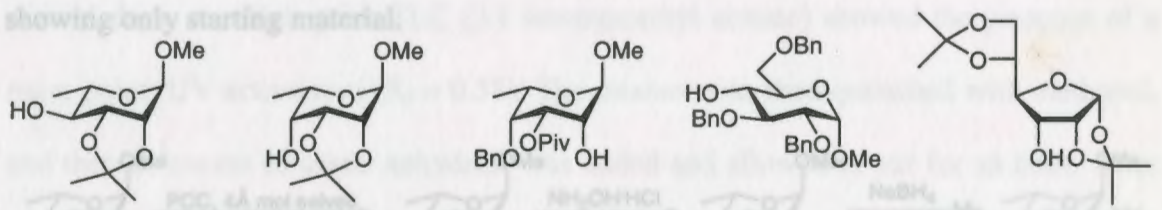

10 **12** **19**

Figure 9: Secondary alcohols used to test azidation method

5. Formation and Reduction of the C-2 Oxime

Since introduction of nitrogen at C-2 could not be accomplished by forming the azidosugar, focus was shifted to the formation and subsequent reduction of an oxime (Scheme 4). A PCC oxidation of **19** was performed, and monitored by TLC (4:1 hexanes:ethyl acetate). Observing the reaction by TLC was difficult, however, as the reactant and product both have similar R_f values (0.28 and 0.32, respectively in 4:1 hexanes:ethyl acetate) and can barely be resolved in a variety of different solvent systems. ^{1}H NMR was used to verify reaction completion, with the disappearance of the signals from the alcohol (4.13 ppm) and proton at C-2 (3.84 ppm). Carbon NMR also showed the formation of the ketone by the appearance of a signal at 195.6 ppm, confirming the formation of compound **25**. To form the oxime, hydroxylamine hydrochloride in pyridine was reacted with **25** over two days. After this time, TLC (4:1 hexanes:ethyl acetate) showed consumption of starting material and a new UV-active spot (R_f = 0.23). ^{13}C NMR showed an upfield shift of C-2 as the less electron-withdrawing oxime replaced the ketone to confirm product **26**. Reduction of the oxime **26** was attempted with sodium borohydride in methanol. TLC (4:1 hexanes:ethyl acetate) after two days provided no evidence of reaction, and ^{1}H confirmed this observation, showing only starting material.

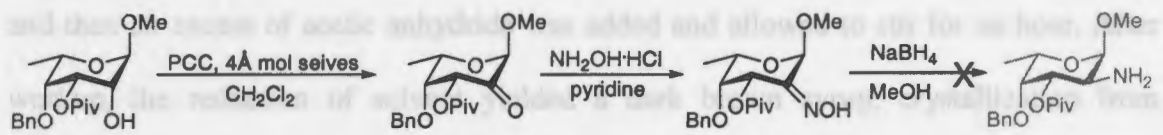

19 **25** **26**

Scheme 7: Oxime synthesis and attempted reduction

An alternate attempt at oxime reduction was used based on an oxime reduction strategy reported by Lichtenthaler *et. al.* in which the oxime is first activated by forming the benzoyl oxime, which is then reduced with BH_3 and reacted with acetic anhydride to form the *N*-acetyl amide.[21] To do so, oxime **26** was reacted with benzoyl chloride in pyridine at room temperature and monitored by TLC (4:1 hexanes:ethyl acetate). After 24 hours, TLC revealed depletion of starting material and a new slightly less polar spot (R_f = 0.27). ^{1}H NMR showed the presence of new signals between 7.5 and 8.2 ppm, indicative of the aromatic ring of the benzoyl oxime. With the exception of very small chemical shifts of protons at C-1 and C-3, the rest of the spectrum remained relatively unchanged, confirming the formation of **27** (Scheme 8).

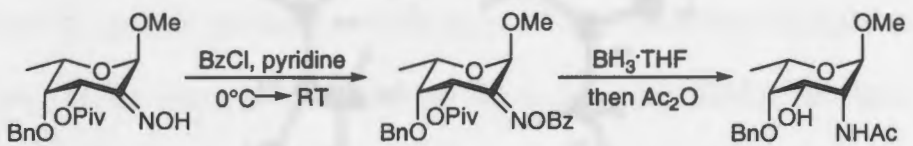

26 **27** **28**

Scheme 8: Benzoylation, reduction, and acylation of the oxime **26** to product **28**

The reduction and acylation of **27** was carried out by reaction with BH_3 over several days, at which point TLC (2:1 hexanes:ethyl acetate) showed the presence of a more polar, UV-active spot (R_f = 0.38). The mixture was then quenched with methanol, and then an excess of acetic anhydride was added and allowed to stir for an hour. After workup, the reduction of solvent yielded a dark brown syrup, crystallization from methanol resulted in small, white crystals. ^{1}H NMR showed the presence of a doublet at 7.05 ppm indicating the presence of an amide proton, as well as a singlet integrating to 3 protons at 1.77 ppm corresponding to the acetyl group. Interestingly, the peak of 9

protons corresponding to pivaloyl ester had disappeared, suggesting the cleaving of the group, possibly the result of the large excess of BH_3. Despite the promising evidence provided by ^1H NMR, X-ray crystallography (Figure 10) showed that the stereochemistry of the amide at C-2 was the *R*-isomer rather than the desired *S*-isomer, resulting in product **28** in a 56% yield.

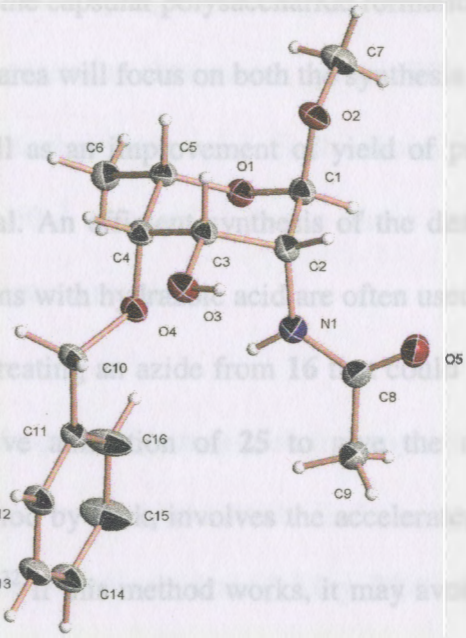

Figure 10: X-ray crystal structure of **28**

Conclusion

Development of a synthesis for an orthogonally-protected *N*-acetyl-L-fucosamine product was unsuccessful. The end product obtained (**28**) has the wrong stereochemistry at C-2. The product may still be useful, however, as the UDP analogue of this product is actually synthesized by *S. aureus* as a precursor to UDP-FucNAc.[7] Therefore, glycomimetic molecules based on this starting material may still show some biological activity in the inhibition of the capsular polysaccharide formation.

Future work in this area will focus on both the synthesis of the desired *N*-acetyl-L-fucosamine product as well as an improvement of yield of product **28** if it is deemed useful as a starting material. An efficient synthesis of the desired product may still be feasible. Mitsunobu reactions with hydrazoic acid are often used to create azides, and this method may be useful in creating an azide from **16** that could then be reduced. Another method may be a reductive amination of **25** to give the desired product. Another possibility, based on a method by Park, involves the accelerated introduction of an azide using microwave radiation.[22] If this method works, it may avoid the by-products **22** and **24** that resulted in azidation attempts from **21**.

Experimental

General Procedures

A Varian Gemini 2000 NMR spectrometer was used to obtain 400 MHz ^{1}H and 100 MHz ^{13}C spectra using $CDCl_3$ (0.1 % w/v TMS) as the solvent. Chemical shifts (δ) are recorded in parts per million (ppm). Multiplicities for NMR spectra are listed as followed: s (singlet), d (doublet), q (quartet), dd (doublet of doublets), dq (doublet of quartets), m (multiplet), and all coupling constants (J) are labeled in Hertz. A Bruker Esquire-HP 1100 LC/MS was used to obtain mass spectra. Whatman aluminum-backed plates were used for thin layer chromatography. Flash column chromatography was performed with 32-60 mesh 60-Å silica gel. A Perkin Elmer 323 automatic polarimeter was used to collect data on optical rotations.

Synthesis of methyl 2,3-*O*-isopropylidene-α-L-rhamnopyranoside (10)

In an oven-dried 250 mL round-bottom flask equipped with a septum and magnetic stirring bar, L-rhamnose monohydrate (13.0 g, 79.4 mmol) was dissolved in 200 proof ethanol (100 mL) and evaporated to remove water of hydration. This process was repeated twice. Next, the L-rhamnose was dissolved in anhydrous methanol (250 mL), which was saturated with HCl gas. The reaction was allowed to run over 24 hours at R.T., at which time TLC (100% ethyl acetate) showed formation of the product (R_f = 0.48). The solvent was removed, and the residue was dissolved in anhydrous DMF (20 mL). A catalytic amount of *p*-toluenesulfonic acid (0.9 g, 4.8 mmol) and 2,2-dimethoxypropane (20 mL) was added to the flask and allowed to stir for 24 hours, after which time TLC (1:2, hexanes : ethyl acetate) showed formation of product (R_f = 0.42). The reaction was

reduced and dissolved in CH_2Cl_2. The solution was washed with a saturated $NaHCO_3$ solution (2 x 25 mL), and water (2 x 25 mL), dried over $MgSO_4$, and evaporated to afford methyl 2,3-*O*-isopropylidene-α-L-rhamnopyranoside as a yellow oil (70 %).

^{1}H NMR ($CDCl_3$): δ 1.30 (d, 3H, CH_3, J = 6.23 Hz), 1.35 (s, 3H, CH_3), 1.53 (s, 3H, CH_3), 3.38 (s, 3H, OCH_3), 3.61 (dq, 1H, H-5, J = 6.25, 9.52 Hz), 4.06 (dd, 1H, H-4, J = 5.86, 7.14 Hz), 4.12 (d, 1H, H-3, J = 5.67 Hz), 4.86 (s, 1H, H-1).

^{13}C NMR ($CDCl_3$): δ 16.8, 25.2, 25.9, 55.0, 64.0, 66.8, 72.9, 73.1, 98.3, 109.1.

m/z calculated : 218.12 *m/z* found: 201.1 (-OH), 241.0 (+Na)

Oxidation of 10 using Swern conditions (11)[23, 24]

In a 3-neck round-bottom flask equipped with two addition funnels, thermometer, septa and a magnetic stirring bar, oxalyl chloride (2.8 mL, 31.8 mmol) was dissolved in CH_2Cl_2 (25 mL) and the flask was cooled to –78 °C. A solution of DMSO (5.0 mL, 63.6 mmol) in CH_2Cl_2 (25 mL) was added dropwise and the mixture was allowed to stir for 15 minutes. Next, a solution of **10** (6.4 g, 28.9 mmol) in CH_2Cl_2 (25 mL) was added dropwise and stirring was continued for 30 minutes. Triethylamine (20 mL, 142 mmol) was added dropwise *via* syringe and the solution was allowed to warm to room temperature and stirred for 24 hours. After 24 hours, TLC (2:1, hexanes : ethyl acetate, product R_f = 0.58) showed consumption of starting material. The mixture was then washed with 5% H_2SO_4 (2 x 50 mL) and water (2 x 50 mL). The organic layer was then dried over $MgSO_4$ and reduced to give **11** as a crude brown syrup, which was purified *via*

column chromatography (2:1 hexanes : ethyl acetate) to afford **11** as a yellow syrup (60 %).

^{1}H NMR ($CDCl_3$): δ 1.37 (s, 3H, CH_3), 1.48 (s, 3H, CH_3), 1.40 (d, 3H, CH_3, J = 6.78 Hz), 3.47 (s, 3H, OCH_3), 4.26 (q, 1H. H-5, J = 6.77 Hz), 4.44 (s, 2H, H-2, H-3), 4.85 (s, 1H, H-1).

^{13}C NMR ($CDCl_3$): δ 15.8, 25.4, 26.6, 55.6, 69.5, 75.7, 78.5, 97.8, 111.0, 204.0.

m/z calculated: 216.10 *m/z* found: 239.1 (+Na)

Sodium borohydride reduction of ketone 11 to give 12

In a 25 mL round-bottom flask fitted with a magnetic stir bar, the ketone **11** (0.9 g, 4.1 mmol) was dissolved in methanol (25 mL). $NaBH_4$ (0.19 g, 4.9 mmol) was added slowly to the solution, which was allowed to stir for two hours at R.T. After two hours, TLC (2:1, hexanes:ethyl acetate) showed consumption of starting material (product R_f = 0.32). The mixture was poured over ice-water (30 mL) and then extracted with CH_2Cl_2 (2 x 25 mL). The organic layer was washed with 5% H_2SO_4 (2 x 25 mL) and water (2 x 25 mL). Drying over $MgSO_4$ and evaporating afforded **12** as yellow syrup (92.7%).

^{1}H NMR ($CDCl_3$): δ 1.34 (d, 3H, CH_3, J = 6.59 Hz), 1.38 (s, 3H, CH_3), 1.59 (s, 3H, CH_3), 2.24 (d, 1H, OH, J = 6.77 Hz), 3.40 (s, 3H, OCH_3), 3.53-3.58 (m, 1H, H-4), 3.83 (q, 1H,

H-5, J = 6.59 Hz), 4.03 (d, 1H, H-2, J = 6.06 Hz), 4.21 (dd, 1H, H-3, J = 4.94, 6.22 Hz), 4.93 (s, 1H, H-1).

m/z calculated : 218.12 *m/z* found: 187.0 (-OCH_3), 241.1 (+Na)

Protection of O-4 of 4 *via* a Williamson ether synthesis (13)

In a 3-neck round-bottom flask equipped with a thermometer, septa and a magnetic stirring bar, **12** (2.3 g, 10.5 mmol) was dissolved in dry DMF (40 mL) and cooled to 0°C. Sodium hydride (0.9 g, 23.2 mmol) was added to the flask and the mixture was allowed to stir for 20 minutes. The flask was then allowed to warm to room temperature and benzyl bromide (1.3 mL, 10.9 mmol) was added dropwise *via* syringe and the reaction was allowed to stir for three hours. TLC (2:1, hexanes:ethyl acetate) showed the consumption of starting material and a new UV-active product (R_f = 0.58). Excess NaH was quenched by adding methanol (10 mL) and the mixture was diluted with CH_2Cl_2 (100 mL). The organics were then washed with saturated $NaHCO_3$ (2 x 50 mL) and water (2 x 50 mL). Drying over $MgSO_4$ and reducing the solution resulted in a crude brown syrup which was purified *via* column chromatography (2:1 hexanes:ethyl acetate) to afford **13** as small white crystals (65%).

^{1}H NMR ($CDCl_3$): δ 1.21 (d, 3H, CH_3, J = 6.59 Hz), 1.37 (s, 3H, CH_3), 1.57 (s, 3H, CH_3), 3.39 (s, 3H, OCH_3), 3.57 (dd, 1H, H-4, J = 3.21, 4.49 Hz), 3.86 (dq, 1H, H-5, J = 3.16, 6.59 Hz), 4.02 (dd, 1H, H-2, J = 1.93, 6.68 Hz), 4.38 (dd, 1H, H-3, J = 4.58, 6.78 Hz), 4.56 (d, 1H, Ph$C\underline{H_2}$OR, J = 12.08 Hz), 4.87 (d, 1H, Ph$C\underline{H_2}$OR, J = 12.08 Hz), 4.83 (d, 1H, H-1, J = 2.02 Hz), 7.25-7.40 (m, 5H, Ar-H).

^{13}C NMR ($CDCl_3$): δ 16.9, 25.5, 26.3, 55.5, 65.5, 72.8, 73.6, 74.2, 98.7, 109.8, 127.6, 127.8, 128.0, 128.1, 128.2, 128.4, 137.8.

m/z calculated : 308.16 *m/z* found: 307.1 (-H), 332.1 (+Na)

Removal of isopropylidene group to afford 14

In a 25 mL round-bottom flask fitted with a magnetic stir bar, the protected sugar **13** was added (3.5 g, 11.2 mmol) and dissolved in a 60% solution of trifluoroacetic acid (35 mL) and allowed to stir for 30 minutes. TLC showed the consumption of starting material (product R_f = 0.33). The mixture was reduced to a syrup and purified *via* column chromatography (1:1 hexanes : ethyl acetate) to afford **14** as a yellow syrup in an 86% yield.

^{1}H NMR ($CDCl_3$): δ 1.28 (d, 3H, CH_3, *J* = 6.59 Hz), 3.36 (s, 3H, OCH_3), 3.62-3.67 (m, 2H), 3.81-3.84 (m, 1H), 3.87 (q, 1H, H-5, *J* = 6.59 Hz), 4.71 (d, 1H, PhC$\underline{H_2}$OR, *J* = 10.99 Hz), 4.87 (d, 1H, PhC$\underline{H_2}$OR, *J* = 10.99 Hz), 4.75 (s, 1H, H-1), 7.30-7.40 (m, 5H, Ar-H).

^{13}C NMR ($CDCl_3$): δ 17.1, 54.9, 65.6, 66.6, 70.7, 81.3, 101.1, 102.7, 127.5, 128.0, 128.4, 128.9, 129.0, 137.2.

m/z calculated : 268.13 *m/z* found: 291.1 (+ Na)

Attempted protection of the C3 hydroxyl of 14 as a benzoyl ester (15, 16, 17)

A 50 mL two-necked round-bottom flask was fitted with a thermometer and stir bar, then flame-dried and cooled under N_2. Sugar **14** (1.2 g, 4.4 mmol) was dissolved in pyridine (7 mL) and the solution was cooled to –10 °C in an ice/acetone bath. Next, benzoyl chloride (0.5 mL, 4.4 mmol) was dissolved in CH_2Cl_2 (5 mL) and added to the solution dropwise *via* syringe. The mixture was left to stir overnight, and monitoring by TLC (97.5:2.5 toluene:methanol) showed the presence of three less polar spots (R_f= 0.36, 0.38, 0.52) and consumption of starting material. The reaction mixture was poured over 25 g of ice, transferred to a separatory funnel, and extracted with CH_2Cl_2 (2 x 25 mL). The organics were then washed with 5% H_2SO_4 (2 x 25 mL), DI H_2O (2 x 25 mL), and dried over $MgSO_4$. Column chromatography (97.5:2.5 toluene:methanol) yielded three products, **15**, **16**, and **17** as yellow oils.

Product **15**

^{1}H NMR ($CDCl_3$): δ 1.44 (d, 3H, CH_3, J = 6.59 Hz), 3.42 (s, 3H, OCH_3), 3.90 (s, 1H, H-4), 4.17 (q, 1H, H-5, J = 6.47 Hz), 4.60 (d, 1H, PhC$\underline{H_2}$OR, J = 4.68 Hz), 4.77 (d, 1H, PhC$\underline{H_2}$OR, J = 4.68 Hz), 4.92 (d, 1H, H-1, J = 1.10 Hz), 5.46-5.50 (m, 1H, H-2), 5.58-5.62 (m, 1H, H-3), 7.10-7.70 (m, 12H, Ar-H), 7.86-8.22 (m, 3H, Ar-H).

m/z calculated : 476.18 *m/z* found: 499.2 (+Na)

Product **16**

^{1}H NMR ($CDCl_3$): δ 1.28 (d, 3H, CH_3, J = 6.41 Hz), 3.39 (s, 3H, OCH_3), 3.88-3.96 (m, 3H), 4.04 (q, 1H, H-5, J = 6.53 Hz), 4.26 (d, 1H, OH, J = 11.17 Hz), 4.59 (d, 1H,

PhC$\underline{H_2}$OR, J = 11.08 Hz), 4.83 (d, 1H, PhC$\underline{H_2}$OR, J = 11.08 Hz), 4.80 (s, 1H, H-1), 5.30-5.34 (m, 1H, H-3), 7.20-7.33 (m, 5H, Ar-H), 7.43-7.49 (m, 2H, Ar-H), 7.56-7.61 (m, 1H, Ar-H), 8.10-8.15 (m, 2H, Ar-H).

m/z calculated : 372.16 *m/z* found: 373.2 (+H), 395.1 (+Na)

Product **17**

^{1}H NMR ($CDCl_3$): δ 1.44 (d, 3H, CH_3, J = 6.60 Hz), 3.37 (s, 3H, OCH_3), 3.64 (d, 1H, H-4, J = 3.30 Hz), 4.00 (q, 1H, H-5, J = 6.59 Hz), 4.09-4.13 (m, 1H, H-3), 4.64 (d, 1H, PhC$\underline{H_2}$OR, J = 10.44 Hz), 4.79 (d, 1H, PhC$\underline{H_2}$OR, J = 10.44 Hz), 4.84 (s, 1H, H-1), 5.10 (d, 1H, H-2, J = 3.85 Hz), 7.11-7.47 (m, 8H, Ar-H), 7.86-7.91 (m, 2H, Ar-H).

m/z calculated : 372.16 *m/z* found: 373.1 (+H), 395.3 (+Na)

Attempted protection of the C3 hydroxyl of 14 with a silyl group[25]

A 100 mL round-bottom flask was fitted with a stir bar, flame-dried and flushed with N_2. Next, **14** was added to the flask (0.44 g, 1.62 mmol) and dissolved in 20 mL of DMF. Imidazole (0.34 g, 4.99 mmol) was added to the flask, then *tert*-butyldiphenylsilyl chloride (0.43 mL, 1.66 mmol) was added dropwise *via* syringe. Monitoring the reaction by TLC (1:1 hexanes:ethyl acetate) over the course of a week showed no evidence of reaction. The mixture was transferred to a separatory funnel containing 25 mL each of DI H_2O and CH_2Cl_2 and extracted with 2 x 25 mL CH_2Cl_2. The organics were then washed with 2 x 25 mL portions of brine and 2 x 25 mL DI H_2O, and dried over Na_2SO_4 and reduced. ^{1}H NMR confirmed no reaction.

Selective protection of the C3 hydroxyl of 14 as a pivaloyl ester (19)[26]

A 50 mL round-bottom flask was fitted with a stir bar, flame-dried and flushed with N_2. Next, **14** was added to the flask and dissolved in 20 mL of CH_2Cl_2. Pyridine was added to the flask (5.0 mL, 61.8 mmol) and the mixture was cooled to –10 °C in an ice/acetone bath. Pivaloyl chloride (0.33 mL, 2.68 mmol) was added dropwise *via* syringe. The ice bath was removed and the flask was allowed to warm to RT. Monitoring the reaction by TLC (4:1 hexanes:ethyl acetate) revealed the formation of three less polar spots (R_f = 0.32, 0.44, and 0.62) after 2 days. The mixture was poured over ice and then transferred to a separatory funnel, and the aqueous layer was extracted with CH_2Cl_2 (2 x 15 mL). The organic layers were combined and washed with saturated aqueous NaCl (2 x 15 mL), and dried over $MgSO_4$. The solvent was removed, and **19** was recrystallized from methanol (58%).

Product **18**

^{1}H NMR ($CDCl_3$): δ 1.14 (s, 9H, $C(CH_3)_3$), 1.23 (s, 9H, $C(CH_3)_3$), 1.31 (d, 3H, CH_3, J = 6.41 Hz), 3.37 (s, 3H, OCH_3), 3.63-3.67 (m, 1H, H-4), 4.03 (q, 1H, H-5, J = 6.28 Hz), 4.49 (d, 1H, PhC$\underline{H_2}$OR, J = 11.45 Hz), 4.82 (d, 1H, PhC$\underline{H_2}$OR, J = 11.45 Hz), 4.66 (s, 1H, H-1), 5.04-5.06 (m, 1H, H-2), 5.24-5.28 (m, 1H, H-3), 7.24-7.41 (m, 5H, Ar-H).

m/z calculated : 436.25 *m/z* found: 459.2 (+Na)

Product **19**

^{1}H NMR ($CDCl_3$): δ 1.25 (d, 3H, CH_3, J = 6.59 Hz), 1.30 (s, 9H, $C(CH_3)_3$), 3.37 (s, 3H, OCH_3), 3.74-3.76 (m, 1H, H-4), 3.79-3.85 (m, 1H, H-2), 3.97 (q, 1H, H-5, J = 6.47 Hz),

4.12 (d, 1H, OH, J = 10.98 Hz), 4.54 (d, 1H, PhC$\underline{H_2}$OR, J = 10.80 Hz), 4.91 (d, 1H, PhC$\underline{H_2}$OR, J = 10.80 Hz), 4.74 (d, 1H, H-1, J = 1.65 Hz), 5.03-5.07 (m, 1H, H-3), 7.29-7.38 (m, 5H, Ar-H).

^{13}C NMR ($CDCl_3$): δ 16.9, 27.4, 39.1, 55.2, 66.1, 69.0, 70.1, 75.8, 78.9, 102.5, 128.0, 128.1, 128.4, 137.0, 177.6.

m/z calculated : 352.19 *m/z* found: 321.1 (-OCH_3), 375.2 (+Na)

Product **20**

^{1}H NMR ($CDCl_3$): δ 1.07 (s, 9H, $C(CH_3)_3$), 1.38 (d, 3H, CH_3, J = 6.59 Hz), 2.63 (d, 1H, OH, J = 10.80 Hz), 3.35 (s, 3H, OCH_3), 3.56 (d, 1H, H-4, J = 3.67 Hz), 3.91-4.04 (m, 2H, H-3, H-5), 4.58 (d, 1H, PhC$\underline{H_2}$OR, J = 11.08 Hz), 4.77 (d, 1H, PhC$\underline{H_2}$OR, J = 11.08 Hz), 4.67 (s, 1H, H-1), 4.81 (d, 1H, H-2, J = 3.66 Hz), 7.25-7.42 (m, 5H, Ar-H).

m/z calculated : 352.19 *m/z* found: 375.2 (+Na)

Formation of the O-2 triflate derivative of compound 19 (21)

A 3-neck round-bottom flask was fitted with a stir bar, two addition funnels, and a thermometer adapter and then flame-dried and flushed with N_2. Pyridine (0.80 mL) and CH_2Cl_2 (5 mL) were added to the flask and cooled to –10 °C in an ice/acetone bath. Once cool, a solution of triflic anhydride (0.33 mL, 1.95 mmol) in 5 mL of CH_2Cl_2 was added dropwise from an addition funnel and the mixture was allowed to stir for 15 minutes. A solution of **19** (0.53 g, 1.49 mmol) in 10 mL of CH_2Cl_2 was then added dropwise and

allowed to stir. The reaction was monitored by TLC (4:1 hexanes:ethyl acetate) and after 3 hours showed the consumption of starting material and the appearance of a less polar spot (R_f = 0.43). The mixture was poured over ice and then transferred to a separatory funnel. The solution was extracted with CH_2Cl_2 (2 x 25 mL), and the combined organics were dried over $MgSO_4$. Reducing the solution resulted in a pink solid (**21**) in good yield (93%).

^{1}H NMR ($CDCl_3$): δ 1.27 (d, 3H, CH_3, J = 6.41 Hz), 1.28 (s, 9H, $C(C\underline{H}_3)_3$), 3.40 (s, 3H, OCH_3), 3.66-3.70 (m, 1H, H-4), 4.03 (dq, 1H, H-5, J = 1.46, 6.53 Hz), 4.51 (d, 1H, $PhC\underline{H}_2OR$, J = 11.26 Hz), 4.89 (d, 1H, $PhC\underline{H}_2OR$, J = 11.26 Hz), 4.88 (d, 1H, H-3, J = 1.46 Hz), 4.96 (d, 1H, H-1, J = 3.29 Hz), 5.23-5.27 (m, 1H, H-2), 7.25-7.40 (m, 5H, Ar-H).

Attempted azidation of 21 using sodium azide

A 25 mL round-bottom flask was fitted with a stir bar, flame-dried, and flushed with N_2. Next, **21** (0.66 g, 1.39 mmol) was dissolved in 5 mL of DMF, and sodium azide (0.30 g, 4.62 mmol) was added. The reaction was monitored over 6 days by TLC (2:1 hexanes:ethyl acetate) and showed no sign of change. The flask was fitted with a reflux condenser and heating mantle, and heated to 80 °C. After three hours, TLC showed the consumption of starting material and the formation of two more polar spots (R_f = 0.38 and 0.52). The mixture was reduced, dissolved in CH_2Cl_2, and transferred to a separatory funnel. The solution was washed with 2 x 25 mL of DI H_2O and dried over $MgSO_4$.

Column chromatography (2:1 hexanes:ethyl acetate) afforded 0.15 g of **22** and 0.074 g of **24**, both as white syrups.

Product **22**

^{1}H NMR ($CDCl_3$): δ 1.26 (s, 9H, C($C\underline{H}_3$)$_3$), 1.36 (d, 3H, CH_3, J = 6.59 Hz), 3.42 (s, 3H, OCH_3), 3.80 (d, 1H, H-4, J = 2.57 Hz), 4.29 (dq, 1H, H-5, J = 2.52, 6.65 Hz), 4.56 (d, 1H, Ph$C\underline{H}_2$OR, J = 11.16 Hz), 4.69 (d, 1H, Ph$C\underline{H}_2$OR, J = 11.16 Hz), 5.12 (d, 1H, H-2, J = 3.29 Hz), 5.79 (d, 1H, H-1, J = 3.48 Hz), 7.23-7.38 (m, 5H, Ar-H).

^{13}C NMR ($CDCl_3$): δ 16.1, 27.0, 27.1, 39.1, 55.4, 55.7, 67.5, 72.2, 72.3, 95.3, 115.3, 127.7, 128.0, 128.2, 137.9, 148.6, 175.9.

m/z calculated : 334.18 *m/z* found: 332.1 (-2H), 356.2 (+Na)

Product **24**

NMR ($CDCl_3$): δ 1.32 (d, 3H, CH_3, J = 6.59 Hz), 2.39 (dt, 1H, H-2*equatorial*, J = 1.38, 13.76 Hz), 3.14 (d, 1H, H-2*axial*, J = 4.57, 13.73 Hz), 3.32 (s, 3H, OCH_3), 3.44 (t, 1H, H-1, J = 1.46), 4.12 (dq, 1H, H-5, J = 1.64, 6.53 Hz), 4.36 (d, 1H, Ph$C\underline{H}_2$OR, J = 11.90 Hz), 4.62 (d, 1H, Ph$C\underline{H}_2$OR, J = 11.90 Hz), 5.08 (dd, 1H, H-4, J = 1.19, 4.48 Hz), 7.27-7.38 (m, 5H, Ar-H).

^{13}C NMR ($CDCl_3$): δ 16.1, 43.4, 54.9, 68.0, 71.8, 82.1, 99.7, 127.9, 128.0, 128.2, 136.7, 204.5.

m/z calculated : 250.12 *m/z* found: 273.1 (+Na)

Attempted azidation of 19 using *p*-ABSA and DBU

A 50 mL round-bottom flask was flame-dried, flushed with N_2, and fitted with a stir bar and septum. Next, 0.03 g (0.082 mmol) of **19** was dissolved in acetonitrile (5 mL). DBU (0.03 mL, 0.17 mmol) and *p*-ABSA (0.04 g, 0.17 mmol) were added to the solution and the mixture was allowed to stir for 48 hours, after which TLC (2:1 hexanes: ethyl acetate) showed no evidence of reaction. The mixture was dissolved in CH_2Cl_2 and washed with 5% H_2SO_4 (2 x 15 mL) and DI H_2O (2 x 15 mL). The organics were then dried over $MgSO_4$ and the solvent evaporated. ^{1}H NMR confirmed no reaction.

Oxidation of 19 with PCC (25)[27]

A 50 mL round-bottom flask was fitted with a stir bar and 4 Å molecular sieves (0.37 g). Next, 0.4 g (1.15 mmol) of **19** dissolved in CH_2Cl_2 (15 mL) was added to the flask, followed by 0.65 g (3.0 mmol) of PCC. The mixture was allowed to stir for 24 hours after which TLC (4:1 hexanes:ethyl acetate) showed the presence of a slightly less polar spot (R_f = 0.32). The mixture was poured onto 25 mL of silica and eluted with a 1:1 mixture of hexanes: ethyl ether. The solvent was evaporated to afford **25** as a white solid in a 95% yield.

^{1}H NMR ($CDCl_3$): δ 1.25 (d, 3H, CH_3, *J* = 6.41 Hz), 1.30 (s, 9H, $C(C\underline{H}_3)_3$), 3.43 (s, 3H, OCH_3), 4.04 (d, 1H, H-4, *J* = 3.30 Hz), 4.47 (q, 1H, H-5, *J* = 6.47 Hz), 4.60 (d, 1H, $PhC\underline{H}_2OR$, *J* = 4.78 Hz), 4.94 (d, 1H, $PhC\underline{H}_2OR$, *J* = 4.78 Hz), 4.66 (s, 1H, H-1), 5.77 (d, 1H, H-3, *J* = 3.30 Hz), 7.25-7.35 (m, 5H, Ar-H).

^{13}C NMR ($CDCl_3$): δ 13.3, 27.2, 38.7, 55.4, 67.4, 74.7, 75.5, 82.2, 100.6, 127.6, 127.8, 128.0, 137.2, 176.6, 194.4.

m/z calculated : 350.17 *m/z* found: 373.1 (+Na)

$[\alpha]_D$ = -78.6 (*c*, 1.0, CH_2Cl_2)

Melting point: 54-57 °C

Formation of the oxime from ketone 25 (26)[28]

A 50 mL round-bottom flask containing 0.10 g (0.29 mmol) of **25** was flushed with N_2 and fitted with a stir bar. The ketone (**25**) was then dissolved in 1.0 mL (12.4 mmol) of pyridine and 0.08 g (1.18 mmol) of $NH_2OH \cdot HCl$ was added to the flask and allowed to stir. After 24 hours, TLC (4:1 hexanes:ethyl acetate) showed the consumption of starting material and a new, more polar spot (R_f = 0.23). The mixture was transferred to a separatory funnel and washed with 1M HCl (25 mL). The organics were then washed with saturated aqueous Na_2SO_4 (25 mL), followed by DI H_2O (25 mL). Drying over $MgSO_4$ and removing the solvent *in vacuo* resulted in **26** as a light pink solid in good yield (97.4 %).

^{1}H NMR ($CDCl_3$): δ 1.18 (d, 3H, CH_3, *J* = 6.41 Hz), 1.26 (s, 9H, $C(C\underline{H}_3)_3$), 3.43 (s, 3H, OCH_3), 3.81 (d, 1H, H-4, *J* = 2.20 Hz), 4.20 (q, 1H, H-5, *J* = 6.47 Hz), 4.58 (d, 1H, $PhC\underline{H}_2OR$, *J* = 11.62 Hz), 4.94 (d, 1H, $PhC\underline{H}_2OR$, *J* = 11.62 Hz), 5.78 (d, 1H, H-3, *J* = 2.74 Hz), 5.91 (s, 1H, H-1), 7.24-7.39 (m ,5H, Ar-H).

^{13}C NMR ($CDCl_3$): δ 16.8, 27.3, 39.0, 55.2, 66.9, 70.7, 74.9, 79.0, 91.4, 127.7, 128.1, 128.2, 137.6, 148.5, 177.1.

m/z calculated : 365.18 *m/z* found: 388.1 (+Na)

$[\alpha]_D$ = -46.4 (*c*, 1.0, CH_2Cl_2)

Melting point: 72-76 °C

Attempted sodium borohydride reduction of 26

A 50 mL flask was fitted with a stir bar and a solution of **26** (0.050g, 0.14 mmol) in 10 mL of methanol was added. Sodium borohydride (0.011 g, 0.29 mmol) was slowly added and the solution was allowed to stir. Progress was checked by TLC (4:1 hexanes: ethyl acetate) and after 24 hours showed no evidence of reaction. The mixture was poured over ice water (30 mL) then extracted with 2 x 25 mL CH_2Cl_2, and the organics washed with 5% H_2SO_4 (2 x 25 mL) and DI H_2O (2 x 25 mL). The organics were dried over $MgSO_4$ and reduced to a clear film. ^1H NMR confirmed no reaction.

Activation of oxime 26 by formation of the benzoyl oxime (27)

A 50 mL round-bottom flask containing 0.49g (1.33 mmol) of **26** was fitted with a stir bar and flushed with N_2. Pyridine (10 mL) was added *via* syringe and the solution was cooled to 0 °C in an ice bath. Benzoyl chloride (1.54 mL, 13.3 mmol) was added dropwise *via* syringe and the mixture was slowly allowed to warm to room temperature. After 24 hours TLC (4:1 hexanes:ethyl acetate) revealed consumption of starting material and formation of a slightly less polar spot (R_f = 0.27). The mixture was poured over ice,

and then extracted with CH_2Cl_2 (2 x 25 mL). The organics were then washed with 5% H_2SO_4 (2 x 25 mL) and DI H_2O (2 x 25 mL). The combined organics were then dried over $MgSO_4$. Purification by flash chromatography (4:1 hexanes : ethyl acetate) afforded **27** as a white solid in a 70.5% yield.

^{1}H NMR ($CDCl_3$): δ 1.23 (d, 3H, CH_3, J = 6.59 Hz), 1.38 (s, 9H, $C(C\underline{H}_3)_3$), 3.48 (s, 3H, OCH_3), 3.88 (d, 1H, H-4, J = 2.93 Hz), 4.25 (q, 1H, H-5, J = 6.59), 4.67 (d, 1H, $PhC\underline{H}_2OR$, J = 11.35 Hz), 5.05(d, 1H, $PhC\underline{H}_2OR$, J = 11.35 Hz), 5.93 (s, 1H, H-1), 5.96 (d, 1H, H-3, J = 2.93 Hz), 7.20-7.62 (m, 8H, Ar-H), 7.90-8.10 (m, 2H, Ar-H).

m/z calculated : 469.21 *m/z* found: 492.3 (+Na)

$[\alpha]_D$ = +6.3 (*c*, 1.0, CH_2Cl_2)

Melting point: 119-122 °C

BH_3 Reduction and subsequent acylation of 27 (28)

A 100 mL round-bottom flask was flame-dried, fitted with a stir bar and a septum, and flushed with N_2. Next, **27** (1.21 g, 2.58 mmol) was added to the flask and dissolved in dry THF (15 mL). The solution was cooled to –10 °C in an ice/acetone bath. Once cool, BH_3·THF (2.7 mL, 2.7 mmol) was added dropwise and the mixture was allowed to stir for 24 hours. TLC (2:1 hexanes:ethyl acetate) showed little evidence of reaction so an additional 5 mL of BH_3·THF was added and the reaction allowed to stir. After 24 hours TLC showed the consumption of starting material and the presence of a more polar spot (R_f = 0.38). The reaction was quenched with methanol, and then 10 mL of acetic

anhydride was added to the reaction flask and stirring was continued for an hour. The mixture was then poured over ice, and extracted with CH_2Cl_2 (2 x 25 mL). The combined organics were then washed with 1M HCl (2 x 15 mL), DI H_2O (2 x 15 mL), and saturated aqueous $NaHCO_3$ (15 mL). The organics were dried over $MgSO_4$ and evaporated to afford crude **28**. Flash chromatography (2:1 hexanes:ethyl acetate) gave the purified product **28** as white crystals in a 56.4% yield.

^{1}H NMR ($CDCl_3$): δ 1.31 (d, 3H, CH_3, J = 6.59 Hz), 1.77 (s, 3H, $NHCOC\underline{H}_3$), 3.32 (s, 3H, OCH_3), 3.61-3.63 (m, 1H, H-4), 3.91 (q, 1H, H-5, J = 6.41 Hz), 4.08-4.11 (m, 1H, H-3), 4.24-4.29 (m, 1H, H-2), 4.58 (d, 1H, H-1, J = 1.09 Hz), 4.69 (d, 1H, H-3, J = 10.43 Hz), 4.82 (d, 1H, H-3, J = 10.43 Hz), 8.98 (d, 1H, NHAc, J = 9.34 Hz), 7.30-7.44 (m, 5H, Ar-H).

m/z calculated : 309.16 *m/z* found: 332.1 (+Na)

$[\alpha]_D$ = -59.1 (*c*, 1.0, CH_2Cl_2)

Melting point: 141-143 °C

References:

1. Splenda. http://www.splenda.com/page.jhtml?id=splenda/hcp/basics.inc (accessed November 2003).
2. Cargill News. http://www.cargill.com/news/plastic.pdf (accessed November 2003)
3. Collins, P.; Ferrier, R. *Monosaccharides*, John Wiley and Sons: Chichester, West Sussex, England; 1995, 510-511.
4. Voet, D.; Voet, J.; Pratt, C. *Fundamentals of Biochemistry*, John Wiley and Sons: New York; 2002, 201.
5. Voet, D.; Voet, J.; Pratt, C. *Fundamentals of Biochemistry*, John Wiley and Sons: New York; 2002, 191-211.
6. Stick, R. *Carbohydrates: The Sweet Molecules of Life*, Academic Press: San Diego; 2001, 233-235.
7. Kneidinger, B.; O'Riordan, K.; Li. J.; Brisson, J.; Lee, J.C.; Lam, J.S. *J. Biol. Chem.* **2003**, *278*, 3615.
8. Lee, J.C. *Trends in Microbiology* **1996**, *4*, 162-166.
9. Chambers, H.F. *N. Engl. J. Med.* **2005**, *352*, 1485-1487.
10. "Surveillance for Methicillin-Resistant *Staphylococcus aureus* in Canadian Hospitals – A Report Update from the Canadian Nosocomial Infection Surveillance Program." [Online] **2005**, *31*, Public Health Agency of Canada. http://www.phac-aspc.gc.ca/publicat/ccdr-rmtc/05vol31/dr3103ea.html.

11. "*Staphylococcus aureus* Resistant to Vancomycin --- United States, 2002." [Online] **2002**, *51*, Centers for Disease Control. http://www.cdc.gov/mmwr/preview/mmwrhtml/mm5126al.htm.

12. Nouwen, J.L.; Fieren, M.W.; Snijders, S.; Verbrugh, H.A.; Belkum, A.V. *Kidney International* **2005**, *67*, 1084-1092.

13. Fridkin, S.K.; Hageman, J.C.; Morrison, M.; Sanza, L.T.; Como-Sabetti, K.; Jernigan, J.A.; Harriman, K.; Harrison, L.H.; Lynfield, R.; Farley, M.M. *N. Engl. J. Med.* **2005**, *352*, 1436-1444.

14. Miller, L.G.; Perdreau-Remington, F.; Rieg, G.; Mehdi, S.; Perlroth, J.; Bayer, A.S.; Tang, A.W.; Phung, T.O.; Spellberg, B. *N. Engl. J. Med.* **2005**, *352*, 1445-1453.

15. Mulrooney, E.F.; Poon, K.K.H.; McNally, D.J.; Brisson, J.R.; Lam, J.S. *J. Biol. Chem.* **2005**, *280*, 19535-19542.

16. Lee, M.; Hesek, D.; Suvorov, M.; Lee, W.; Vakulenko, S.; Mobashery, S. *J. Am. Chem. Soc.* **2003**, *125*, 16322-16326.

17. Gan, Z.; Kong, F. *Carbohydr. Res.* **1995**, *270*, 211-215.

18. Collins, P.M.; Overend, W.G. *J. Chem. Soc.* **1965**, 1912-1918.

19. Garegg, P.J.; Samuelsson, B. *Carbohydr. Res.* **1978**, *67*, 267-270.

20. J. Sacui, Youngstown State University, unpublished.

21. Kaji, E.; Osa, Y.; Takahashi, K.; Hirooka, M.; Zen, S.; Lichtenthaler, F.W. *Bull. Chem. Soc. Jpn.* **1994**, *67*, 1130-1140.

22. Park, S.H. *Bull. Korean Chem. Soc.* **2003**, *24*, 253-255.

23. Kobayashi, T.; Kobayashi, A. *Molecules* **2000**, *5*, 1062-1067.

24. Tidwell, T.T. *Synthesis* **1990**, 857.

25. Sever, M.J.; Wilker, J.J. *Tetrahedron* **2001**, *57*, 6139-6146.

26. Saito, N. *Tetrahedron* **2004**, *60*, 7951-7961.

27. Rauter, A.P.; Piedade, F.; Almeida, T.; Ramalho, R.; Ferreira, M.J.; Resende, R.; Amado, J.; Pereira, H.; Justino, J.; Neves, A.; Silva, F.V.M.; Canda, T. *Carbohydr. Res.* **2004**, *339*, 1889-1897.

28. Oare, D.A.; Heathcock, C.H. *J. Org. Chem.* **1990**, *55*, 157-173.

Appendix A

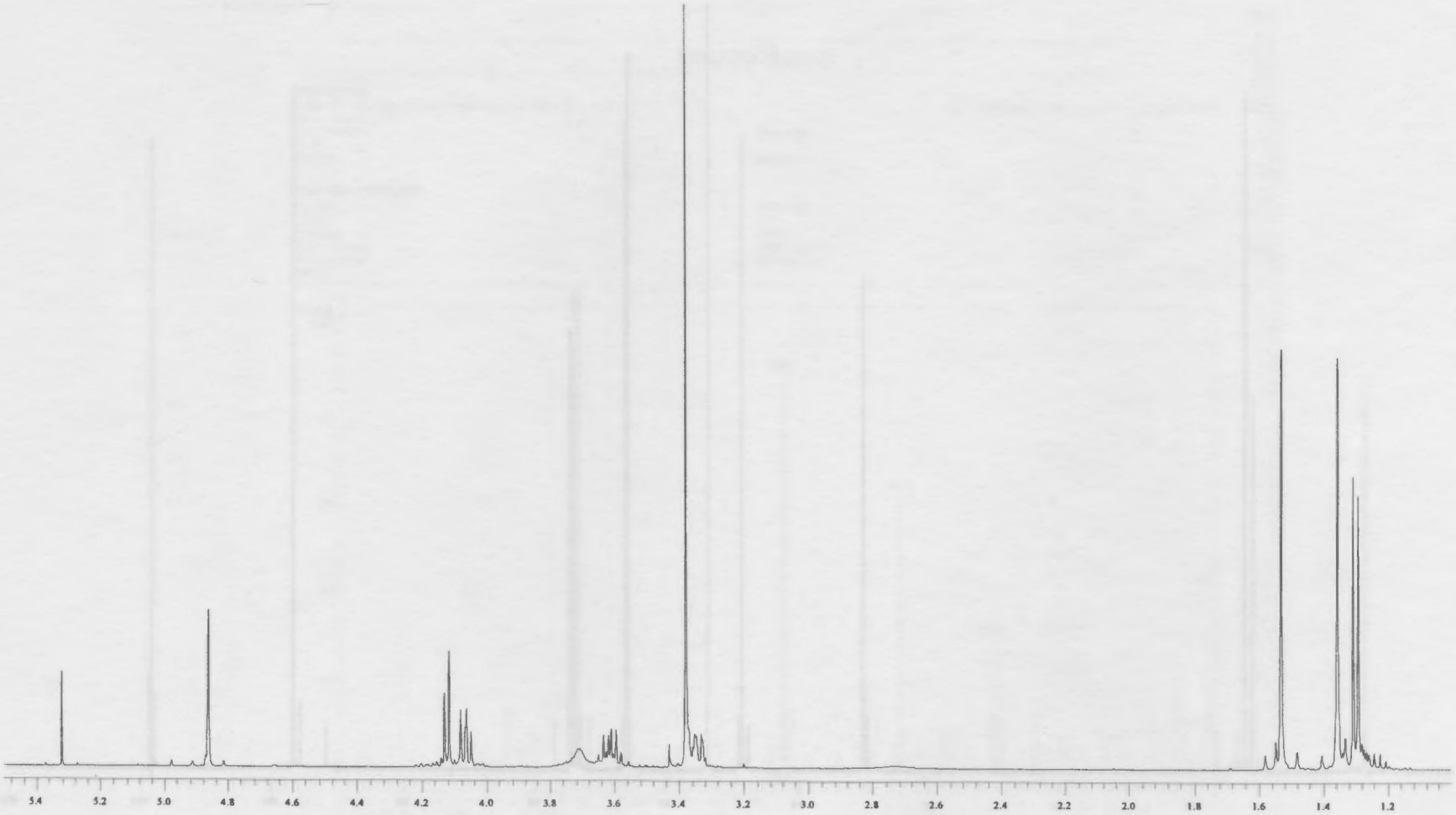

Figure 11: 400 MHz ^{1}H NMR spectrum of **10**

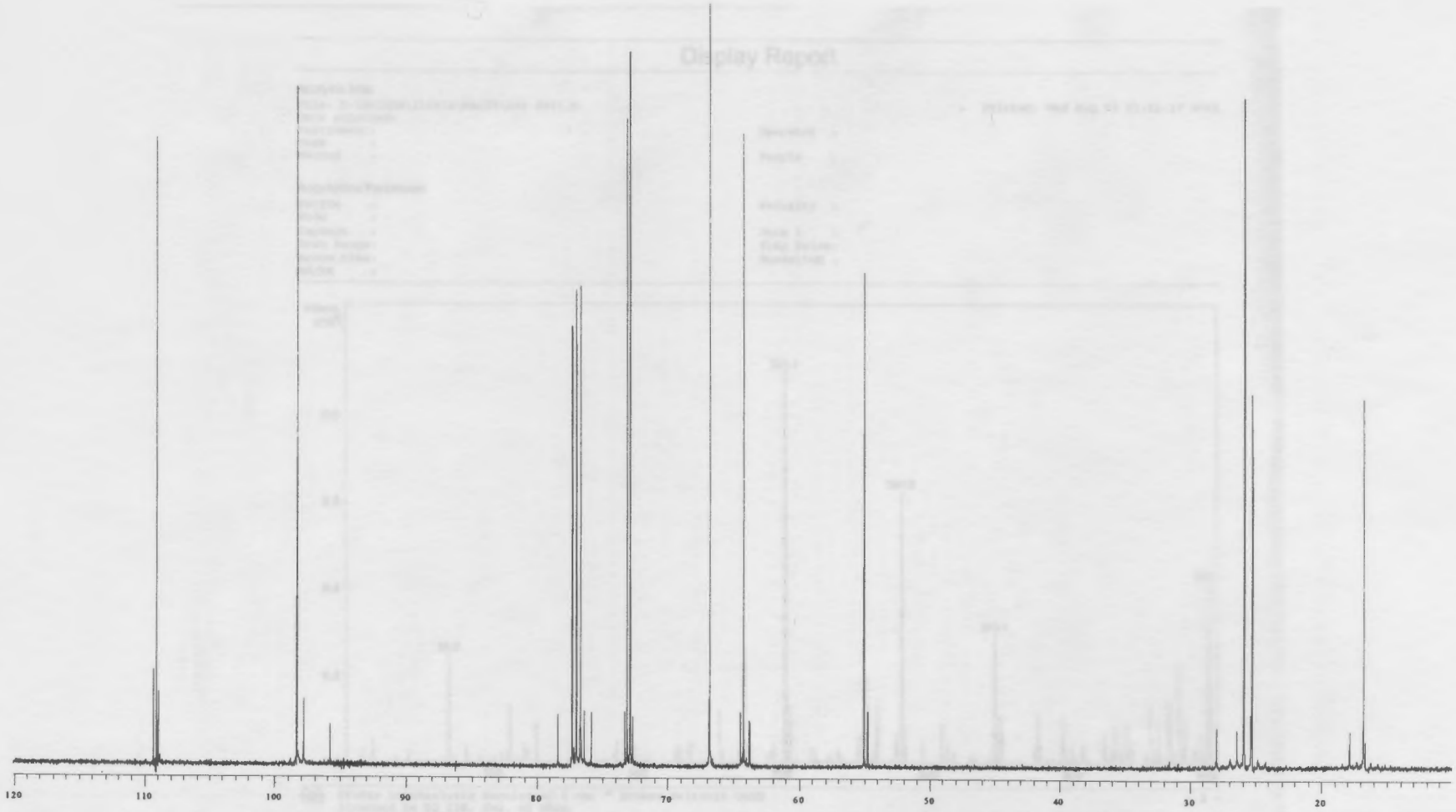

Figure 12: 100 MHz ^{13}C spectrum of **10**

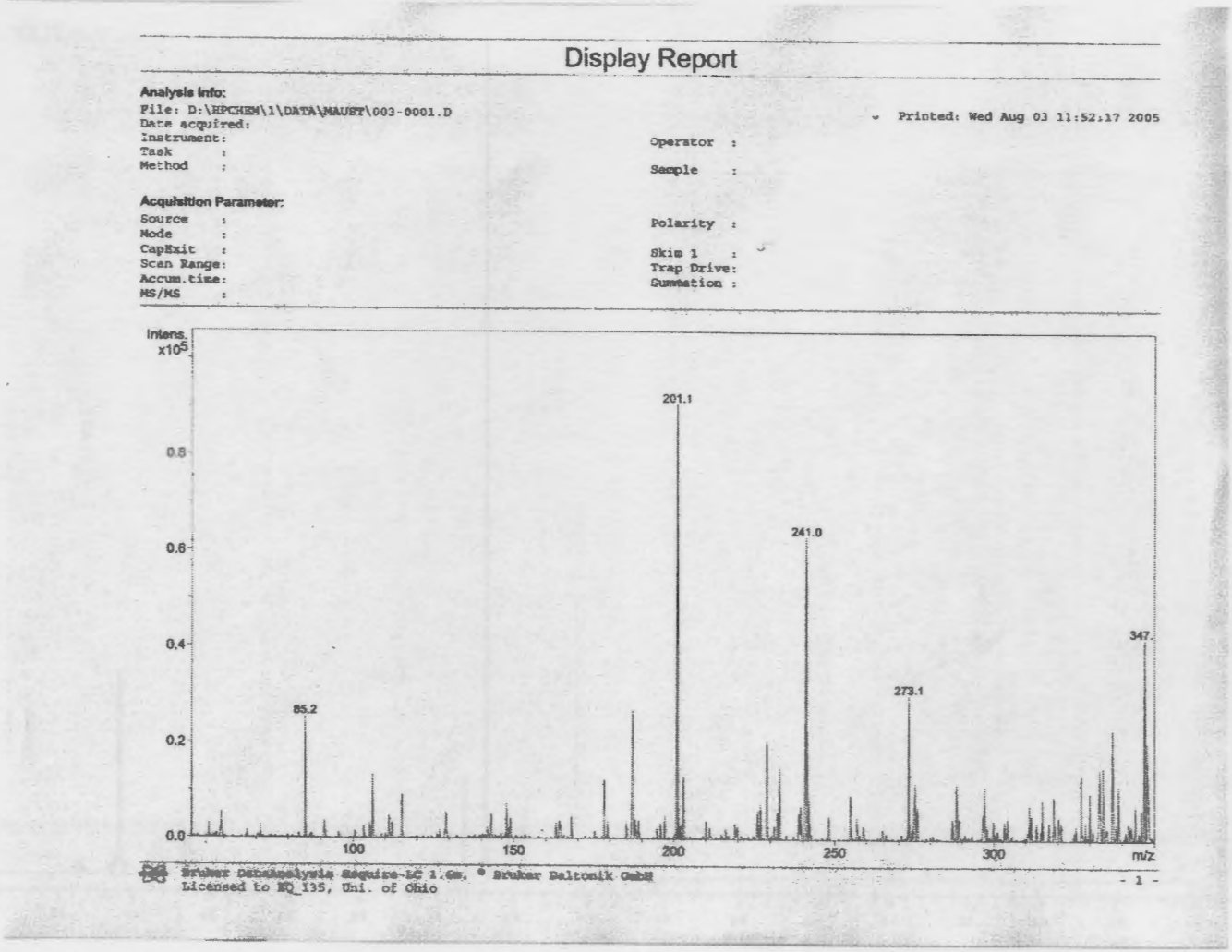

Figure 13: Mass spectrum of **10**

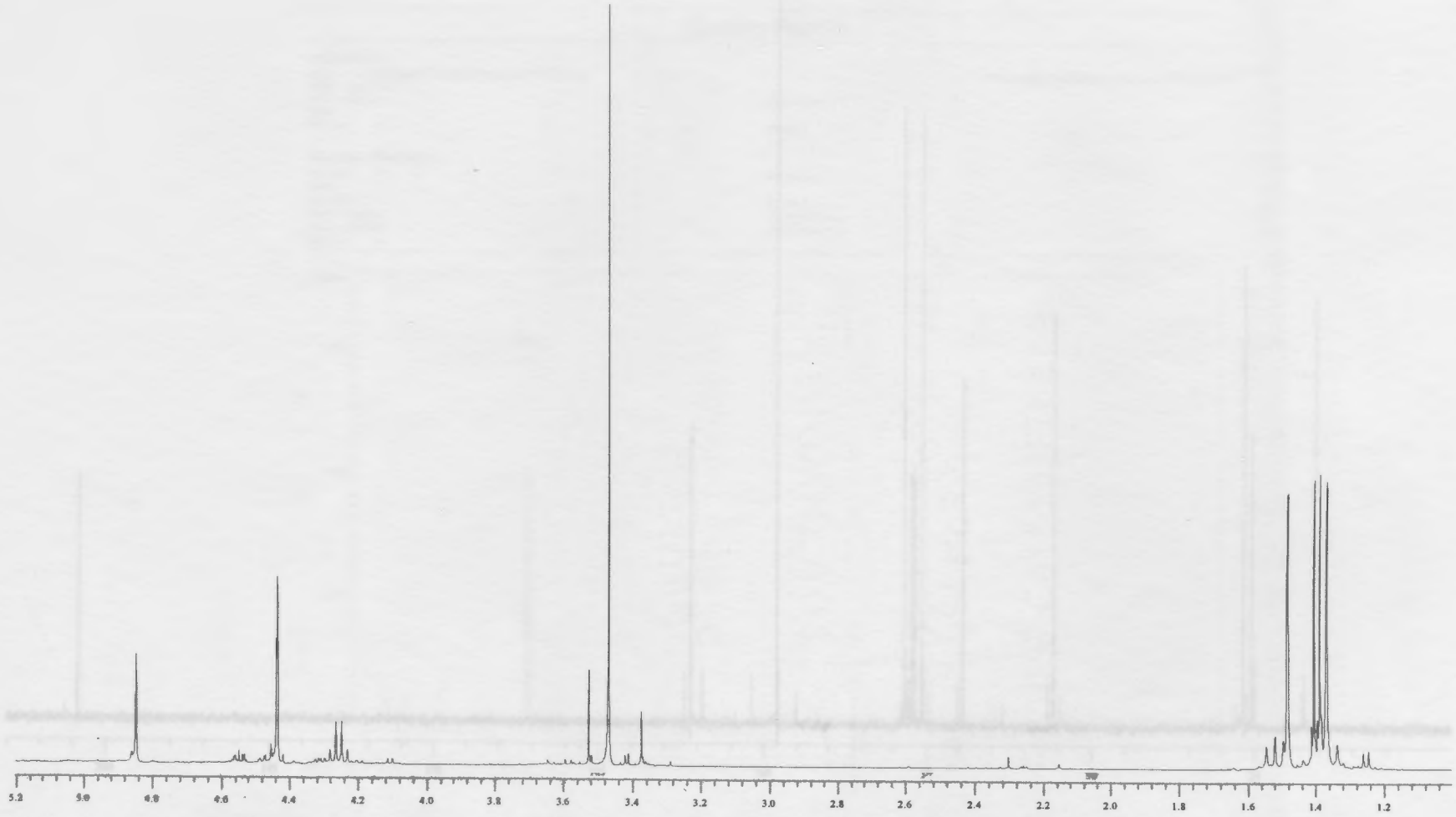

Figure 14: 400 MHz ^{1}H NMR spectrum of **11**

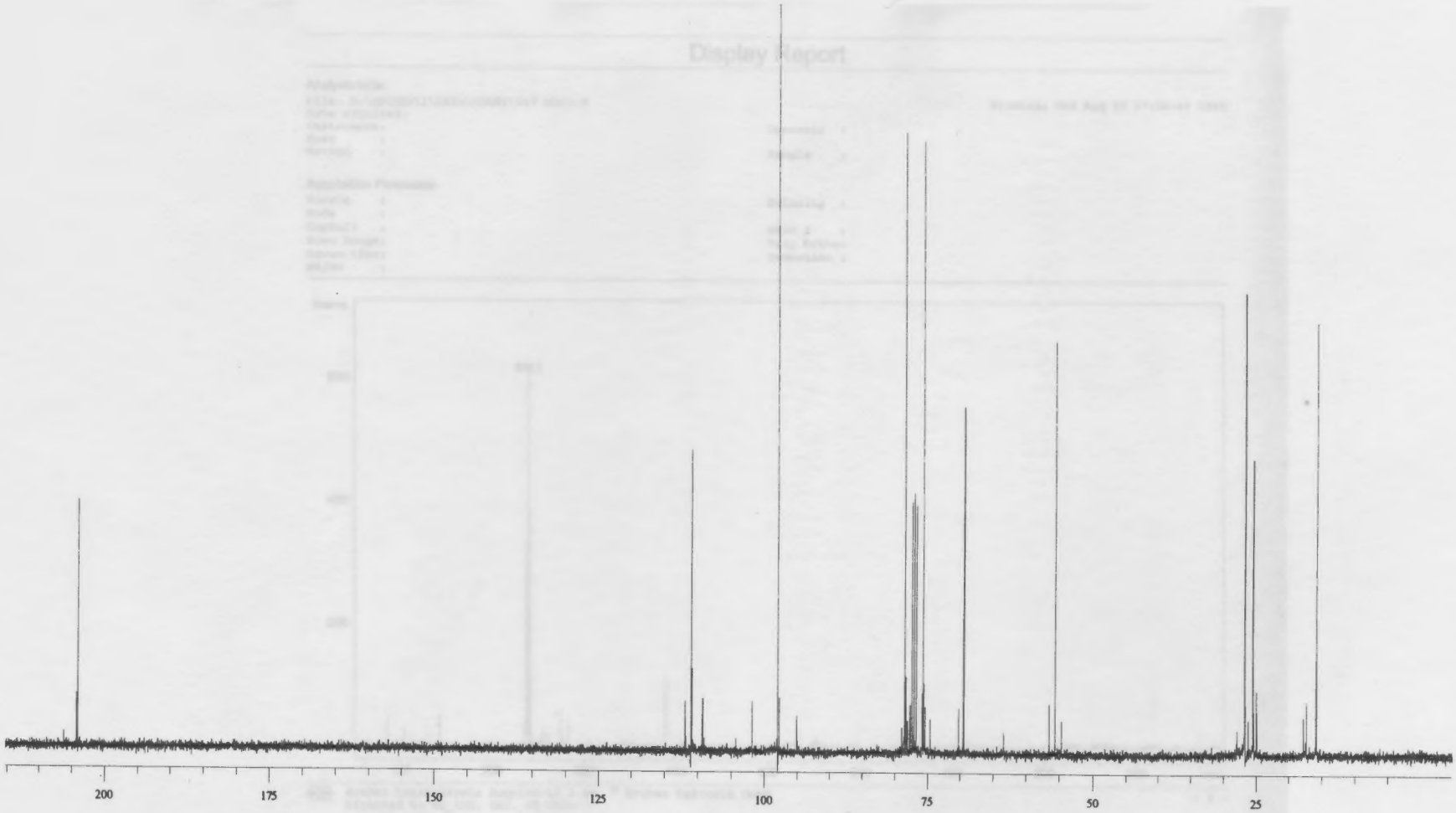

Figure 15: 100 MHz ^{13}C spectrum of **11**

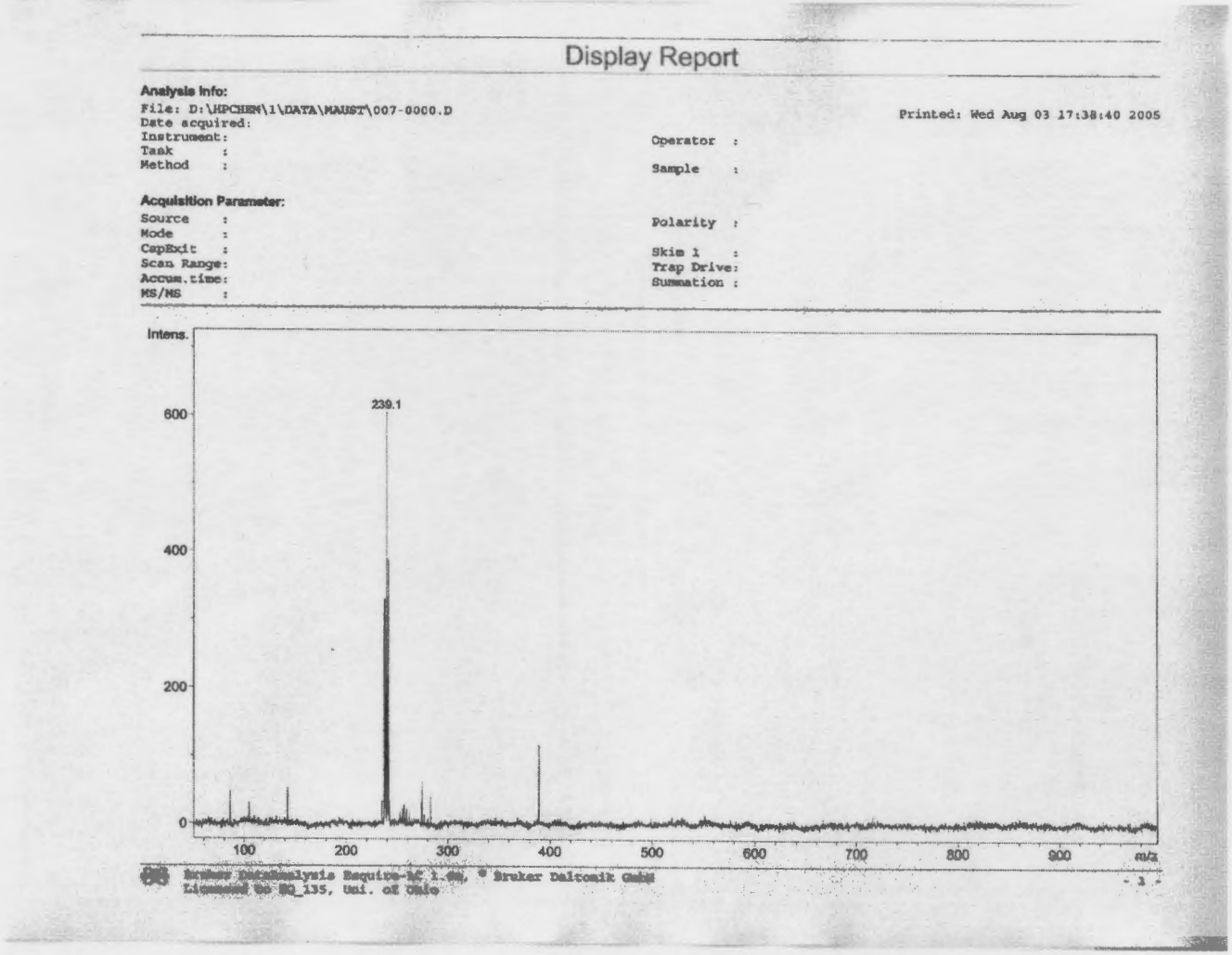

Figure 16: Mass spectrum of **11**

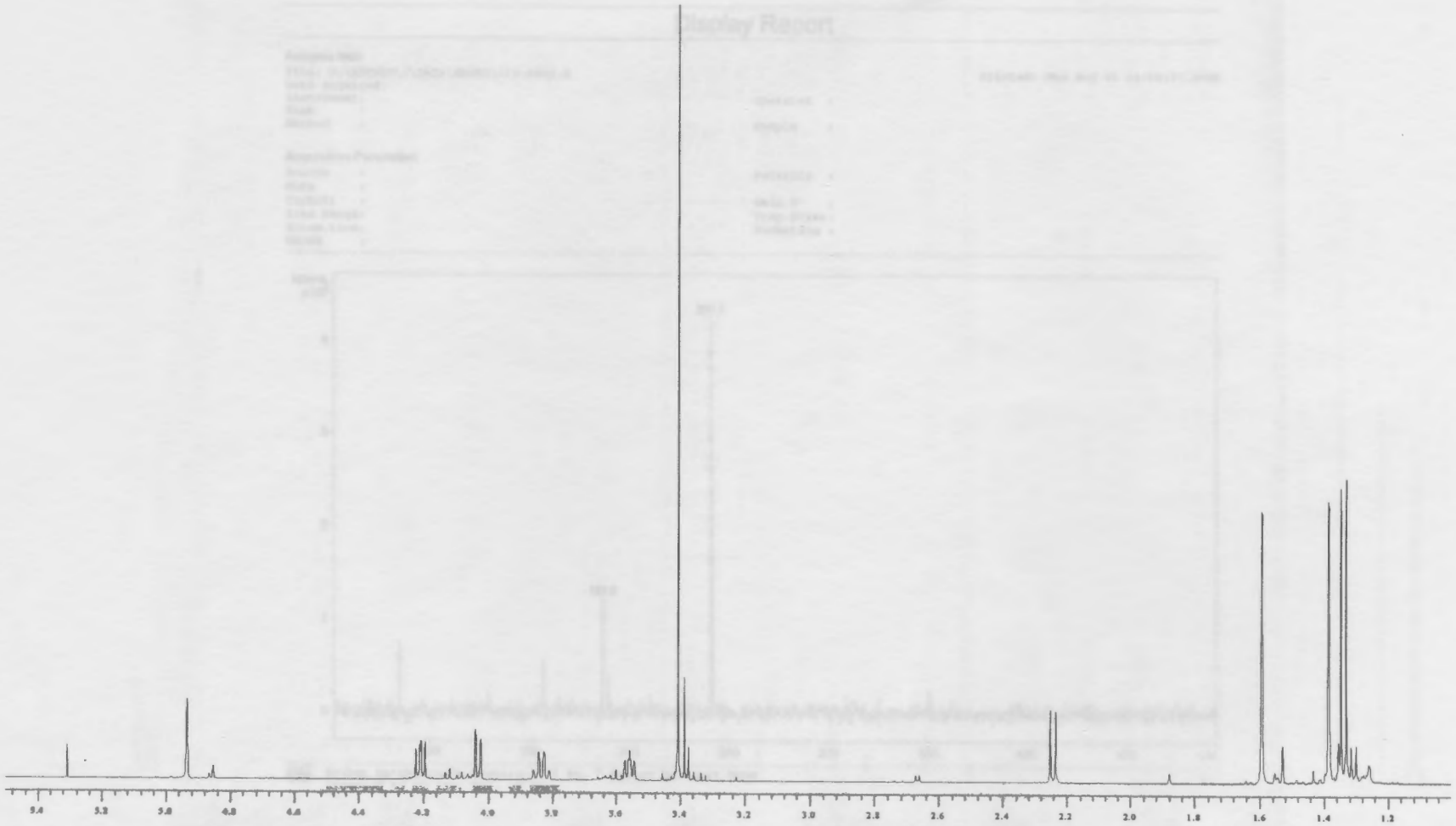

Figure 17: 400 MHz ^{1}H NMR spectrum of **12**

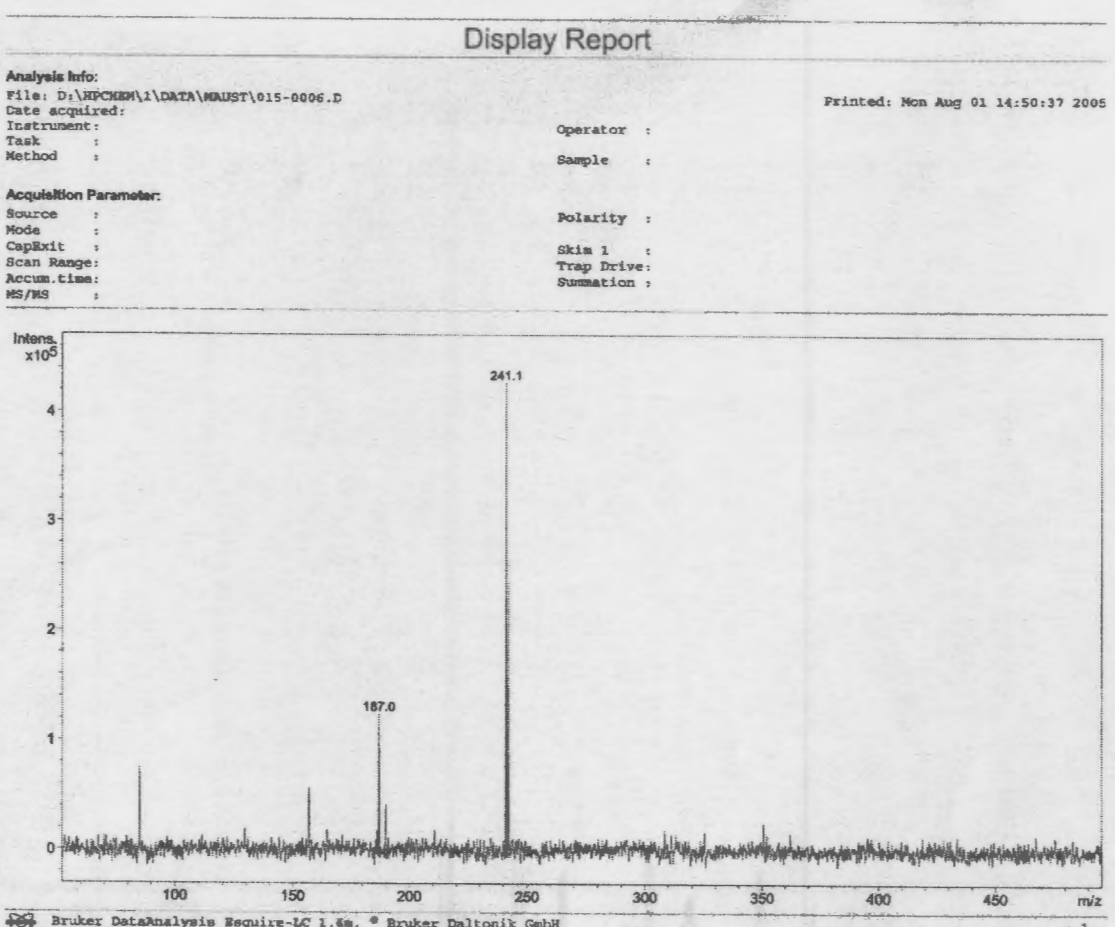

Figure 18: Mass spectrum of **12**

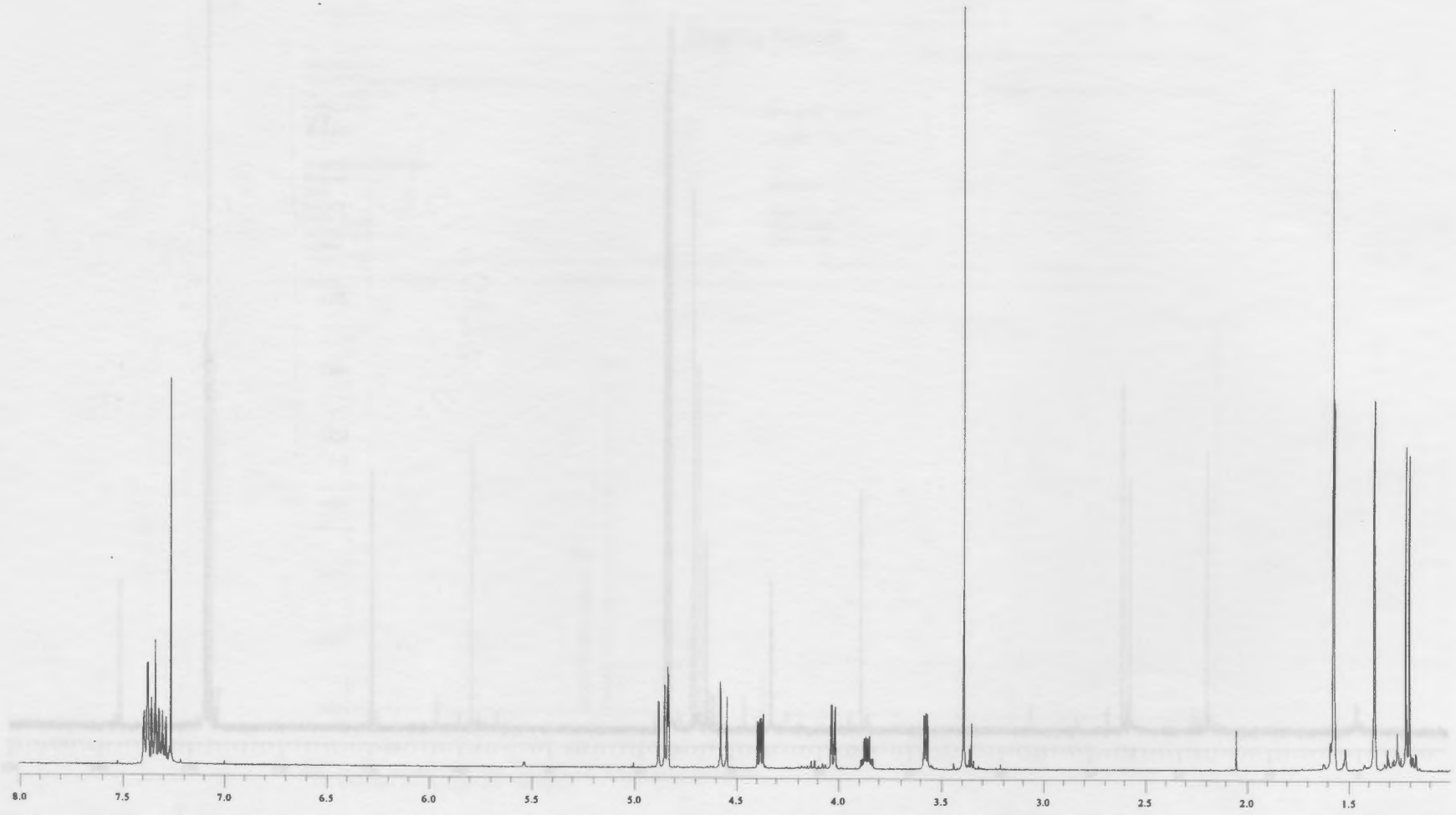

Figure 19: 400 MHz ^{1}H NMR spectrum of **13**

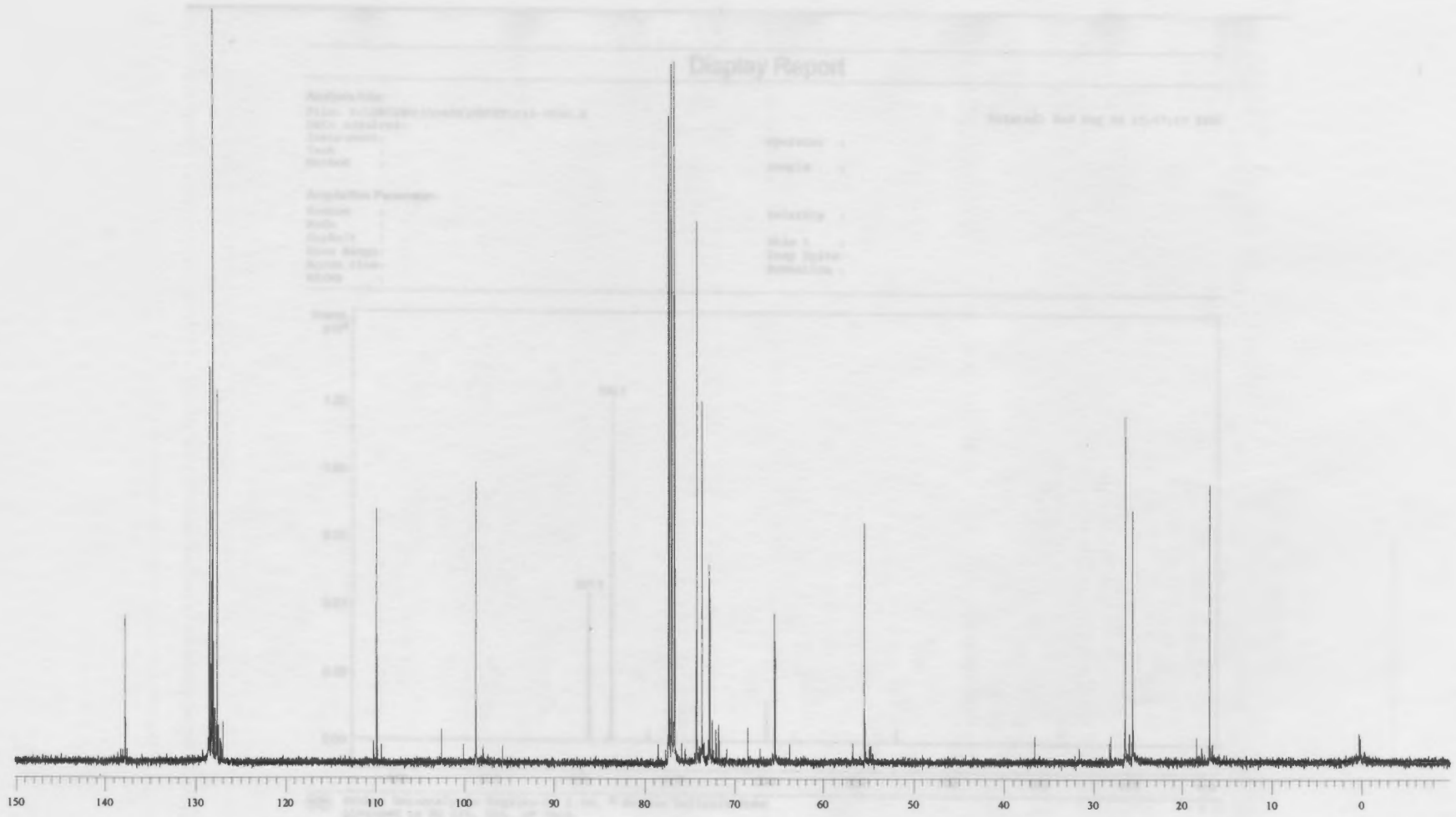

Figure 20: 100 MHz ^{13}C spectrum of **13**

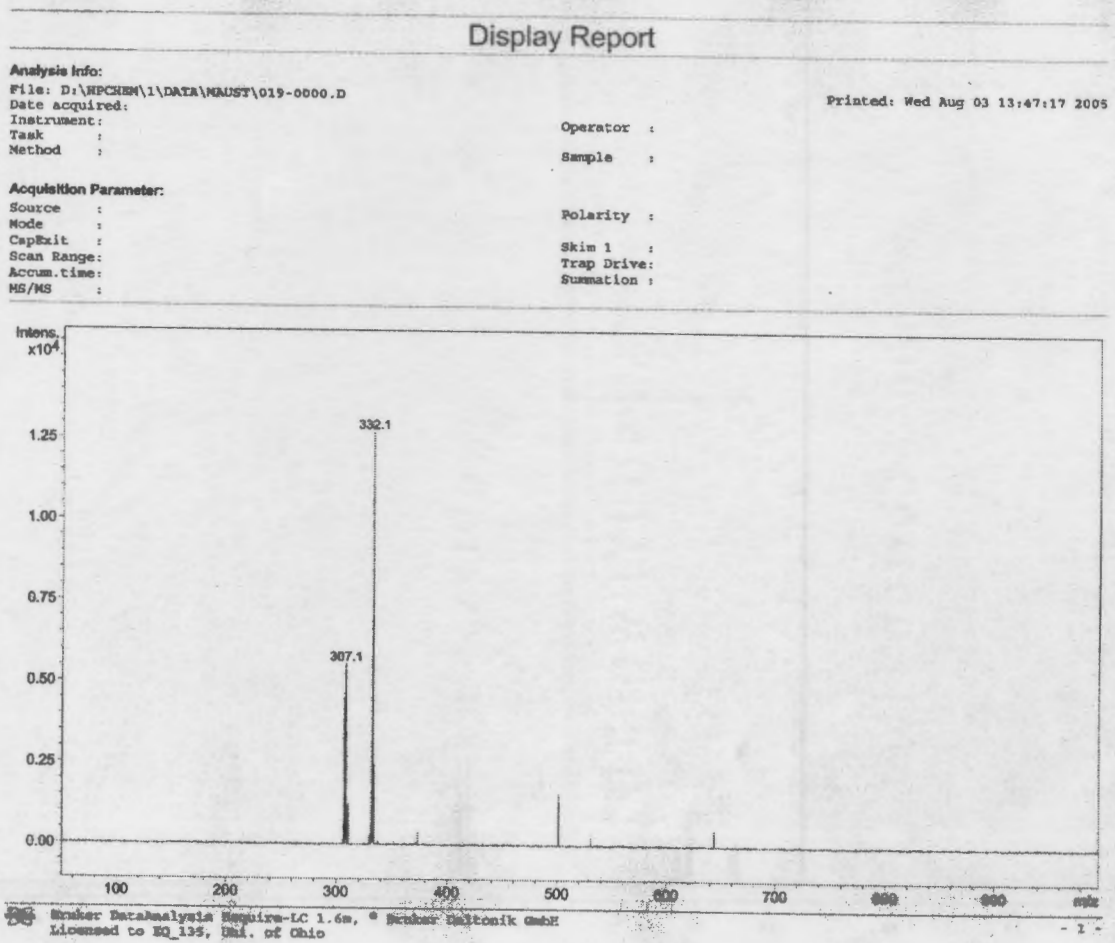

Figure 21: Mass spectrum of **13**

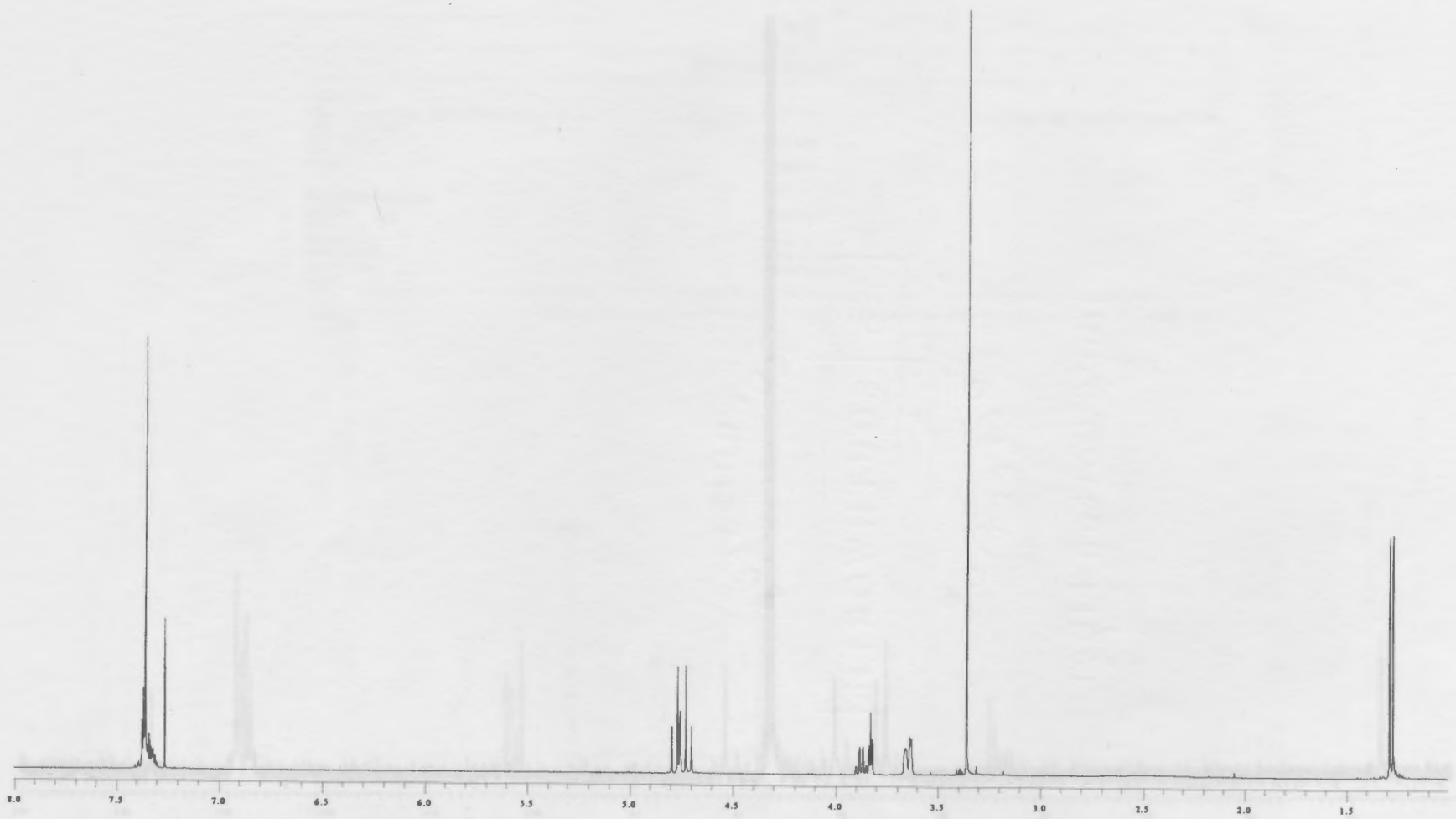

Figure 22: 400 MHz ^{1}H NMR spectrum of **14**

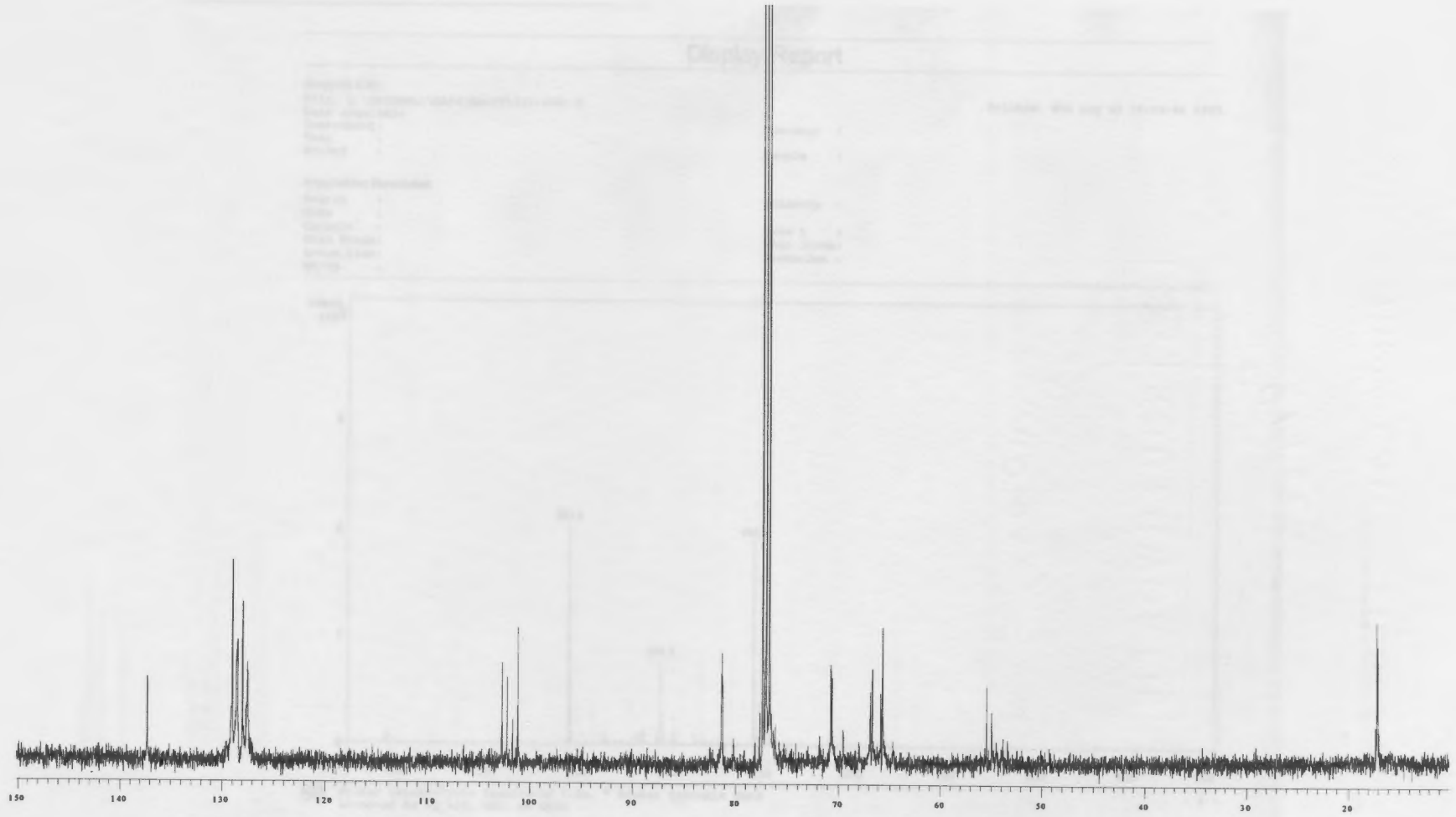

Figure 23: 100 MHz ^{13}C spectrum of **14**

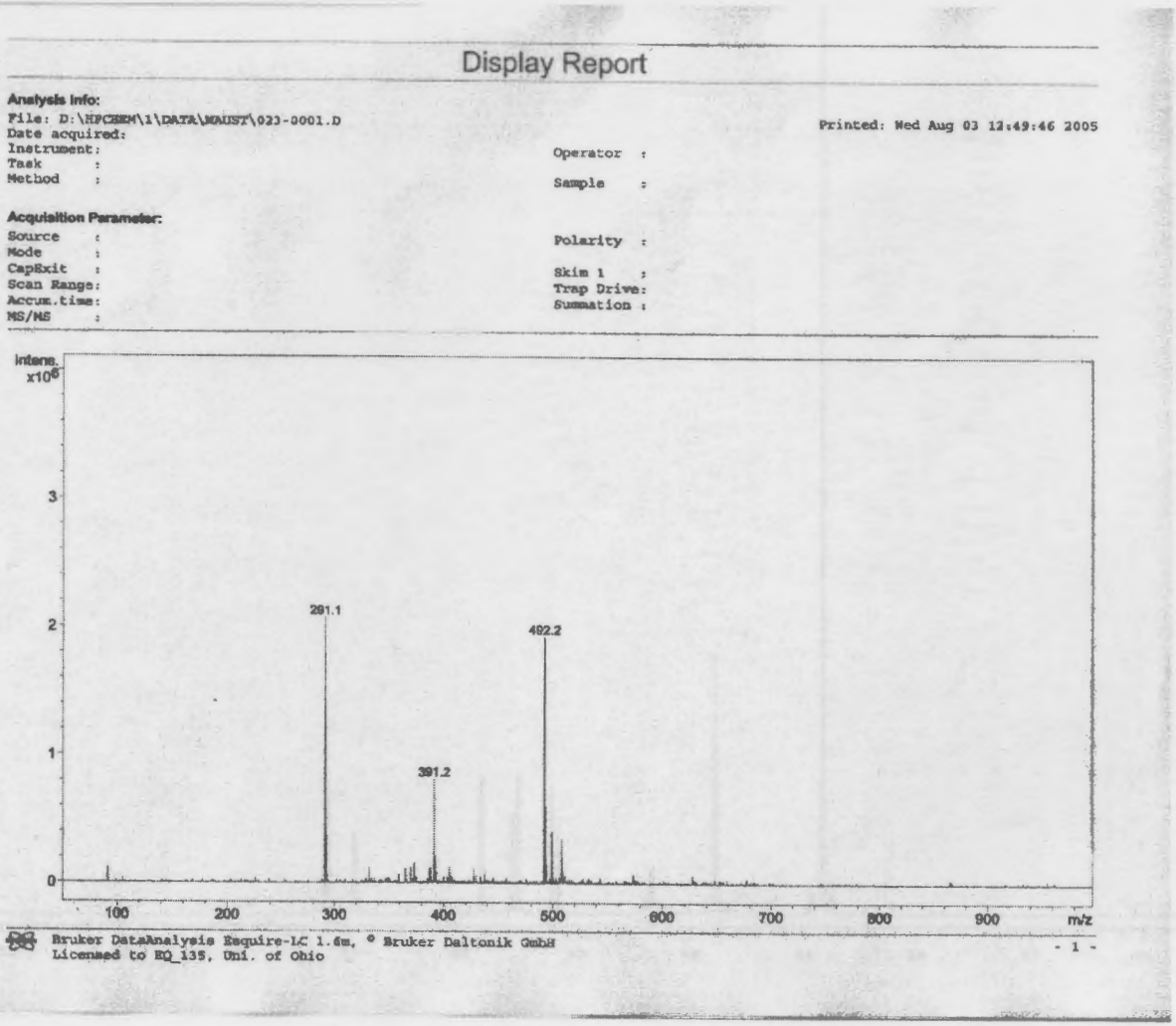

Figure 24: Mass spectrum of **14**

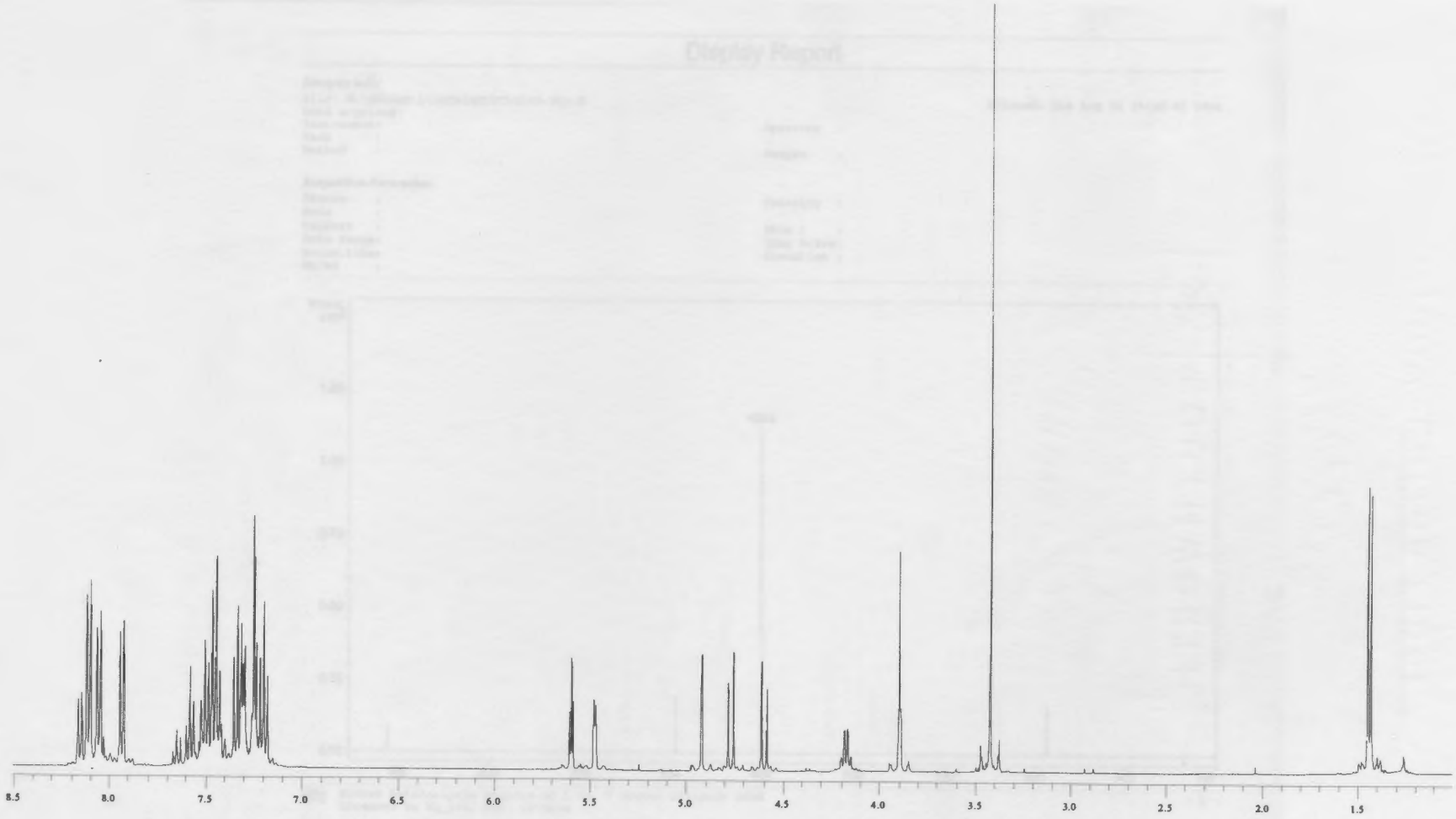

Figure 25: 400 MHz ^{1}H spectrum of **15**

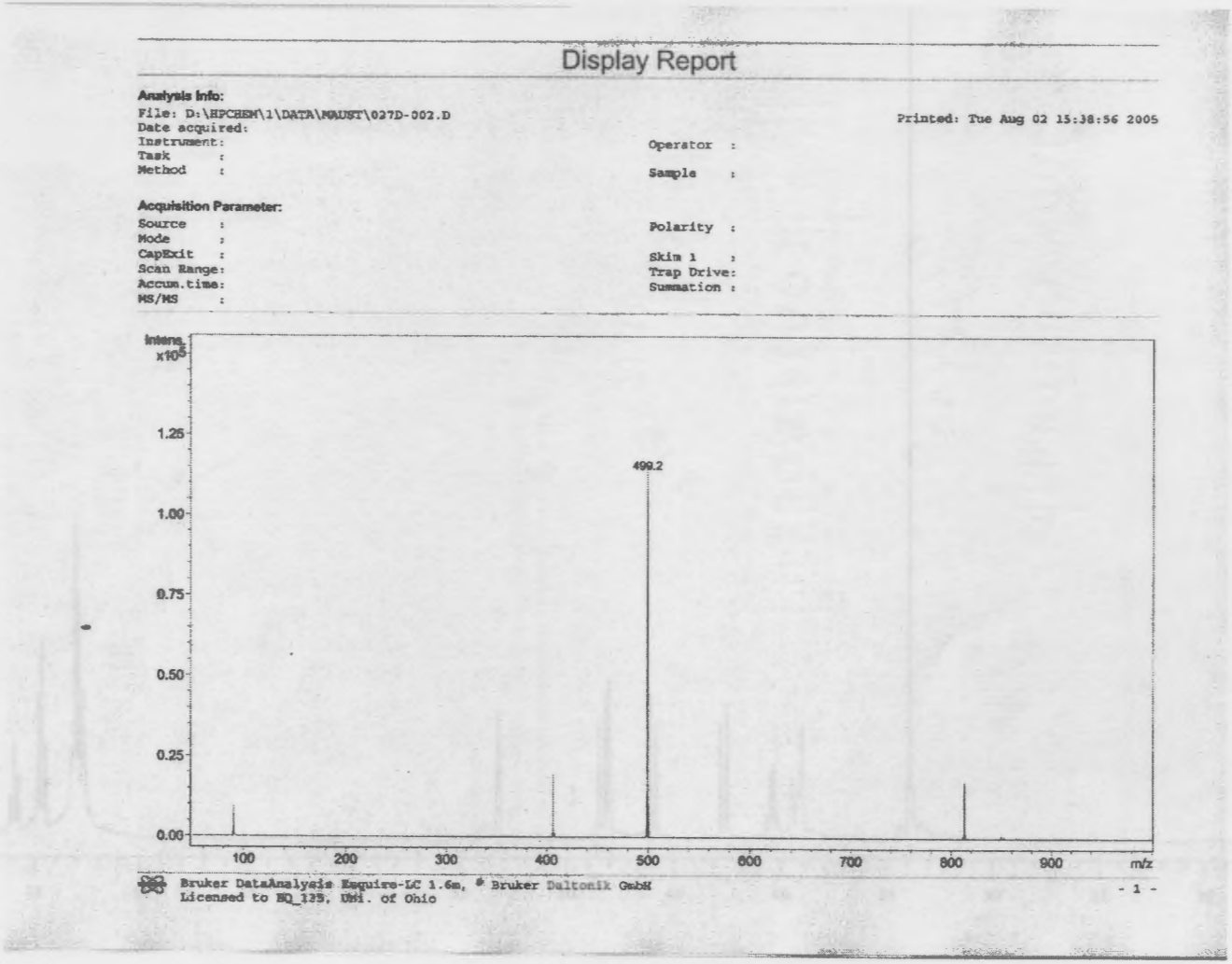

Figure 26: Mass spectrum of **15**

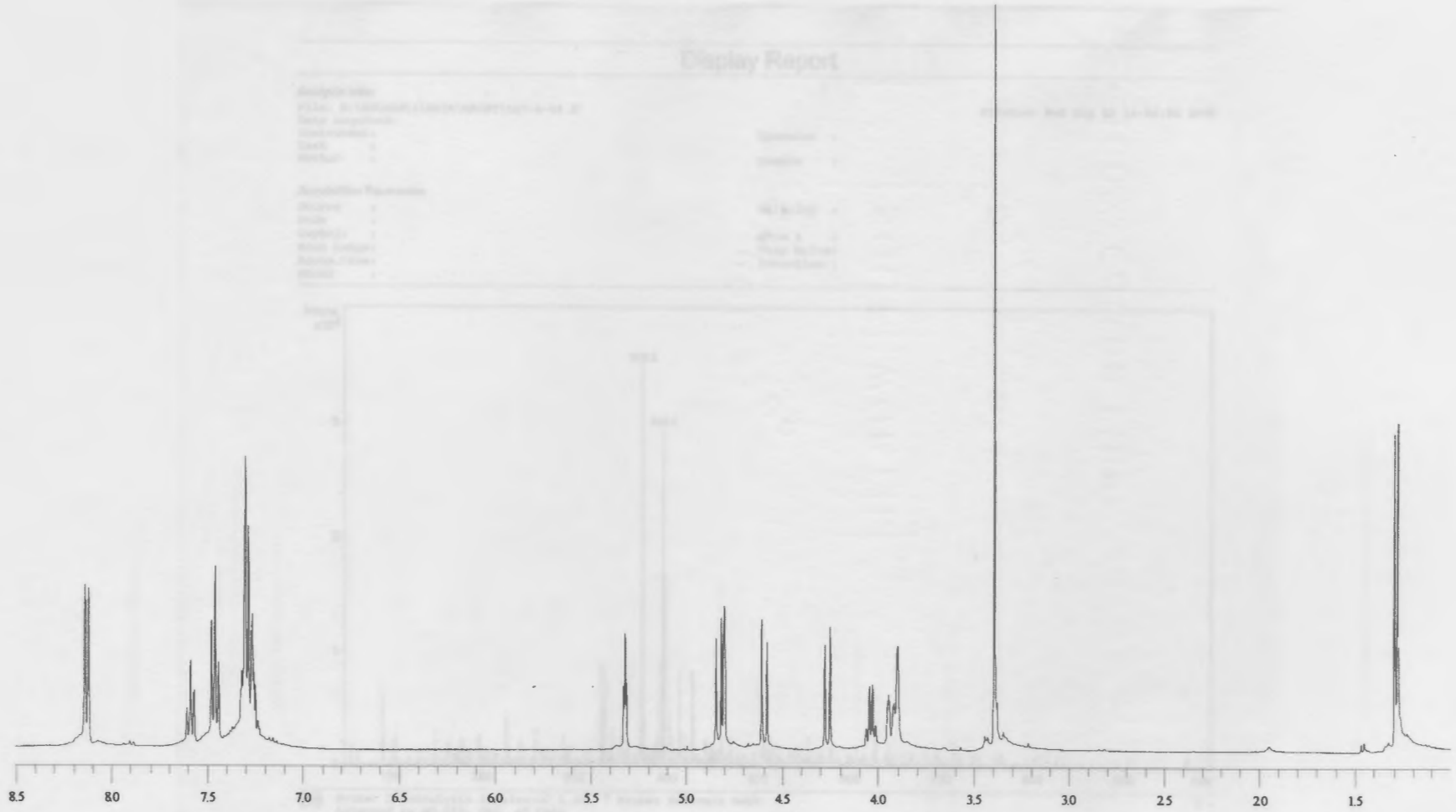

Figure 27: 400 MHz ^{1}H spectrum of **16**

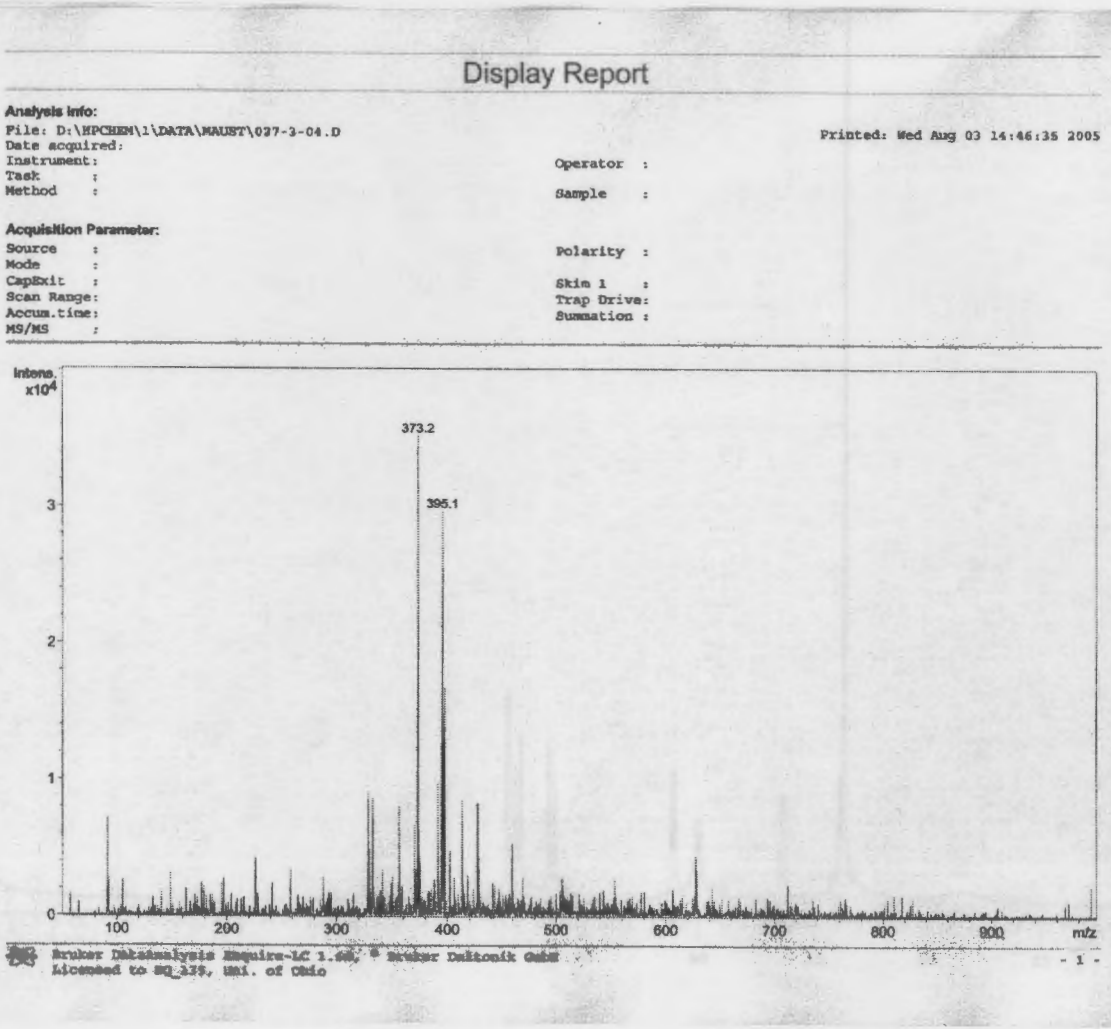

Figure 28: Mass spectrum of **16**

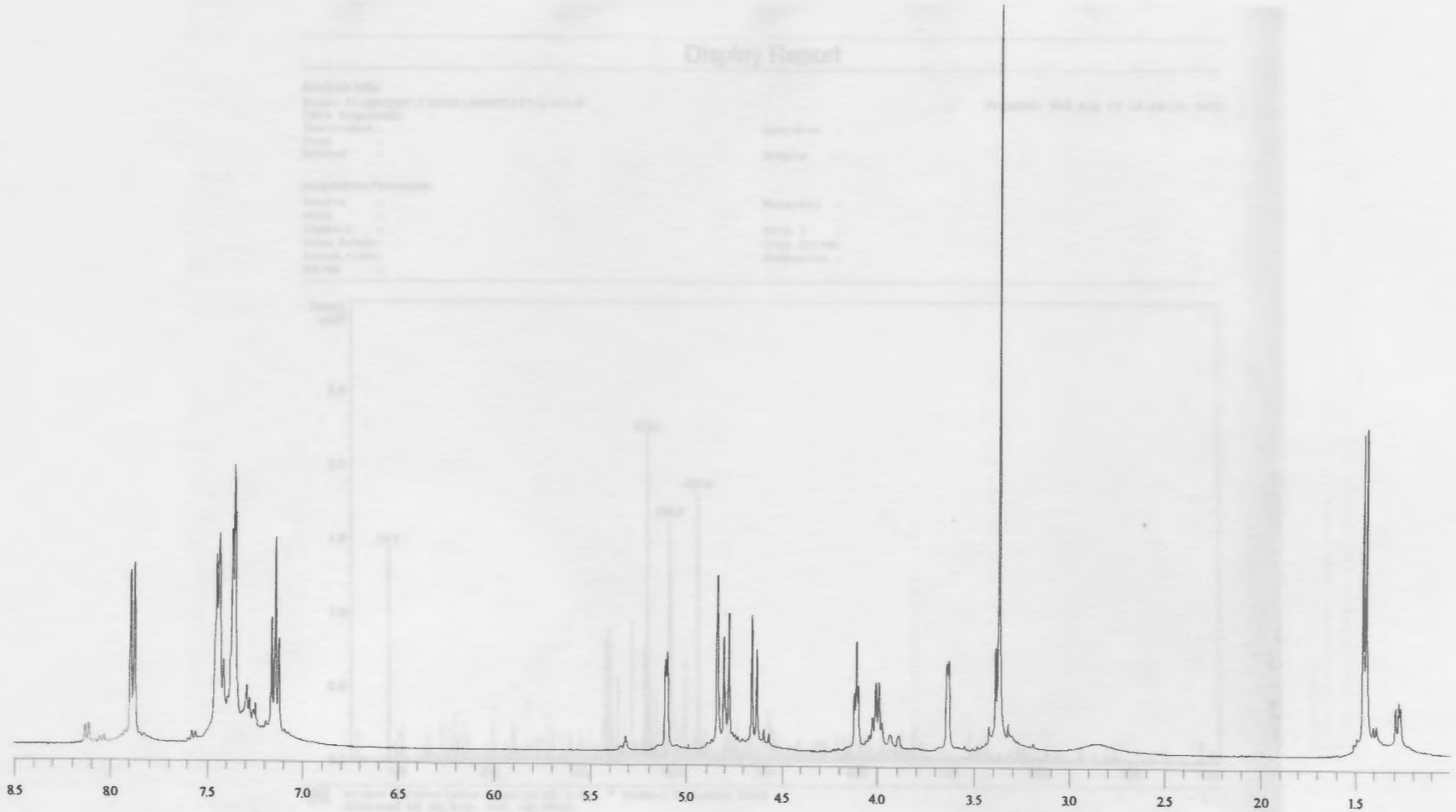

Figure 29: 400 MHz ^{1}H spectrum of **17**

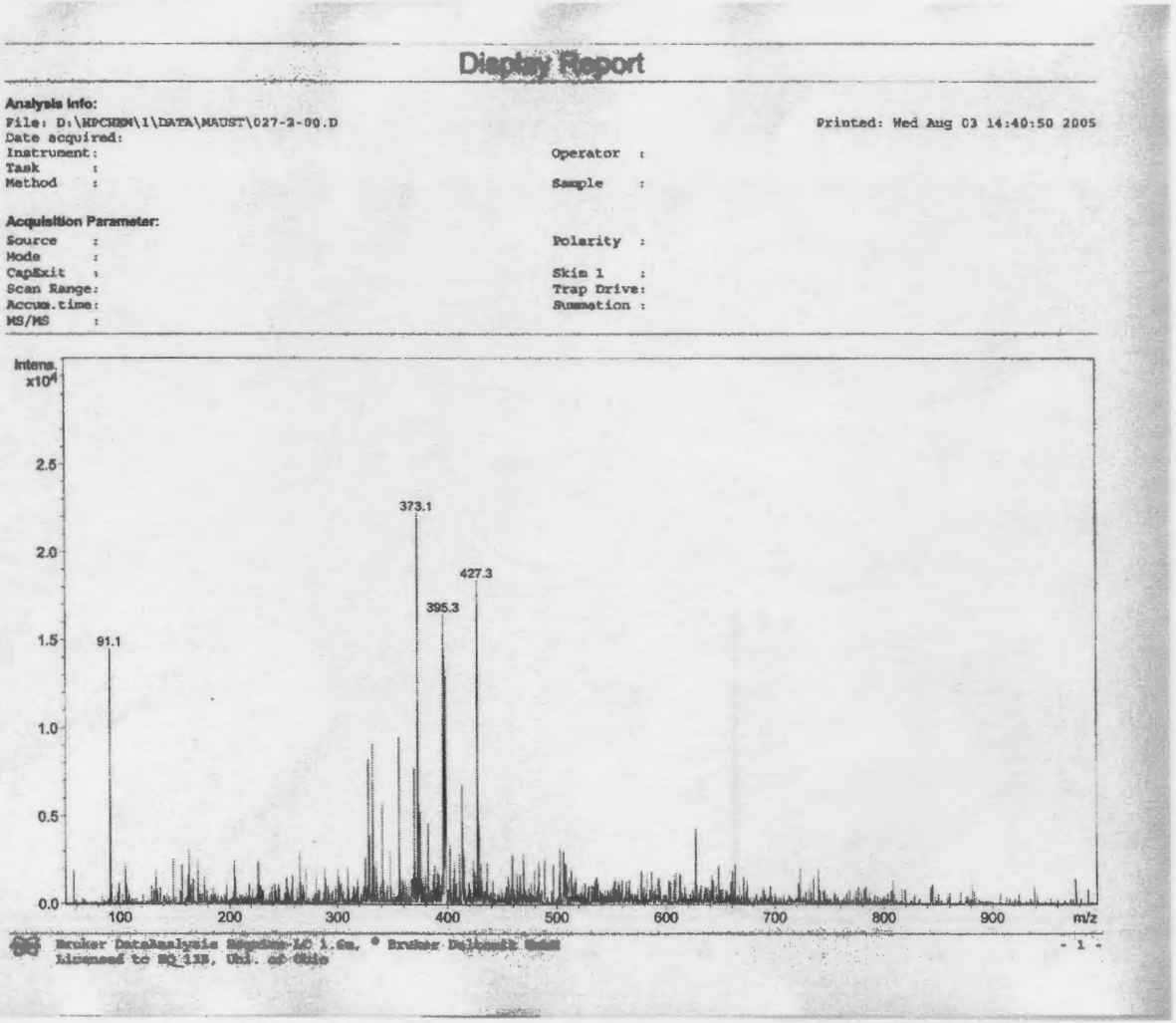

Figure 30: Mass spectrum of **17**

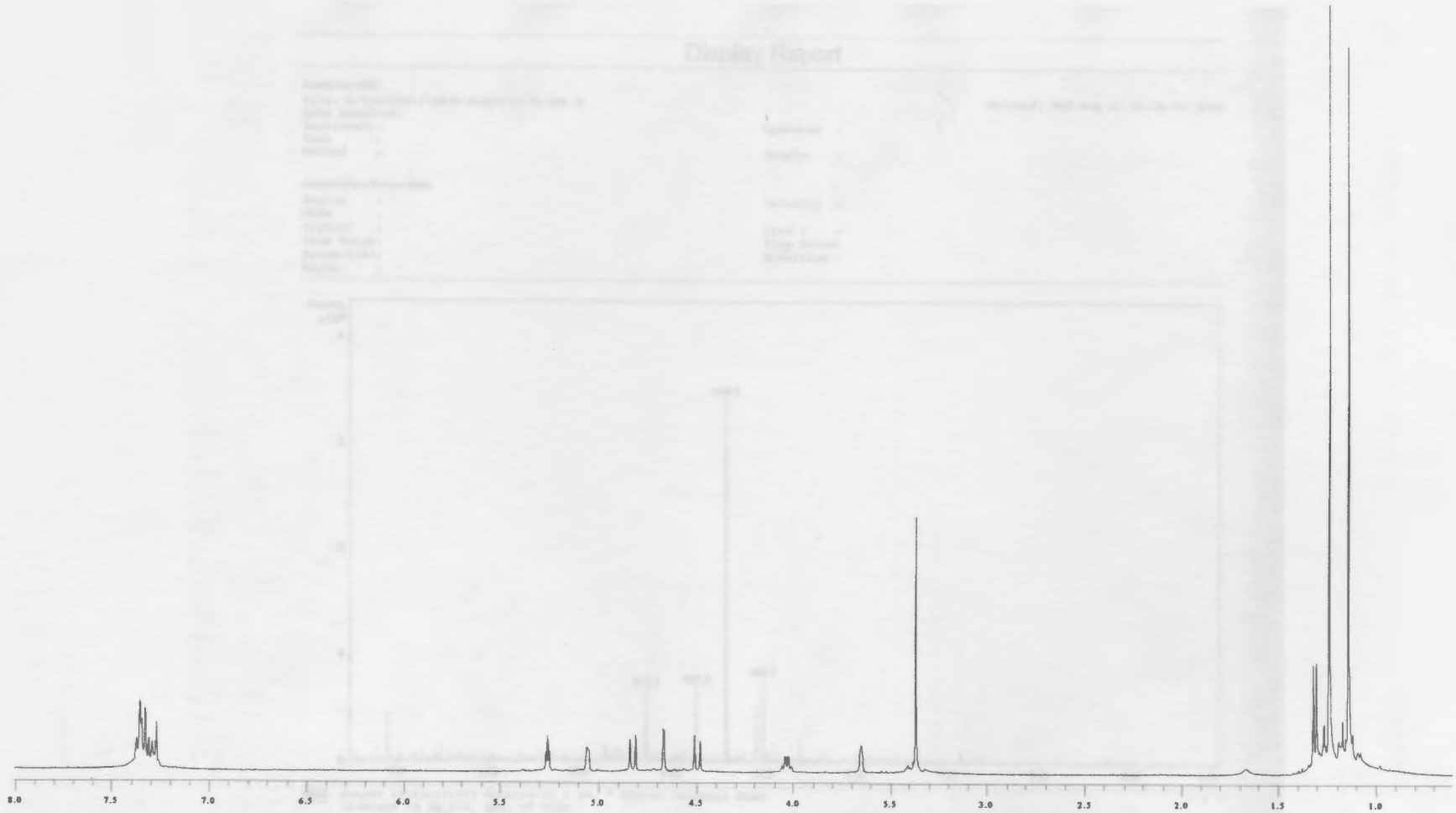

Figure 31: 400 MHz ^{1}H spectrum of **18**

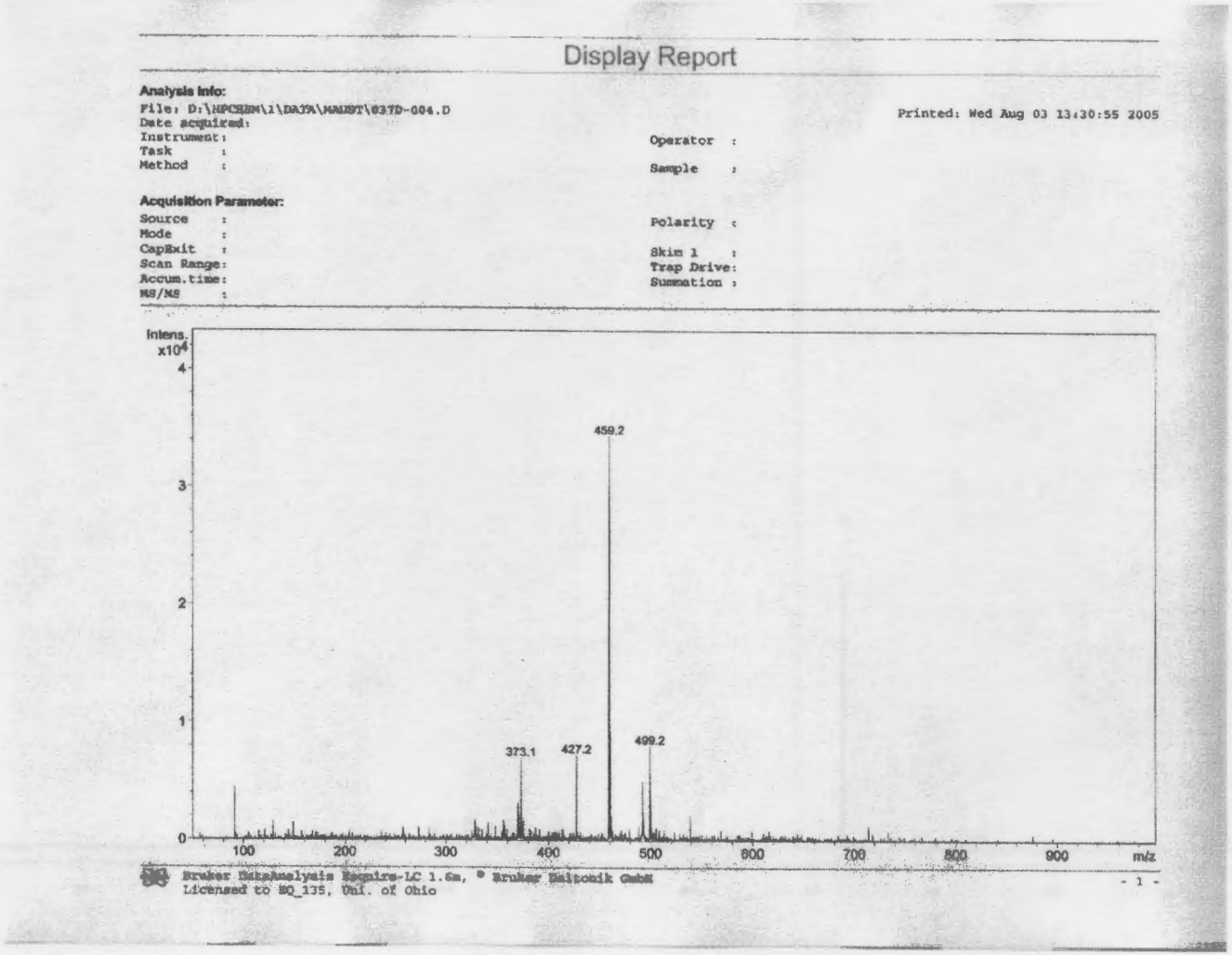

Figure 32: Mass spectrum of **18**

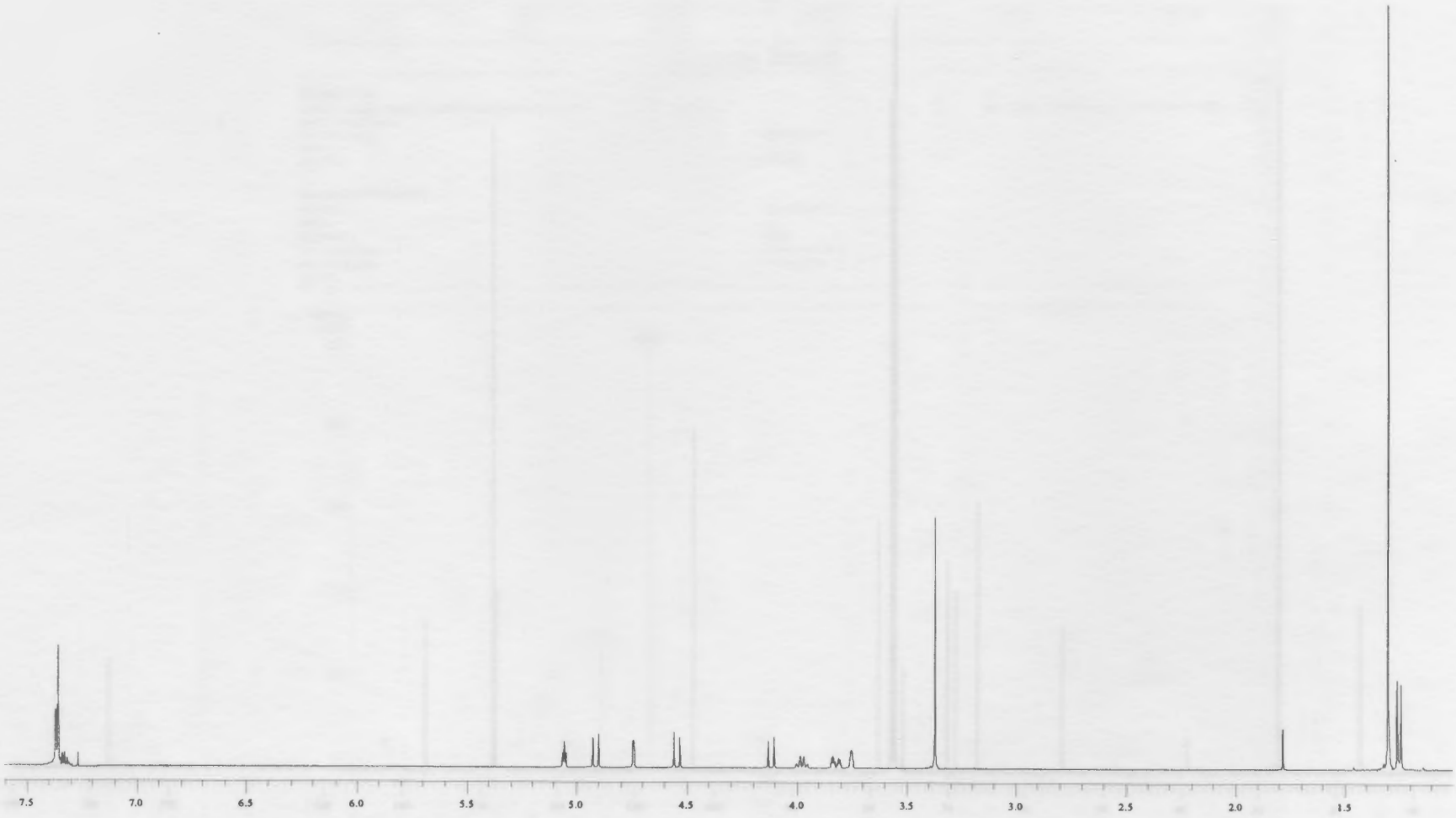

Figure 33: 400 MHz ^{1}H spectrum of **19**

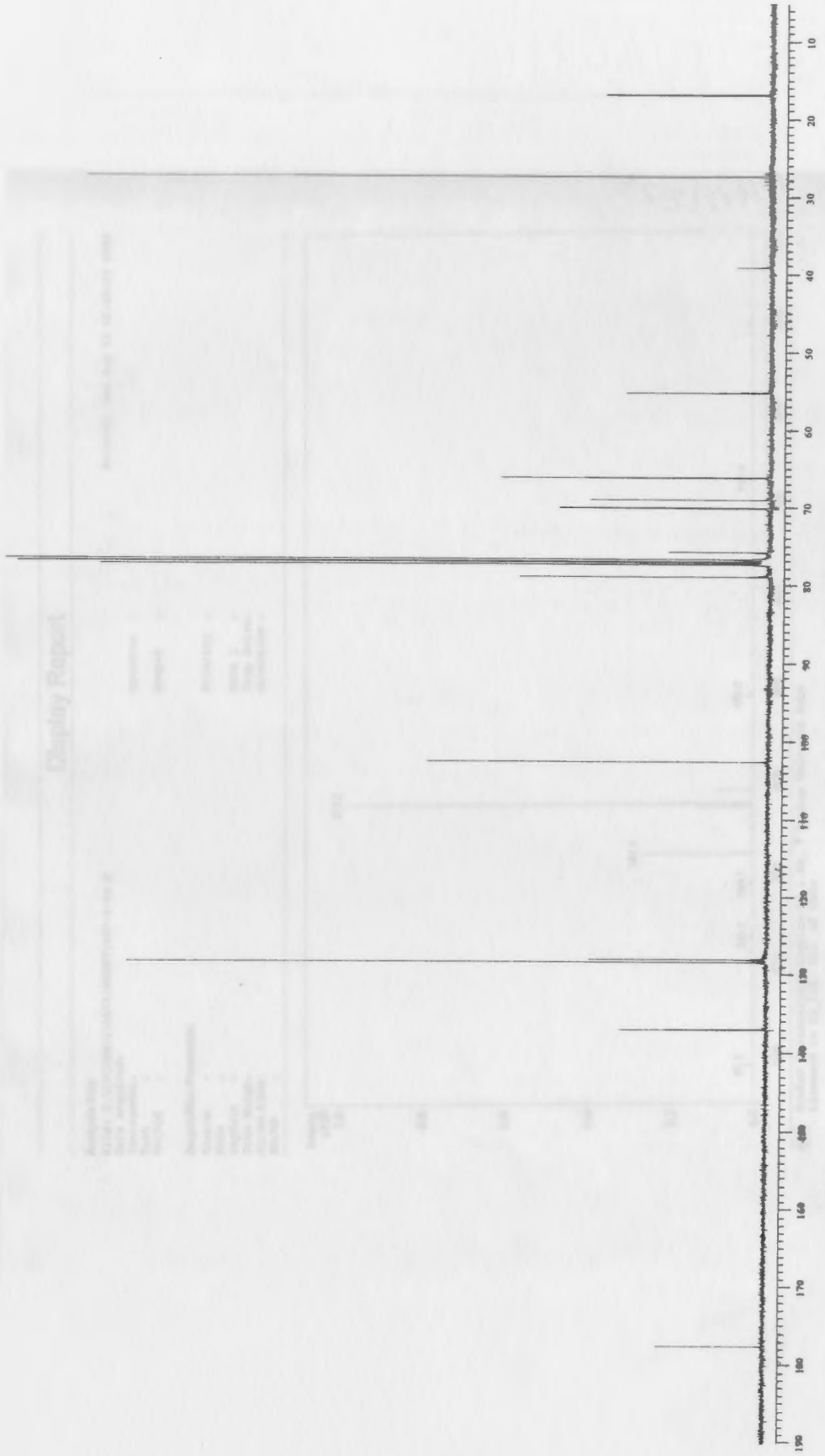

Figure 34: 100 MHz ^{13}C spectrum of **19**

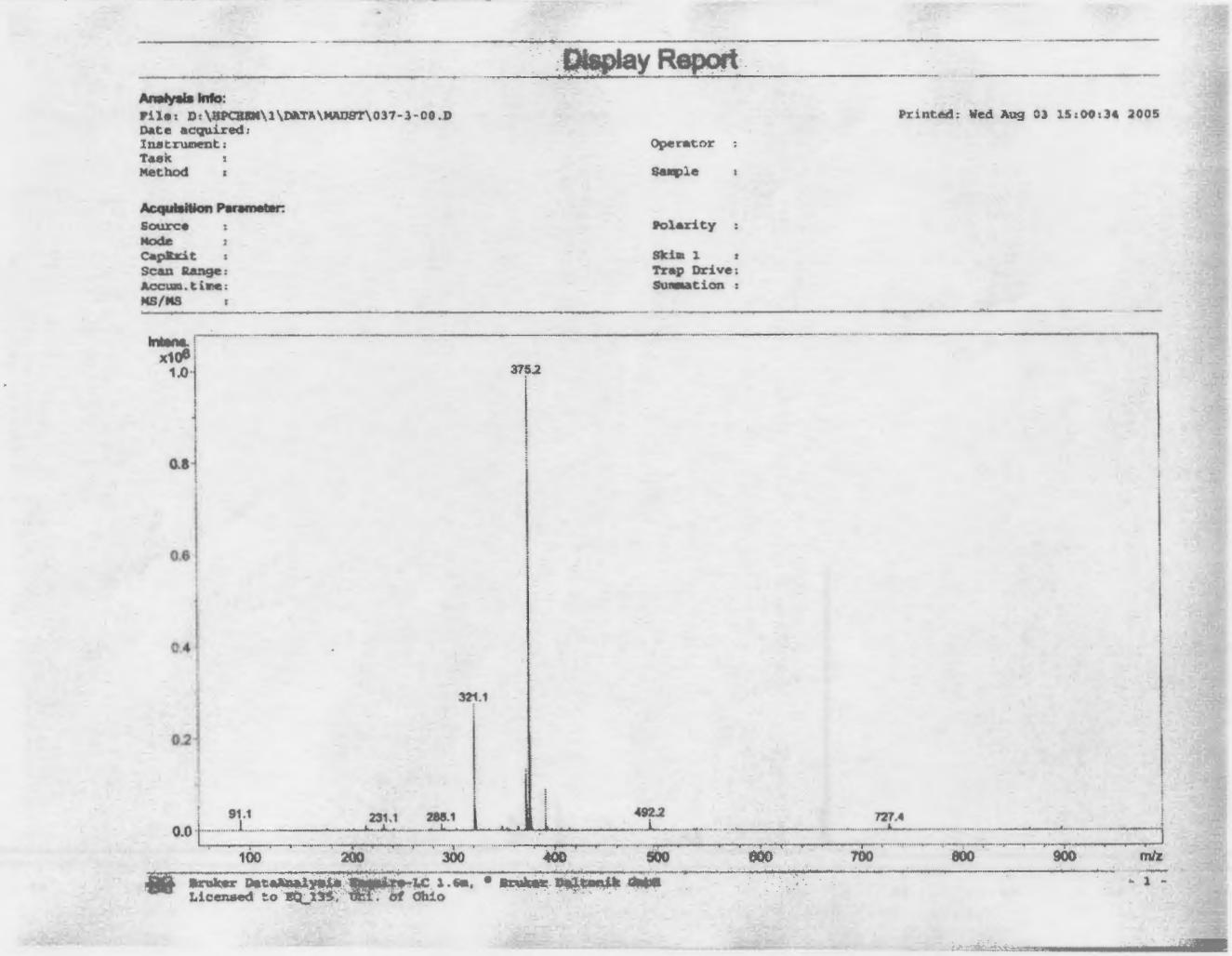

Figure 35: Mass spectrum of **19**

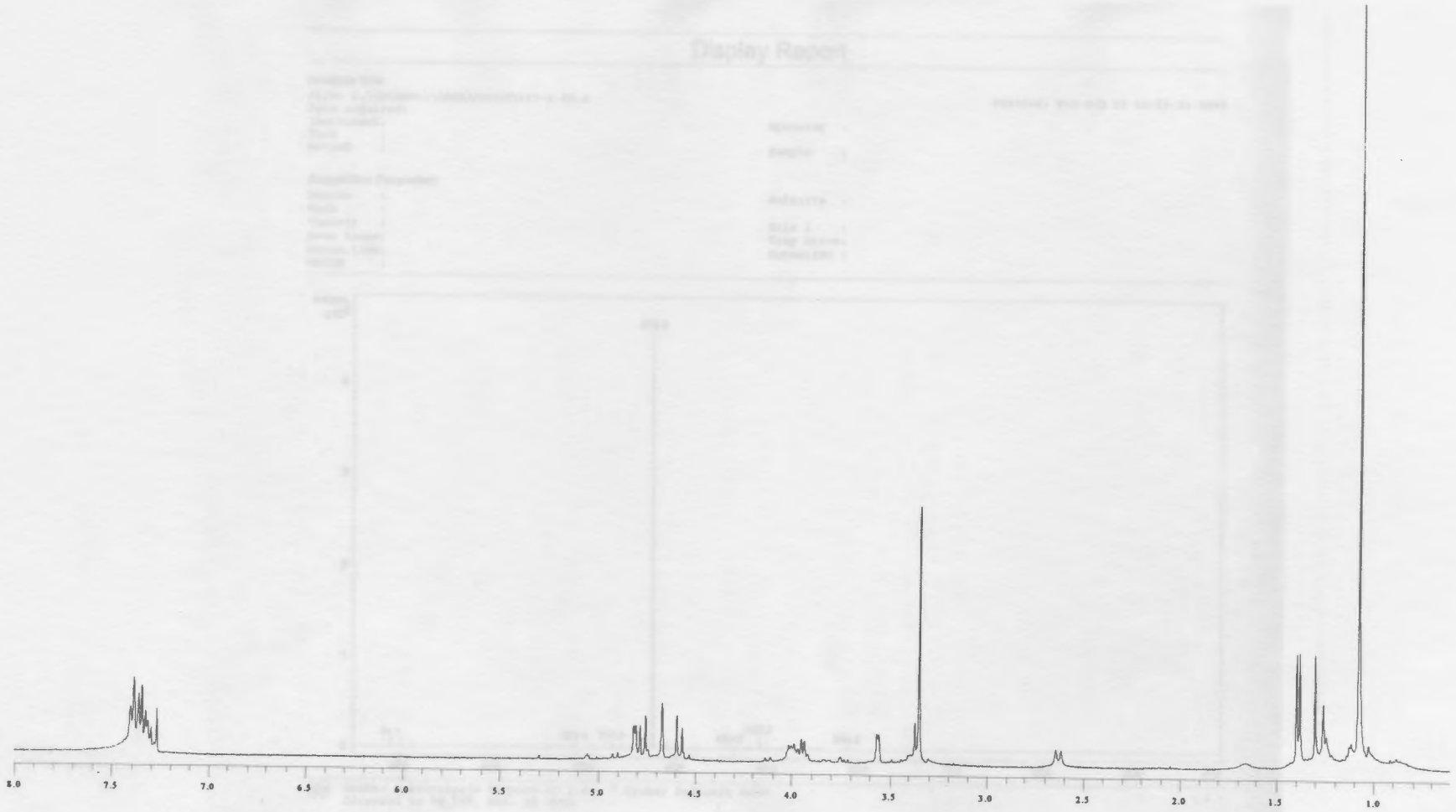

Figure 36: 400 MHz ^{1}H spectrum of **20**

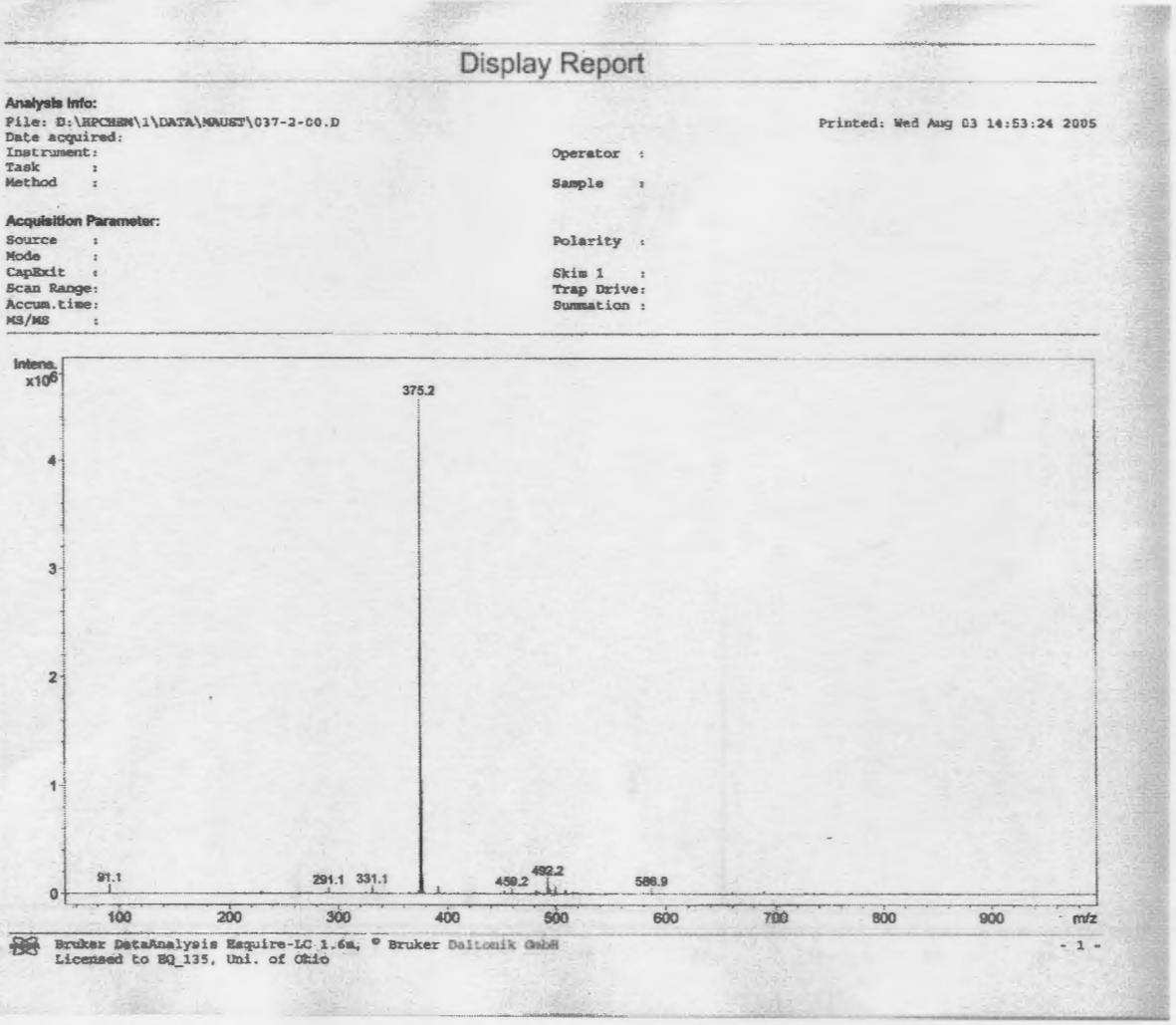

Figure 37: Mass spectrum of **20**

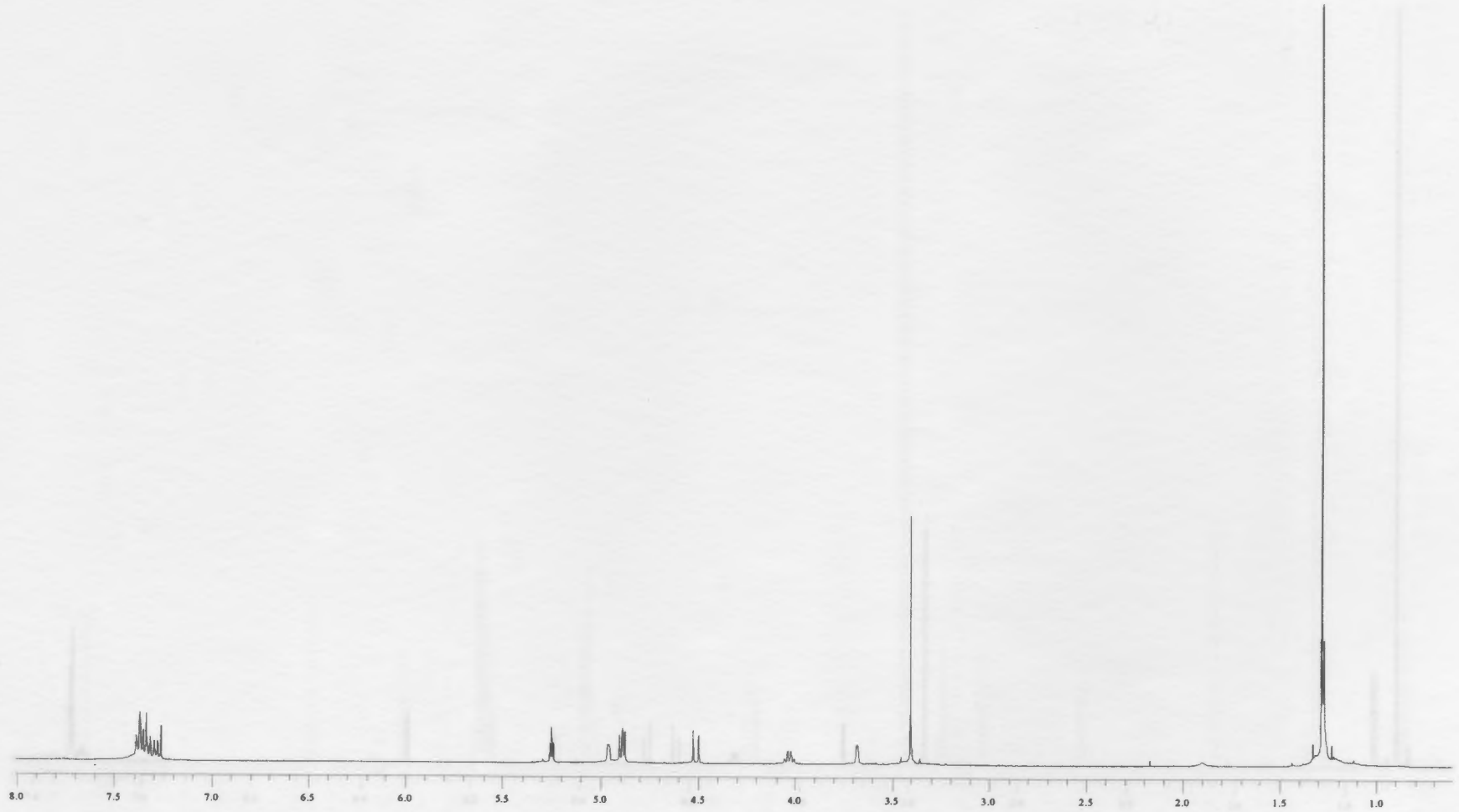

Figure 38: 400 MHz ^{1}H spectrum of **21**

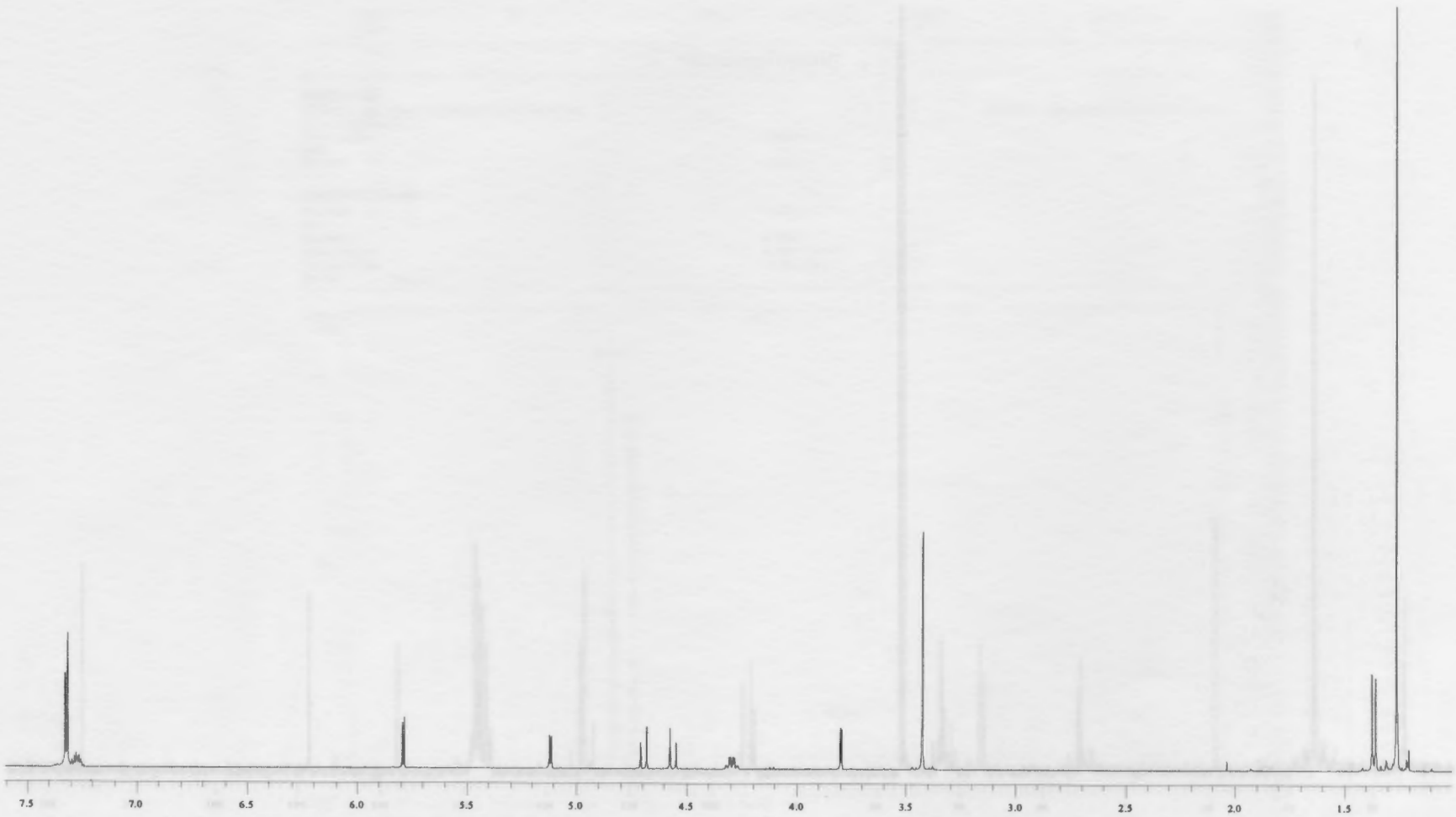

Figure 39: 400 MHz ^{1}H spectrum of **22**

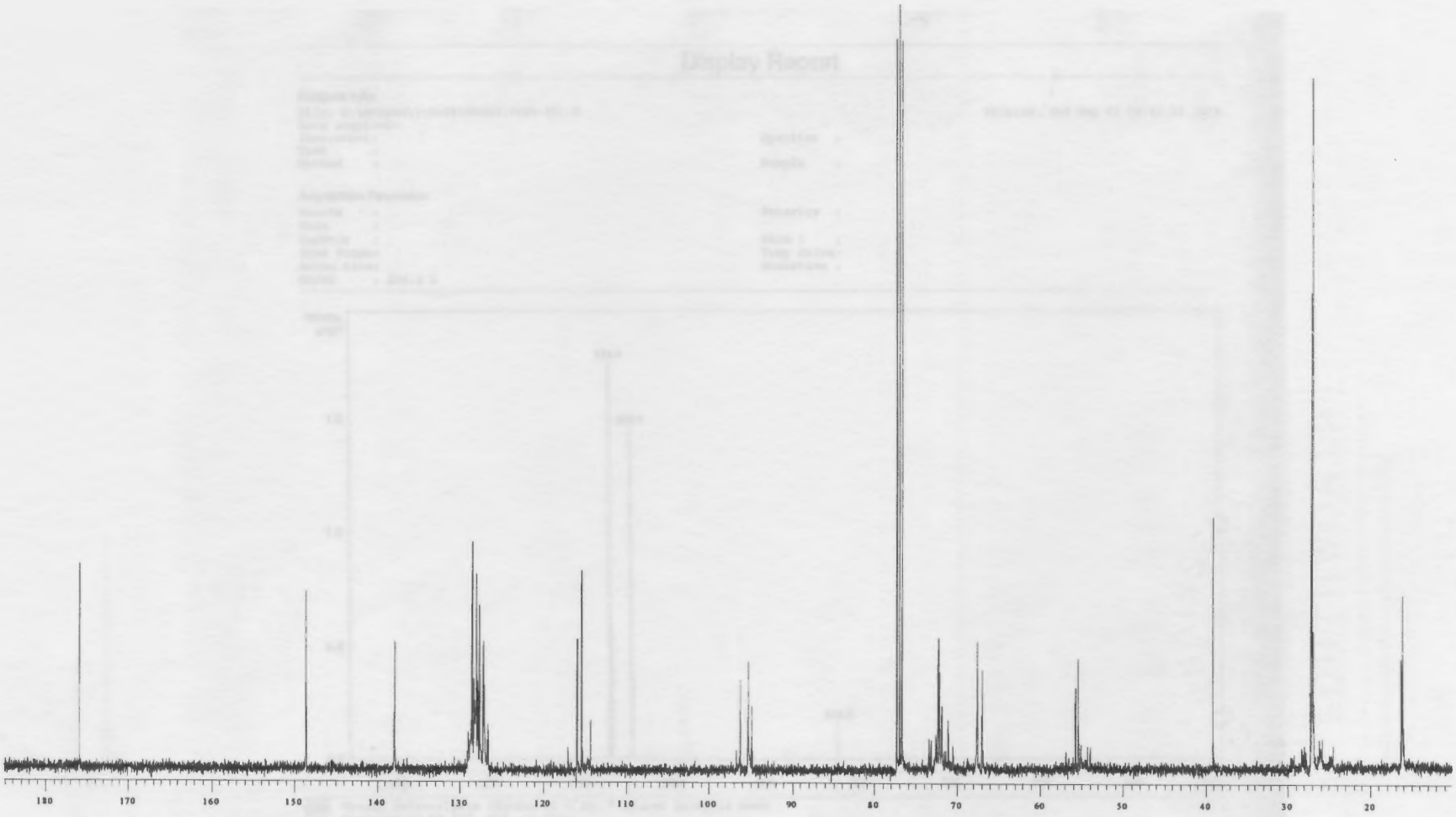

Figure 40: 100 MHz ^{13}C spectrum of **22**

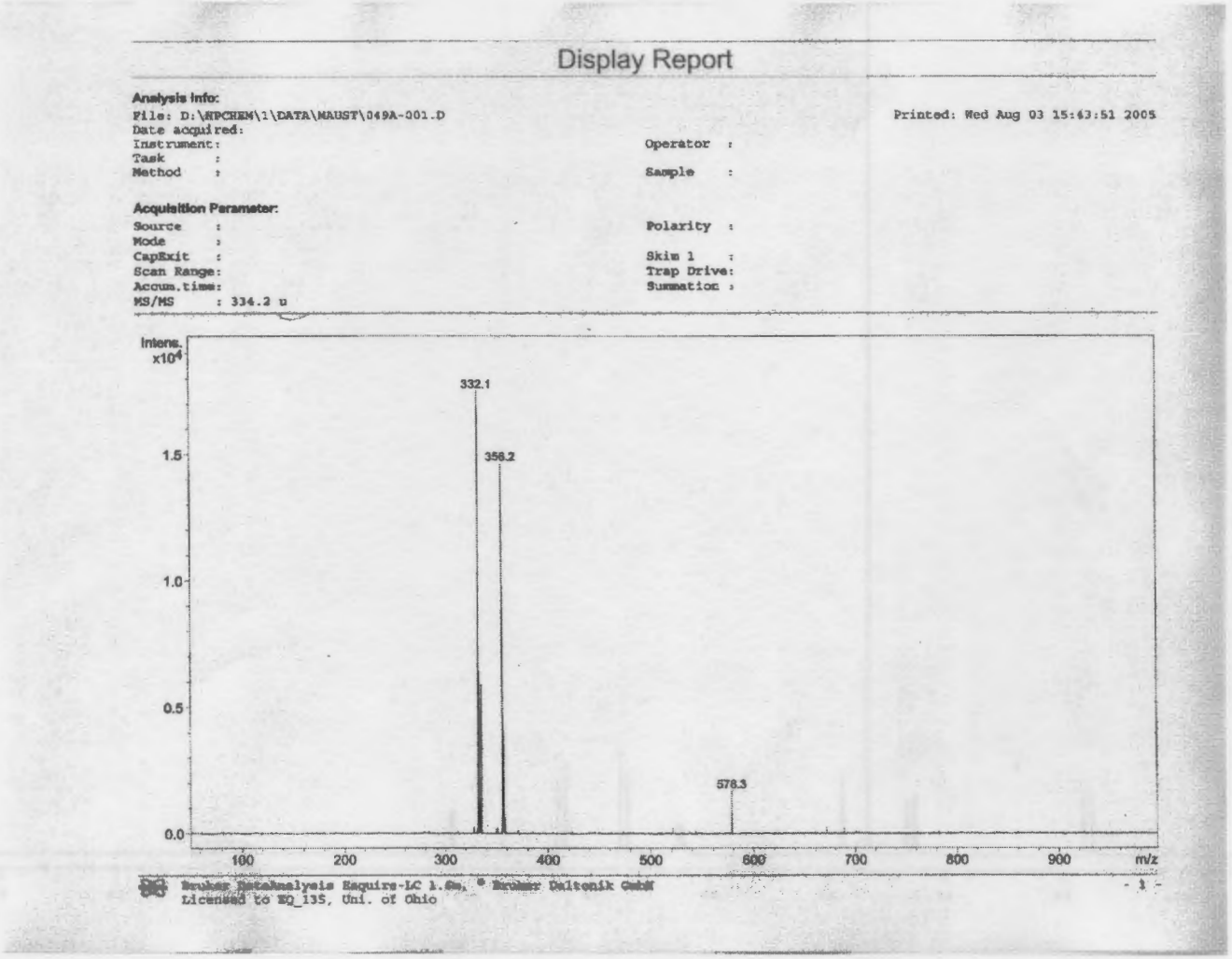

Figure 41: Mass spectrum of **22**

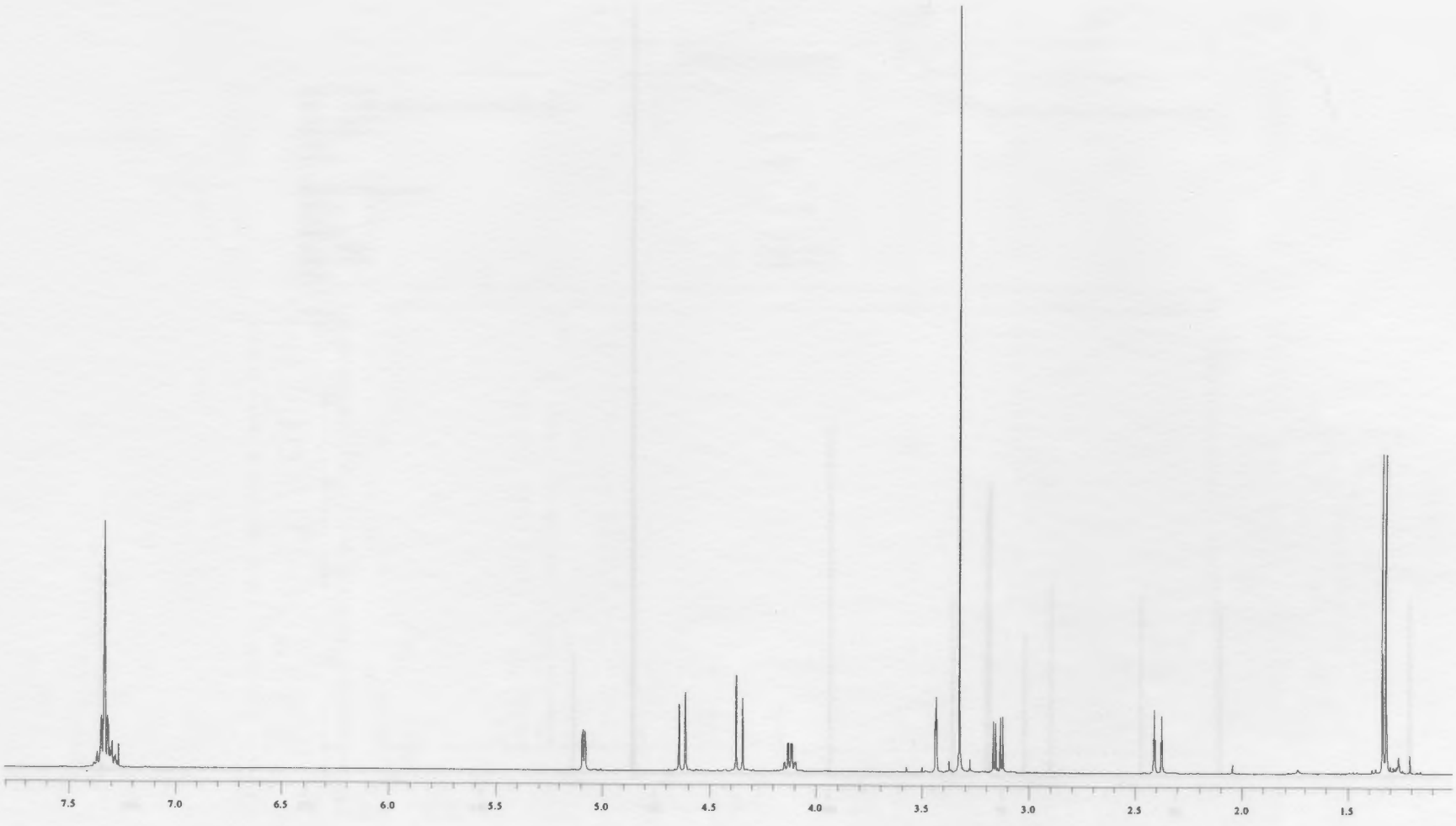

Figure 42: 400 MHz ^{1}H spectrum of **24**

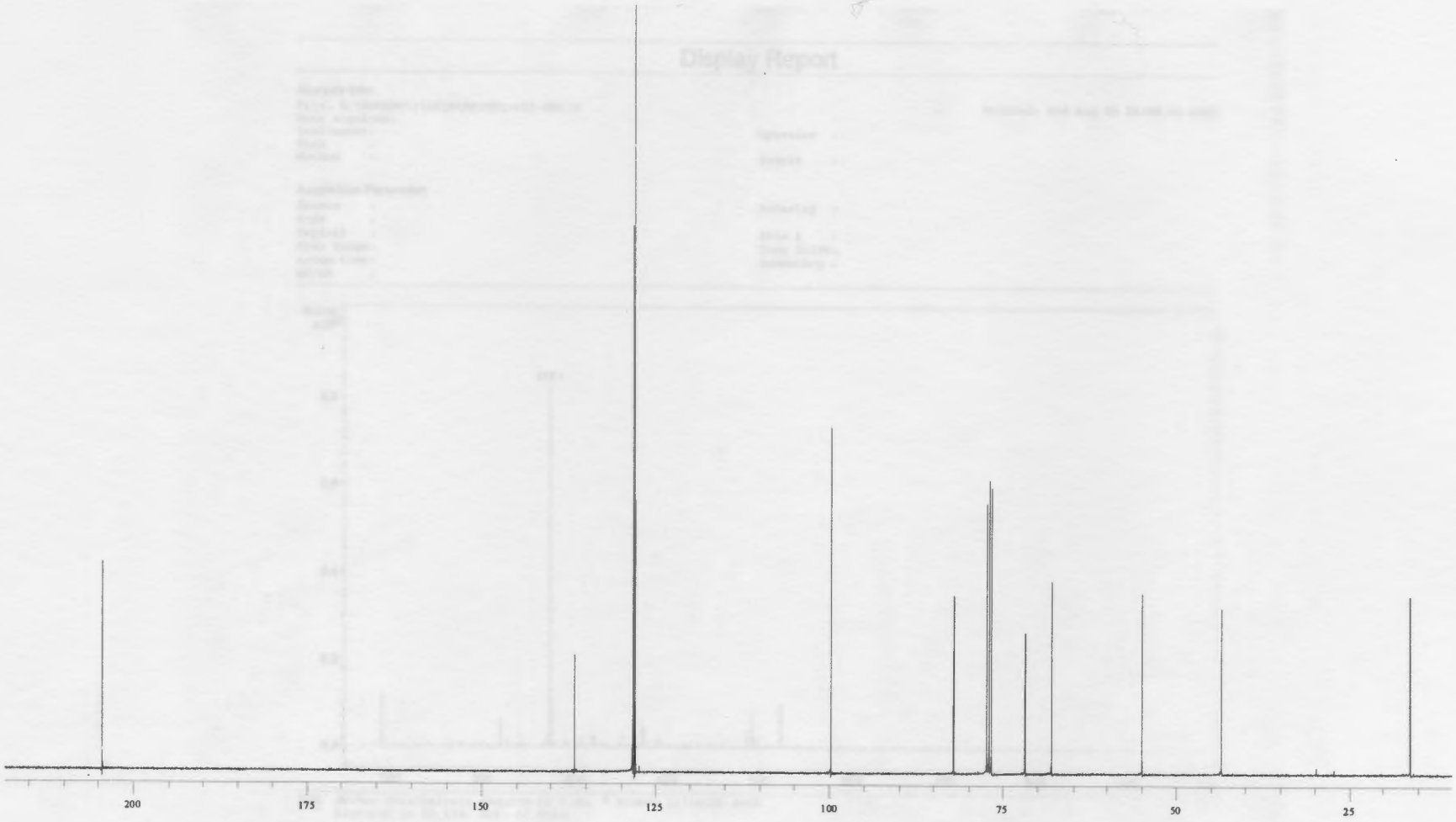

Figure 43: 100 MHz ^{13}C spectrum of **24**

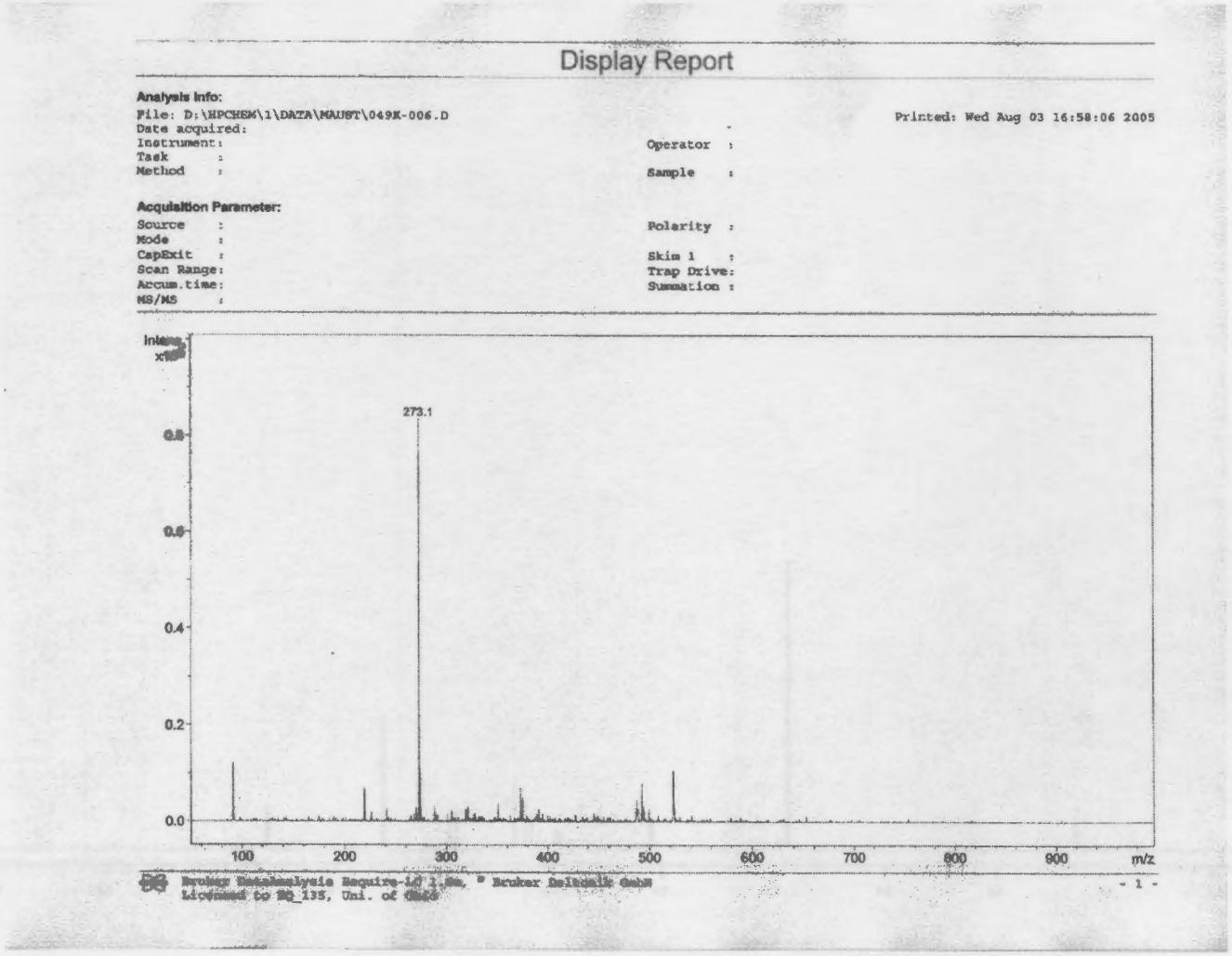

Figure 44: Mass spectrum of **24**

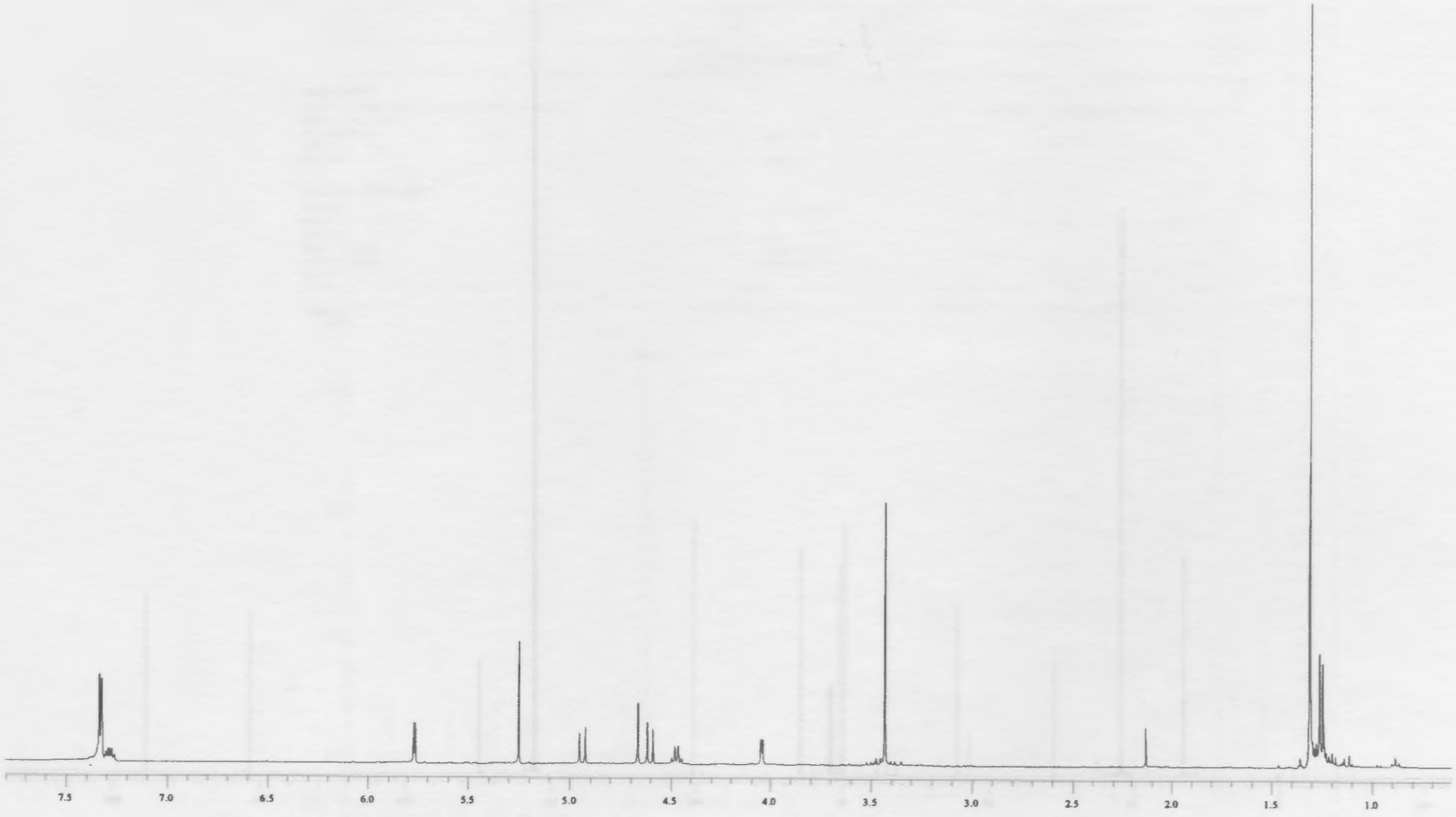

Figure 45: 400 MHz ^{1}H spectrum of **25**

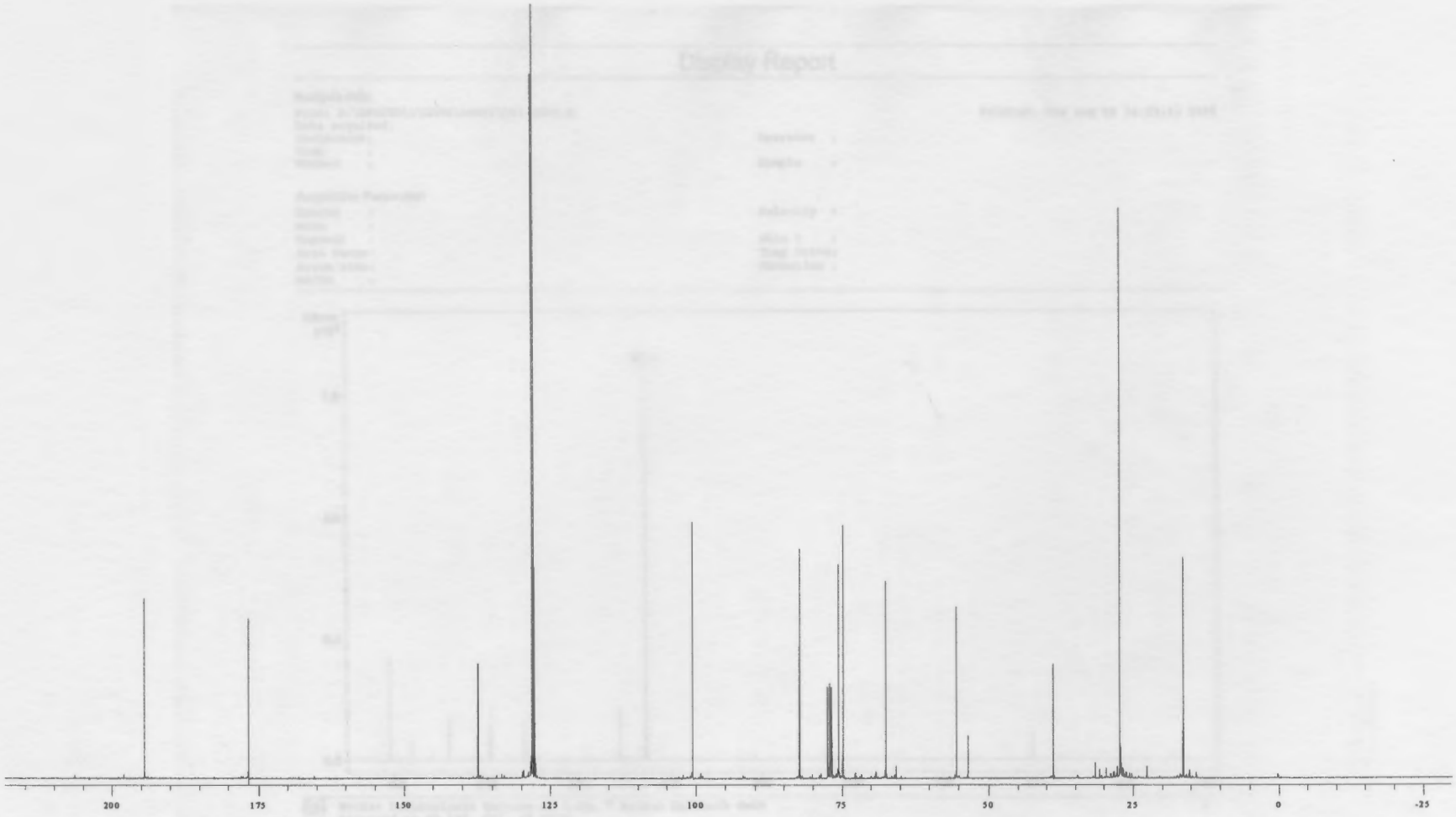

Figure 46: 100 MHz ^{13}C spectrum of **25**

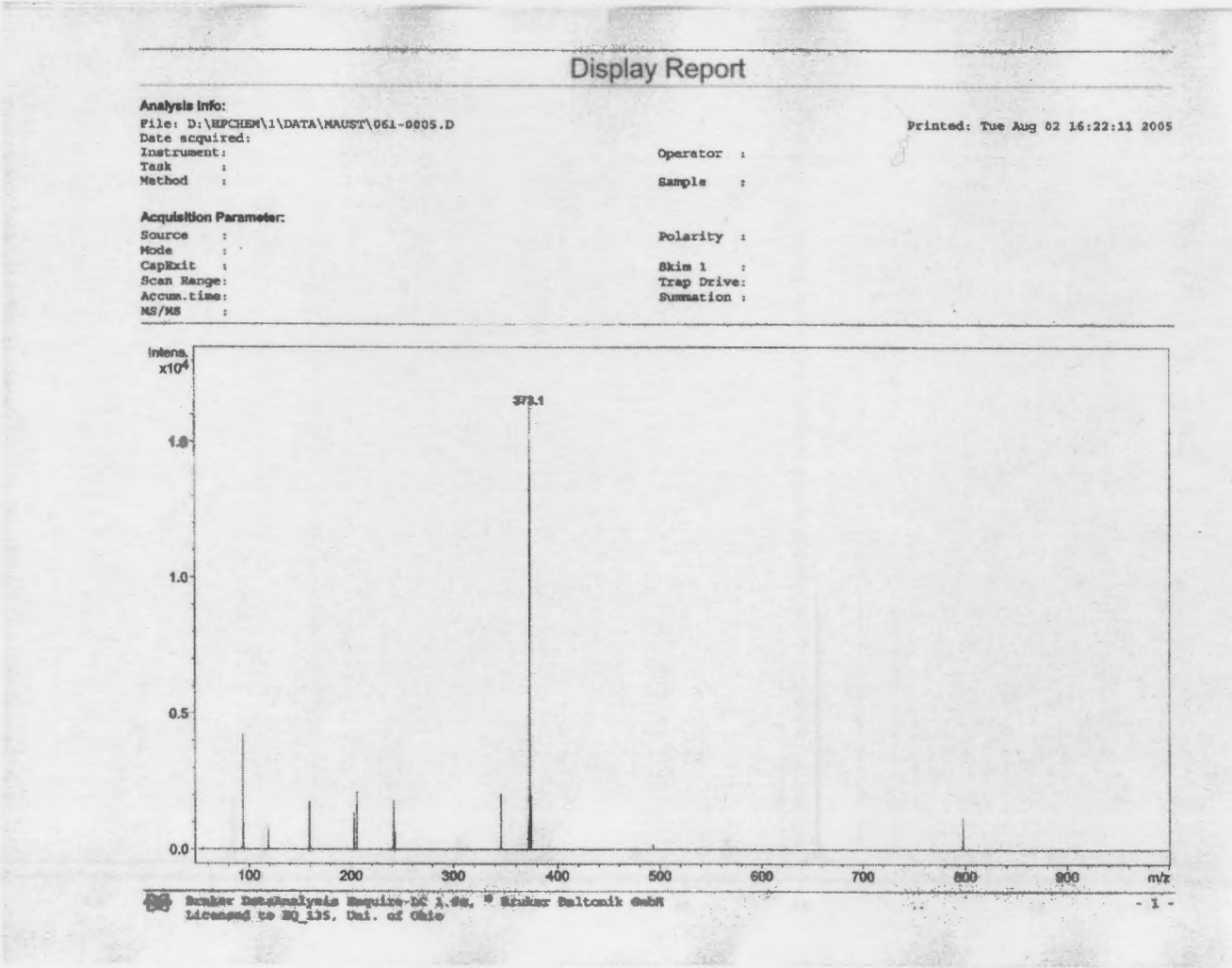

Figure 47: Mass spectrum of **25**

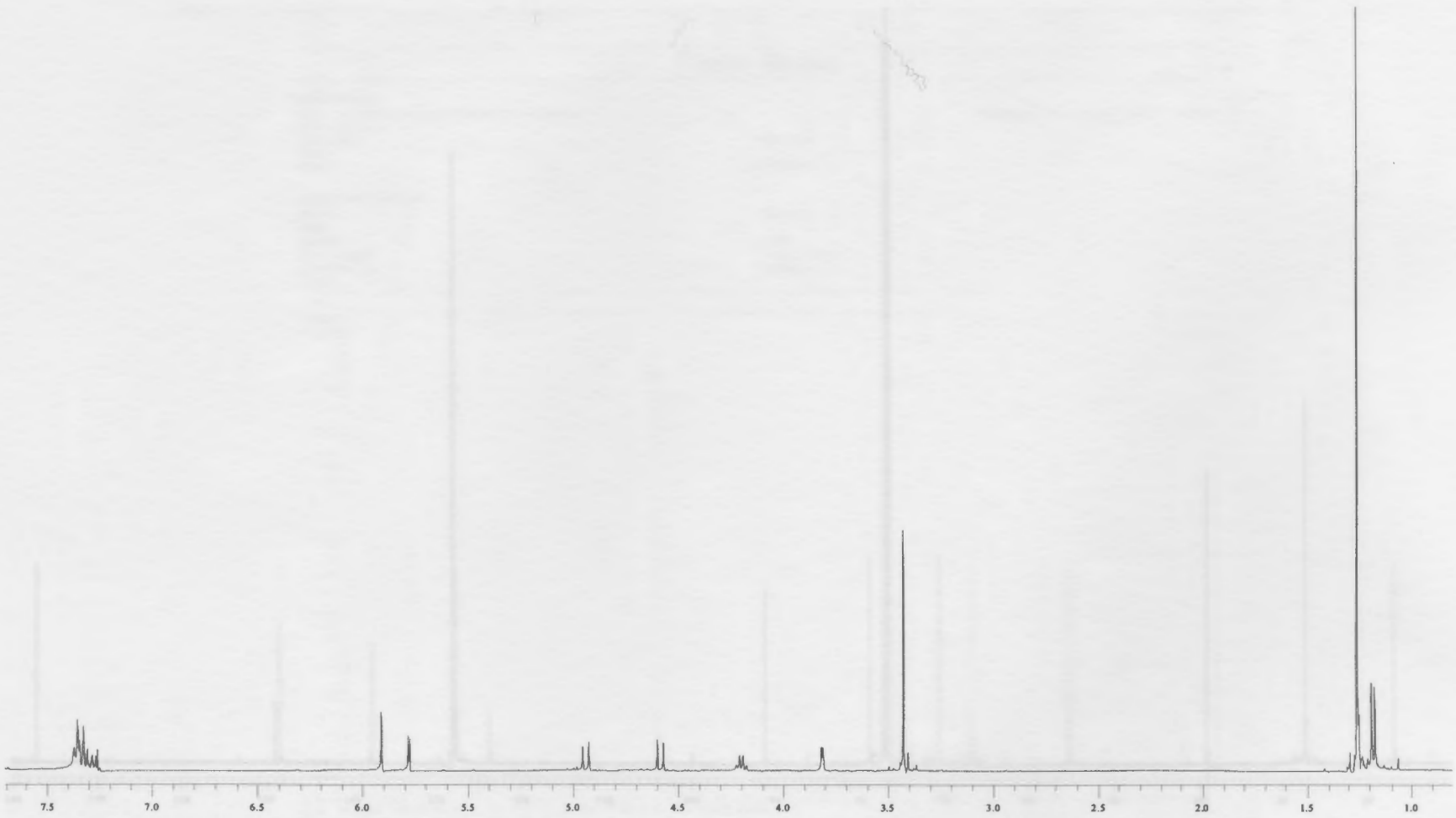

Figure 48: 400 MHz ^{1}H spectrum of **26**

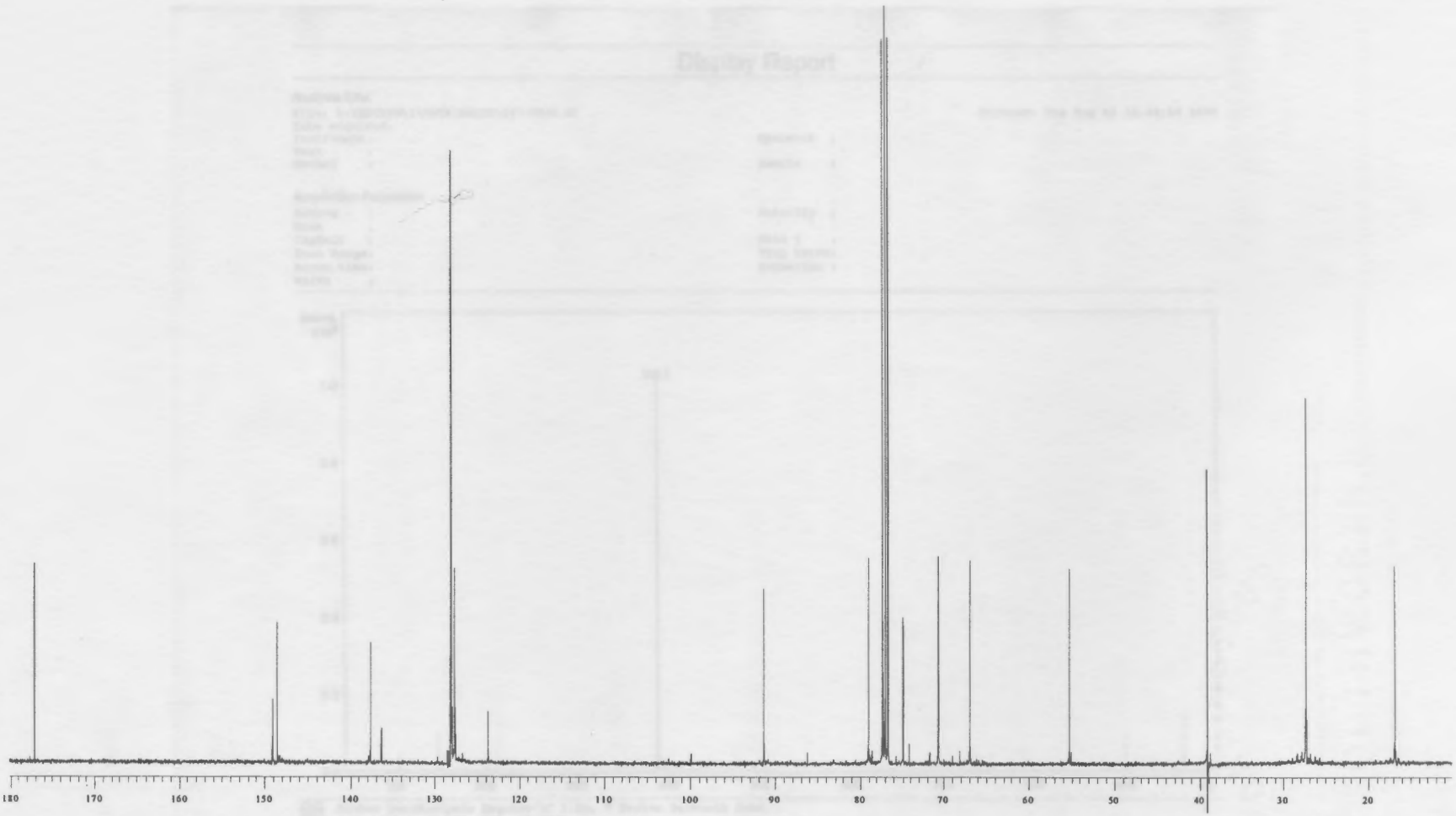

Figure 49: 100 MHz ^{13}C spectrum of **26**

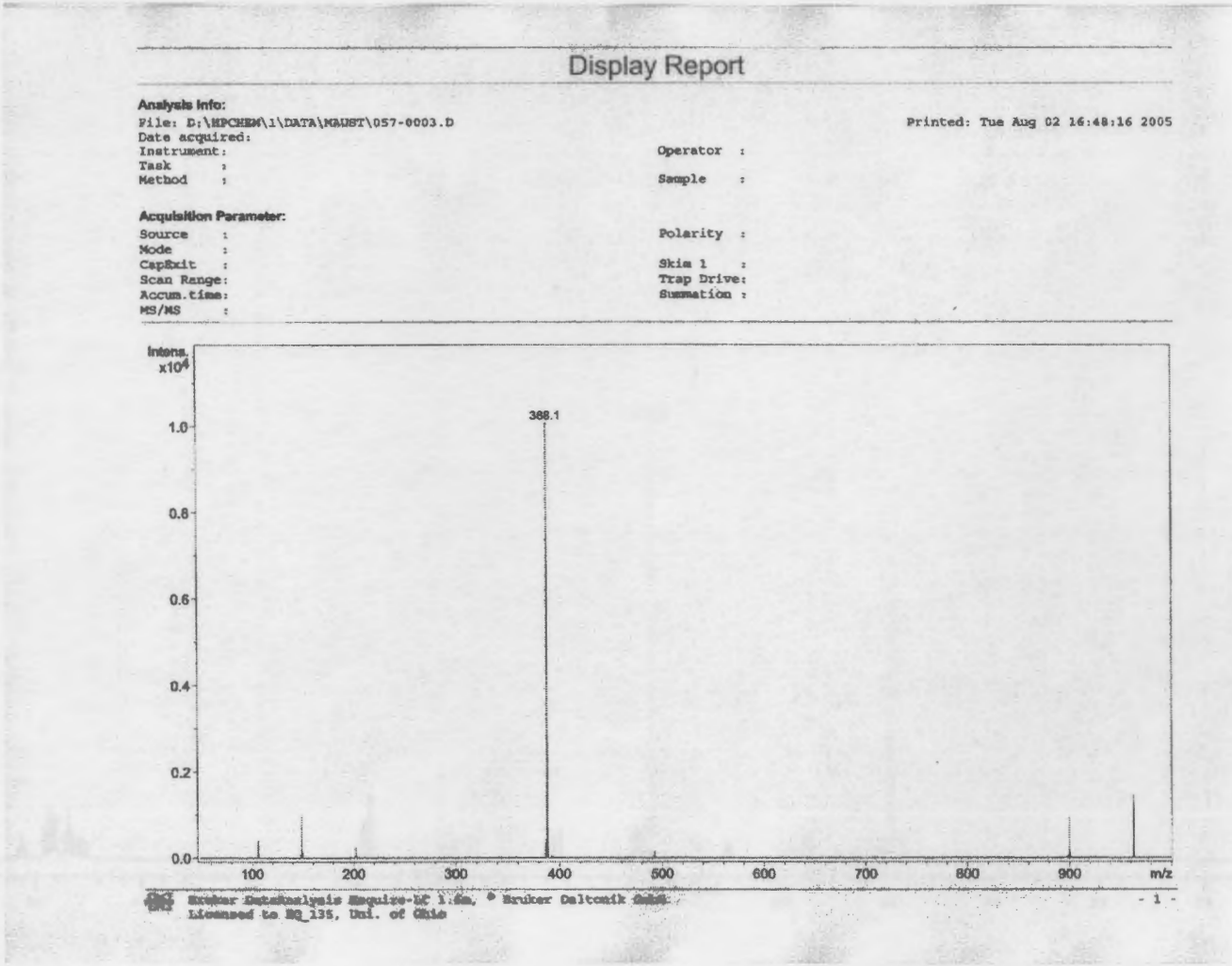

Figure 50: Mass spectrum of **26**

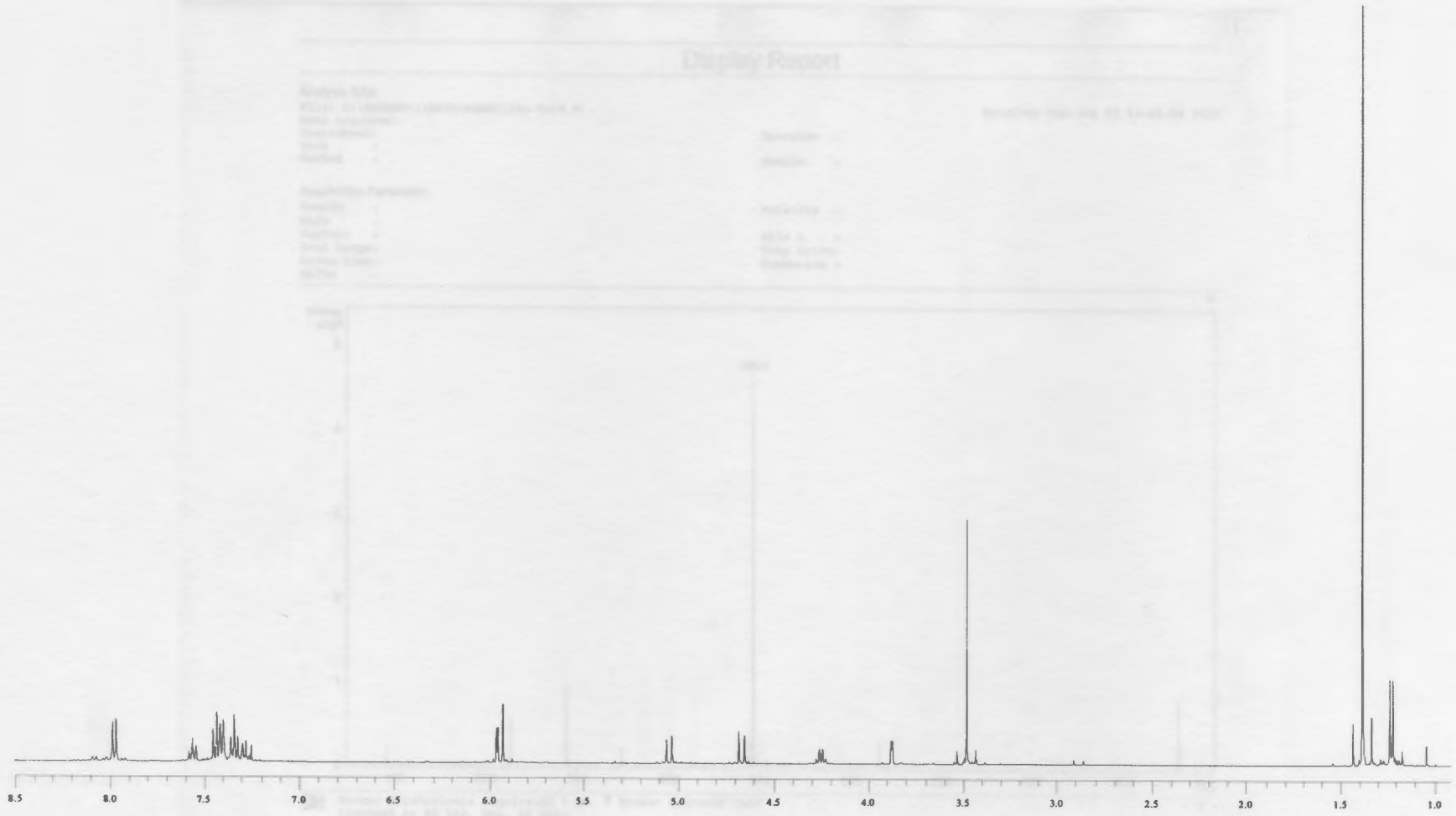

Figure 51: 400 MHz ^{1}H spectrum of **27**

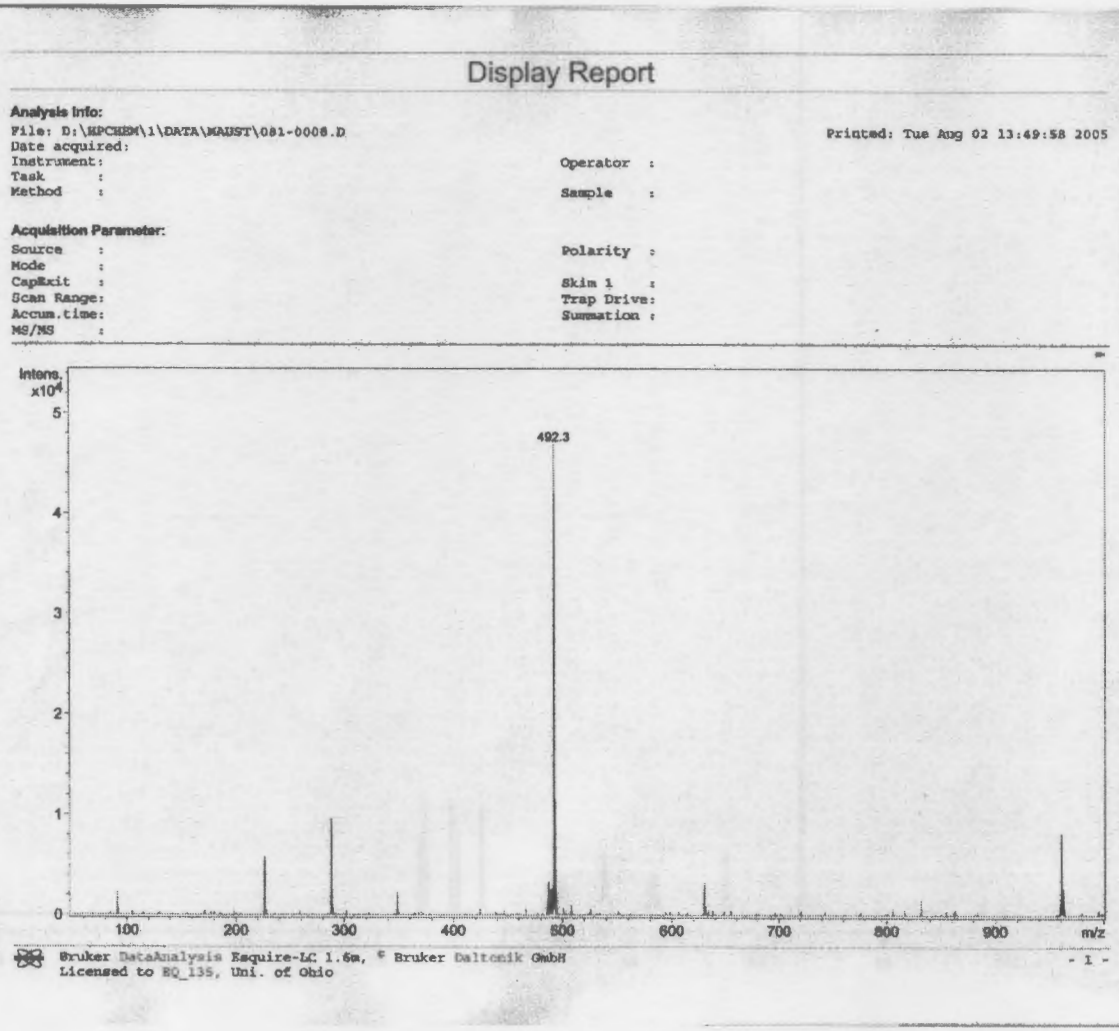

Figure 52: Mass spectrum of **27**

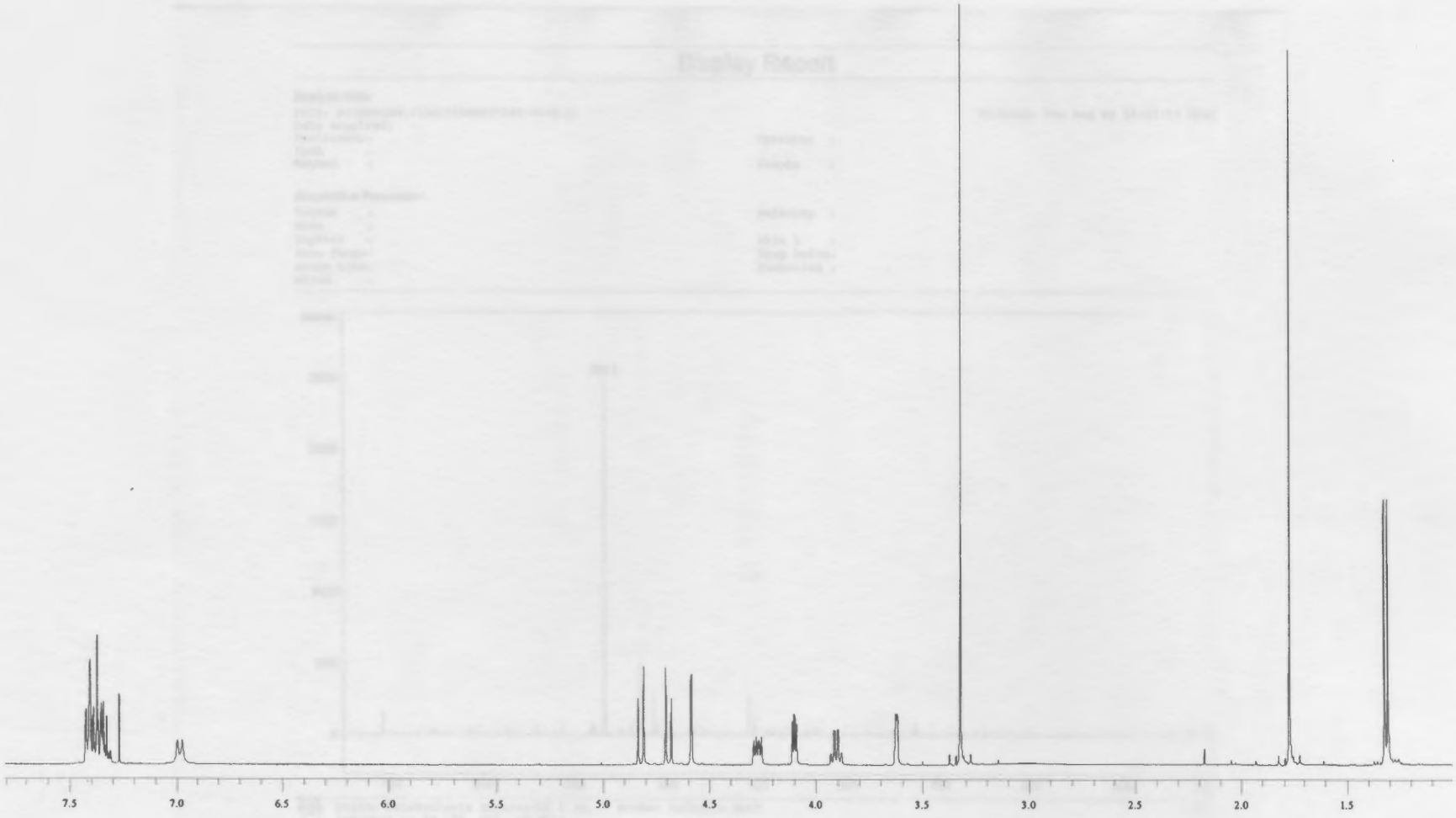

Figure 53: 400 MHz ^{1}H spectrum of **28**

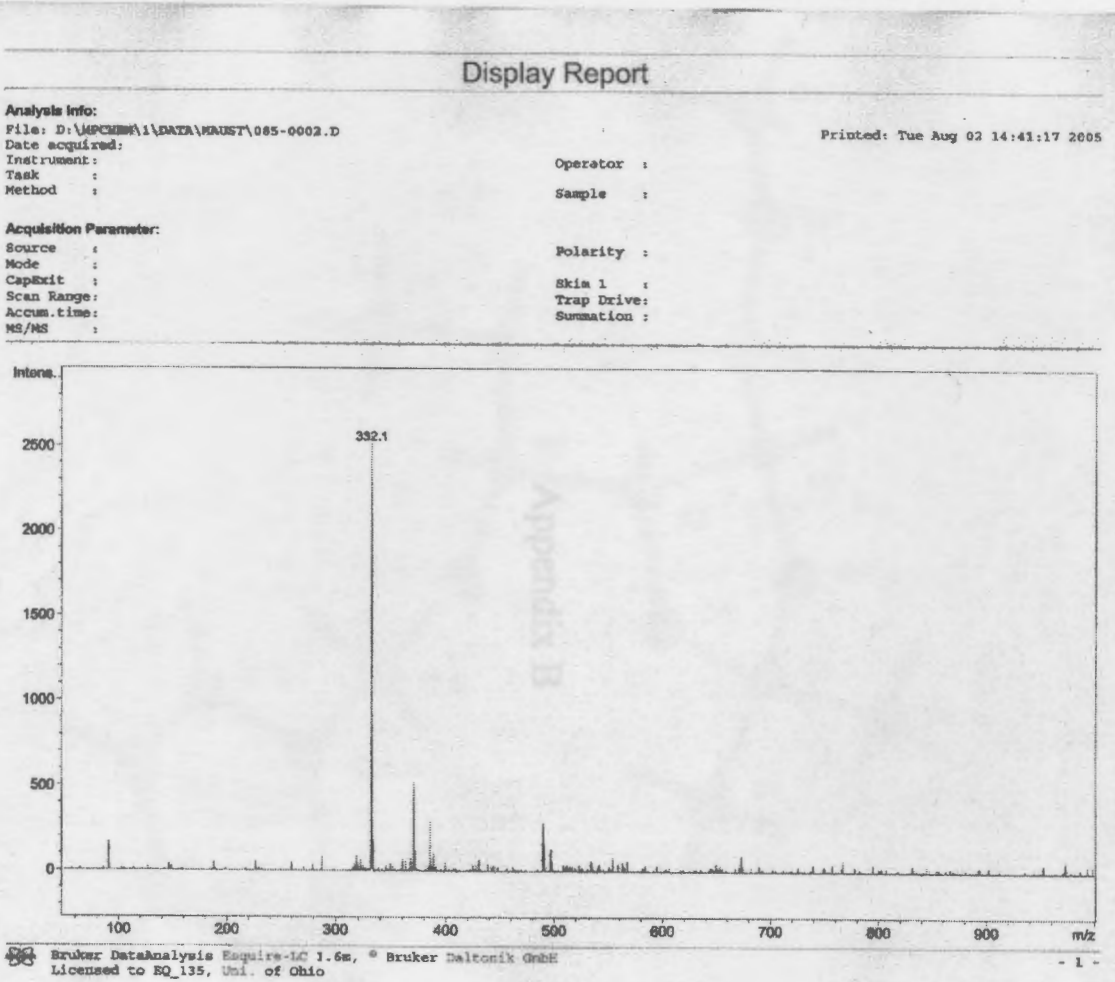

Figure 54: Mass spectrum of **28**

Appendix B

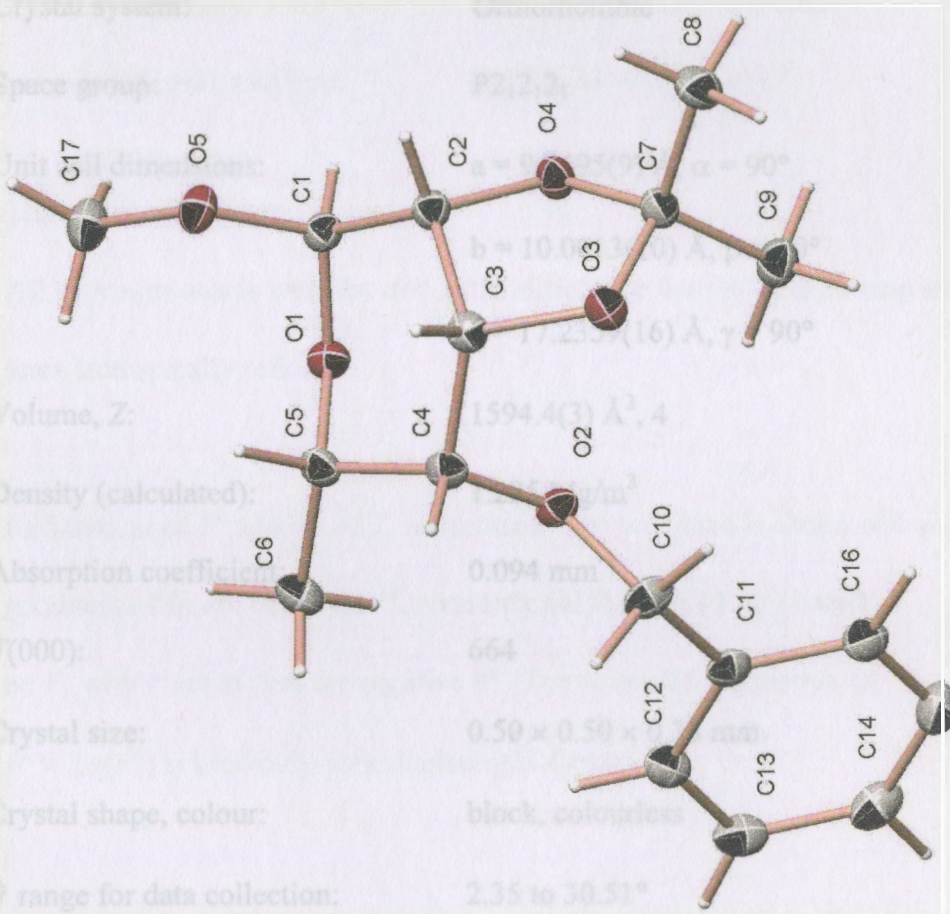

Figure 55: X-Ray crystal structure of **13**

Table 1: Crystal data and structure refinement for **13**

Empirical formula:	$C_{17}H_{24}O_5$
Formula weight:	308.36
Temperature:	100(2) K
Wavelength:	0.71073 Å
Crystal system:	Orthorhombic
Space group:	$P2_12_12_1$
Unit cell dimensions:	a = 9.2495(9) Å, α = 90°
	b = 10.0013(10) Å, β = 90°
	c = 17.2359(16) Å, γ = 90°
Volume, *Z*:	1594.4(3) $Å^3$, 4
Density (calculated):	1.285 Mg/m^3
Absorption coefficient:	0.094 mm^{-1}
F(000):	664
Crystal size:	0.50 × 0.50 × 0.38 mm
Crystal shape, colour:	block, colourless
θ range for data collection:	2.35 to 30.51°
Limiting indices:	$-13 \le h \le 13$, $-14 \le k \le 14$, $-24 \le l \le 24$
Reflections collected:	19051
Independent reflections:	2759 (R(int) = 0.0253)
Completeness to θ = 30.51°:	99.8 %
Absorption correction:	multi-scan

Max. and min. transmission:	0.96 and 0.75805
Refinement method:	Full-matrix least-squares on F^2
Data / restraints / parameters:	2759 / 0 / 295
Goodness-of-fit on F^2:	1.150
Final R indices [$I>2\sigma(I)$]:	R1 = 0.0390, wR2 = 0.0979
R indices (all data):	R1 = 0.0398, wR2 = 0.0987
Largest diff. peak and hole:	0.402 and -0.180 e × Å^{-3}

Treatment of hydrogen atoms:

All hydrogen atoms were located in the difference density Fourier map and were isotropically refined.

Refinement of F^2 against ALL reflections. The weighted R-factor wR and goodness of fit are based on F^2, conventional R-factors R are based on F, with F set to zero for negative F^2. The threshold expression of $F^2 > 2\sigma(F^2)$ is used only for calculating R-factors.

Table 2: Atomic coordinates [$\times 10^4$] and equivalent isotropic displacement parameters [$Å^2 \times 10^3$] for **13**

U(eq) is defined as one third of the trace of the orthogonalized U_{ij} tensor.

	x	y	z	U(eq)
C(1)	9310(1)	5653(1)	1859(1)	16(1)
C(2)	8563(2)	4611(1)	1356(1)	16(1)
C(3)	7203(1)	5082(1)	930(1)	17(1)
C(4)	7145(1)	6587(1)	735(1)	17(1)
C(5)	7801(2)	7395(1)	1395(1)	18(1)
C(6)	7917(2)	8873(2)	1214(1)	25(1)
C(7)	8617(2)	3701(1)	140(1)	18(1)
C(8)	8462(2)	2193(2)	210(1)	25(1)
C(9)	9257(2)	4120(2)	-631(1)	23(1)
C(10)	6953(2)	7024(2)	-622(1)	21(1)
C(11)	7725(2)	7822(1)	-1233(1)	18(1)
C(12)	7911(2)	9195(2)	-1130(1)	21(1)
C(13)	8589(2)	9960(2)	-1694(1)	23(1)
C(14)	9112(2)	9358(2)	-2366(1)	25(1)
C(15)	8930(2)	7993(2)	-2473(1)	27(1)
C(16)	8235(2)	7229(2)	-1911(1)	22(1)
C(17)	9269(2)	6505(2)	3132(1)	24(1)
O(1)	9252(1)	6948(1)	1545(1)	17(1)
O(2)	7891(1)	6911(1)	38(1)	17(1)
O(3)	7201(1)	4278(1)	244(1)	19(1)
O(4)	9505(1)	4242(1)	737(1)	18(1)
O(5)	8641(1)	5586(1)	2597(1)	20(1)

All esds (except the esd in the dihedral angle between two l.s. planes) are estimated using the full covariance matrix. The cell esds are taken into account individually in the estimation of esds in distances, angles and torsion angles; correlations between esds in cell parameters are only used when they are defined by crystal

symmetry. An approximate (isotropic) treatment of cell esds is used for estimating esds involving l.s. planes.

Table 3. Bond lengths [Å] and angles [deg] for **13**

C(1)-O(1)	1.4039(16)	C(14)-H(14)	0.95(2)
C(1)-O(5)	1.4147(15)	C(15)-C(16)	1.391(2)
C(1)-C(2)	1.5217(19)	C(15)-H(15)	0.96(2)
C(1)-H(1)	0.962(18)	C(16)-H(16)	0.96(2)
C(2)-O(4)	1.4261(16)	C(17)-O(5)	1.4261(18)
C(2)-C(3)	1.5309(19)	C(17)-H(17A)	0.96(3)
C(2)-H(2)	0.92(2)	C(17)-H(17B)	0.94(2)
C(3)-O(3)	1.4291(16)	C(17)-H(17C)	0.95(2)
C(3)-C(4)	1.5429(19)		
C(3)-H(3)	0.962(19)	O(1)-C(1)-O(5)	111.95(11)
C(4)-O(2)	1.4224(16)	O(1)-C(1)-C(2)	113.23(10)
C(4)-C(5)	1.5214(19)	O(5)-C(1)-C(2)	106.31(10)
C(4)-H(4)	0.93(2)	O(1)-C(1)-H(1)	105.0(12)
C(5)-O(1)	1.4391(17)	O(5)-C(1)-H(1)	109.3(11)
C(5)-C(6)	1.514(2)	C(2)-C(1)-H(1)	111.2(11)
C(5)-H(5)	1.017(19)	O(4)-C(2)-C(1)	109.06(11)
C(6)-H(6A)	0.96(2)	O(4)-C(2)-C(3)	102.87(10)
C(6)-H(6B)	0.97(3)	C(1)-C(2)-C(3)	115.85(11)
C(6)-H(6C)	1.03(3)	O(4)-C(2)-H(2)	108.5(13)
C(7)-O(4)	1.4236(16)	C(1)-C(2)-H(2)	107.6(13)
C(7)-O(3)	1.4426(16)	C(3)-C(2)-H(2)	112.7(14)
C(7)-C(9)	1.5149(19)	O(3)-C(3)-C(2)	103.00(10)
C(7)-C(8)	1.519(2)	O(3)-C(3)-C(4)	111.65(11)
C(8)-H(8A)	0.97(3)	C(2)-C(3)-C(4)	115.68(11)
C(8)-H(8B)	0.97(3)	O(3)-C(3)-H(3)	108.5(11)
C(8)-H(8C)	0.91(3)	C(2)-C(3)-H(3)	109.6(11)
C(9)-H(9A)	1.02(2)	C(4)-C(3)-H(3)	108.2(12)
C(9)-H(9B)	0.98(2)	O(2)-C(4)-C(5)	108.46(11)
C(9)-H(9C)	0.97(2)	O(2)-C(4)-C(3)	112.88(10)
C(10)-O(2)	1.4352(16)	C(5)-C(4)-C(3)	109.97(11)
C(10)-C(11)	1.5007(19)	O(2)-C(4)-H(4)	112.4(12)
C(10)-H(10A)	0.95(3)	C(5)-C(4)-H(4)	107.5(13)
C(10)-H(10B)	0.98(2)	C(3)-C(4)-H(4)	105.5(13)
C(11)-C(16)	1.394(2)	O(1)-C(5)-C(6)	105.92(12)
C(11)-C(12)	1.3957(19)	O(1)-C(5)-C(4)	109.98(10)
C(12)-C(13)	1.387(2)	C(6)-C(5)-C(4)	113.19(12)
C(12)-H(12)	0.95(2)	O(1)-C(5)-H(5)	108.8(11)
C(13)-C(14)	1.392(2)	C(6)-C(5)-H(5)	110.5(11)
C(13)-H(13)	0.87(3)	C(4)-C(5)-H(5)	108.4(11)
C(14)-C(15)	1.388(2)	C(5)-C(6)-H(6A)	109.6(15)

C(5)-C(6)-H(6B)	109.6(16)	C(16)-C(11)-C(12)	118.86(13)
H(6A)-C(6)-H(6B)	108(2)	C(16)-C(11)-C(10)	121.57(13)
C(5)-C(6)-H(6C)	109.9(14)	C(12)-C(11)-C(10)	119.55(13)
H(6A)-C(6)-H(6C)	107.5(19)	C(13)-C(12)-C(11)	120.68(14)
H(6B)-C(6)-H(6C)	112(2)	C(1)-O(5)-C(17)	111.84(11)
O(4)-C(7)-O(3)	106.39(10)	C(13)-C(12)-H(12)	119.9(15)
O(4)-C(7)-C(9)	107.67(11)	C(11)-C(12)-H(12)	119.4(15)
O(3)-C(7)-C(9)	110.70(11)	C(12)-C(13)-C(14)	120.15(14)
O(4)-C(7)-C(8)	111.98(12)	C(12)-C(13)-H(13)	120.5(16)
O(3)-C(7)-C(8)	107.55(12)	C(14)-C(13)-H(13)	119.1(16)
C(9)-C(7)-C(8)	112.42(12)	C(15)-C(14)-C(13)	119.52(14)
C(7)-C(8)-H(8A)	109.9(16)	C(15)-C(14)-H(14)	121.1(14)
C(7)-C(8)-H(8B)	107.8(15)	C(13)-C(14)-H(14)	119.3(14)
H(8A)-C(8)-H(8B)	106(2)	C(14)-C(15)-C(16)	120.32(15)
C(7)-C(8)-H(8C)	112.5(16)	C(14)-C(15)-H(15)	121.7(15)
H(8A)-C(8)-H(8C)	110(2)	C(16)-C(15)-H(15)	117.9(15)
H(8B)-C(8)-H(8C)	110(2)	C(15)-C(16)-C(11)	120.47(14)
C(7)-C(9)-H(9A)	105.9(12)	C(15)-C(16)-H(16)	119.5(14)
C(7)-C(9)-H(9B)	111.7(13)	C(11)-C(16)-H(16)	120.0(13)
H(9A)-C(9)-H(9B)	108.0(18)	O(5)-C(17)-H(17A)	110.9(15)
C(7)-C(9)-H(9C)	109.1(12)	O(5)-C(17)-H(17B)	107.0(14)
H(9A)-C(9)-H(9C)	111.7(19)	H(17A)-C(17)-H(17B)	107(2)
H(9B)-C(9)-H(9C)	110.4(18)	O(5)-C(17)-H(17C)	112.0(14)
O(2)-C(10)-C(11)	108.08(11)	H(17A)-C(17)-H(17C)	110(2)
O(2)-C(10)-H(10A)	110.9(16)	H(17B)-C(17)-H(17C)	110(2)
C(11)-C(10)-H(10A)	110.1(16)	C(1)-O(1)-C(5)	113.07(10)
O(2)-C(10)-H(10B)	109.0(12)	C(4)-O(2)-C(10)	113.22(10)
C(11)-C(10)-H(10B)	110.1(13)	C(3)-O(3)-C(7)	109.06(10)
H(10A)-C(10)-H(10B)	109(2)	C(7)-O(4)-C(2)	106.64(10)

Table 4: Anisotropic displacement parameters [$Å^2 \times 10^3$] for **13**

The anisotropic displacement factor exponent takes the form: $-2\pi^2 [(h\,a^*)^2 U11 + ... + 2\,h\,k\,a^*\,b^*\,U12]$

	U11	U22	U33	U23	U13	U12
C(1)	16(1)	18(1)	16(1)	1(1)	0(1)	0(1)
C(2)	17(1)	16(1)	15(1)	0(1)	1(1)	-1(1)
C(3)	14(1)	18(1)	18(1)	0(1)	2(1)	-2(1)
C(4)	12(1)	19(1)	19(1)	1(1)	2(1)	2(1)
C(5)	16(1)	18(1)	19(1)	-1(1)	2(1)	3(1)
C(6)	31(1)	17(1)	28(1)	-2(1)	1(1)	5(1)
C(7)	17(1)	18(1)	18(1)	-2(1)	-1(1)	1(1)
C(8)	30(1)	16(1)	28(1)	-3(1)	-2(1)	1(1)
C(9)	23(1)	29(1)	18(1)	0(1)	3(1)	1(1)
C(10)	18(1)	23(1)	21(1)	5(1)	-6(1)	-4(1)
C(11)	15(1)	19(1)	19(1)	2(1)	-6(1)	0(1)
C(12)	19(1)	19(1)	24(1)	-2(1)	-3(1)	0(1)
C(13)	21(1)	18(1)	31(1)	3(1)	-6(1)	-3(1)
C(14)	22(1)	30(1)	24(1)	7(1)	-5(1)	-6(1)
C(15)	32(1)	31(1)	19(1)	-1(1)	-1(1)	-2(1)
C(16)	27(1)	19(1)	22(1)	0(1)	-5(1)	-1(1)
C(17)	28(1)	27(1)	18(1)	-3(1)	-1(1)	-4(1)
O(1)	16(1)	16(1)	18(1)	2(1)	1(1)	-1(1)
O(2)	14(1)	20(1)	16(1)	3(1)	-1(1)	0(1)
O(3)	16(1)	20(1)	21(1)	-3(1)	-1(1)	0(1)
O(4)	16(1)	21(1)	17(1)	-3(1)	0(1)	2(1)
O(5)	24(1)	22(1)	14(1)	0(1)	1(1)	-5(1)

Table 5. Hydrogen coordinates ($\times 10^4$) and isotropic displacement parameters ($Å^2 \times 10^3$) for **13**

	x	y	z	U(eq)
H(1)	10320(20)	5461(19)	1913(10)	12(4)
H(2)	8400(20)	3870(20)	1661(12)	20(5)
H(3)	6360(20)	4863(19)	1231(11)	13(4)
H(4)	6170(20)	6800(20)	710(11)	20(5)
H(5)	7190(20)	7250(20)	1879(11)	17(4)
H(6A)	8560(30)	9000(20)	785(14)	35(6)
H(6B)	6980(30)	9220(30)	1070(14)	36(6)
H(6C)	8340(30)	9370(30)	1682(14)	34(6)
H(8A)	8090(30)	1960(30)	715(15)	39(7)
H(8B)	7740(30)	1900(30)	-165(14)	36(6)
H(8C)	9310(30)	1750(30)	125(14)	35(6)
H(9A)	10260(20)	3700(20)	-654(13)	26(5)
H(9B)	8690(30)	3780(20)	-1069(12)	26(5)
H(9C)	9310(20)	5080(20)	-652(11)	23(5)
H(10A)	6710(30)	6170(30)	-819(15)	38(7)
H(10B)	6060(30)	7480(20)	-465(12)	26(5)
H(12)	7570(30)	9600(20)	-671(14)	33(6)
H(13)	8630(30)	10830(30)	-1652(14)	34(6)
H(14)	9580(20)	9890(20)	-2748(12)	29(5)
H(15)	9260(30)	7550(20)	-2934(14)	34(6)
H(16)	8100(30)	6280(20)	-1997(13)	33(6)
H(17A)	8890(30)	7390(30)	3055(13)	34(6)
H(17B)	8990(30)	6230(20)	3629(12)	26(5)
H(17C)	10300(30)	6520(20)	3095(13)	30(6)

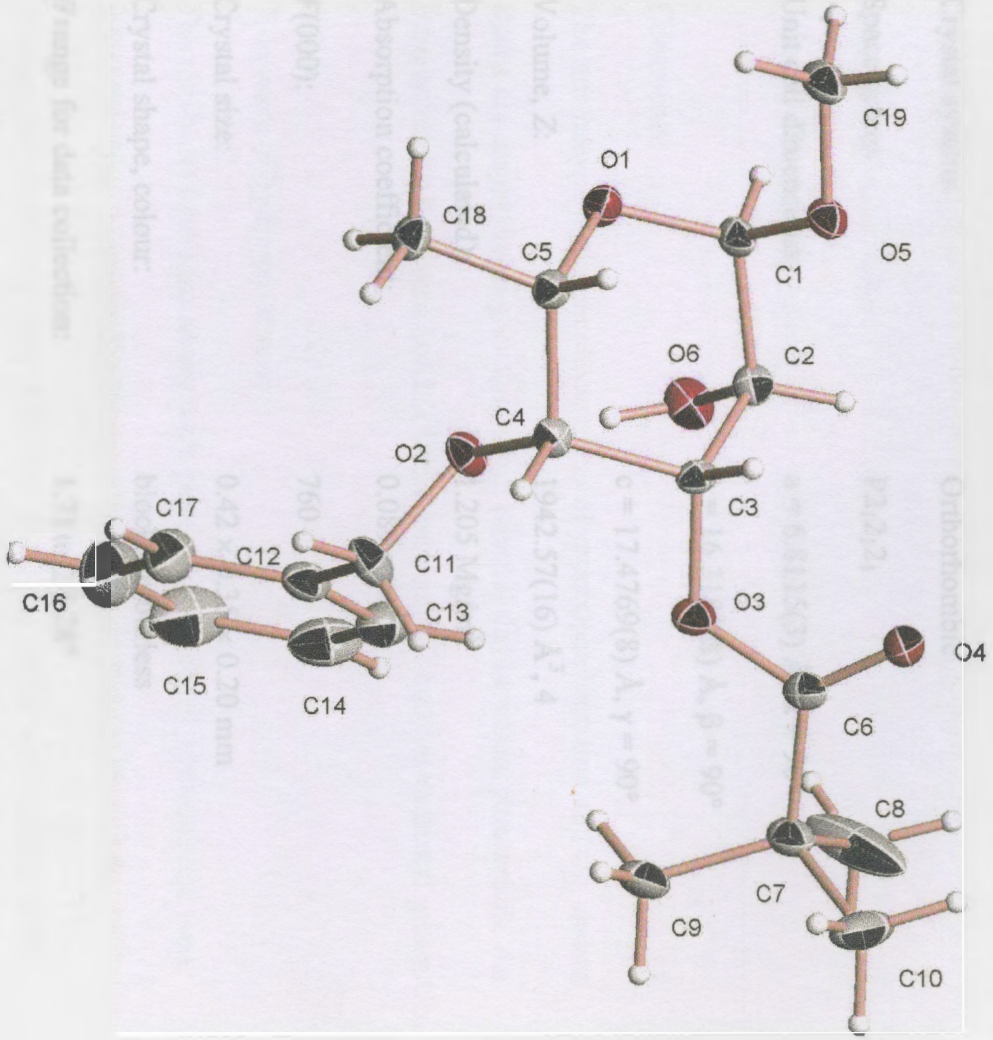

Figure 56: X-Ray crystal structure of **19**

Table 6: Crystal data and structure refinement for **19**

Empirical formula:	$C_{19}H_{28}O_6$
Formula weight:	352.41
Temperature:	100(2) K
Wavelength:	0.71073 Å
Crystal system:	Orthorhombic
Space group:	$P2_12_12_1$
Unit cell dimensions:	a = 6.8115(3) Å, α = 90°
	b = 16.3181(8) Å, β = 90°
	c = 17.4769(8) Å, γ = 90°
Volume, *Z*:	1942.57(16) $Å^3$, 4
Density (calculated):	1.205 Mg/m^3
Absorption coefficient:	0.089 mm^{-1}
F(000):	760
Crystal size:	0.42 × 0.35 × 0.20 mm
Crystal shape, colour:	block, colourless
θ range for data collection:	1.71 to 28.28°
Limiting indices:	$-9 \le h \le 9$, $-21 \le k \le 21$, $-22 \le l \le 23$
Reflections collected:	20054
Independent reflections:	2750 (R(int) = 0.0273)
Completeness to θ = 28.28°:	99.9 %
Absorption correction:	multi-scan

Max. and min. transmission:	0.9800 and 0.8099
Refinement method:	Full-matrix least-squares on F^2
Data / restraints / parameters:	2750 / 0 / 304
Goodness-of-fit on F^2:	1.203
Final R indices [$I>2\sigma(I)$]:	R1 = 0.0425, wR2 = 0.1048
R indices (all data):	R1 = 0.0431, wR2 = 0.1052
Number of Friedel Pairs:	2964
Largest diff. peak and hole:	0.313 and -0.238 e × $Å^{-3}$

Comments:

The tert-butyl substituent shows signs of pronounced rotation and the carbon atoms are displaying higher than usual thermal displacement parameters. An intramolecular hydrogen bond is found between O2 and the hydroxyl group O6.

Treatment of hydrogen atoms:

The tert-butyl hydrogen atoms were placed in calculated positions and were refined with an isotropic displacement parameter 1.5 times that of the adjacent non hydrogen atom. All other hydrogen atoms were located in the density Fourier map. The hydroxyl hydrogen atom H6 was refined with an isotropic displacement parameter 1.5 times that of the adjacent oxygen atom, all others were refined isotropically.

Refinement of F^2 against ALL reflections. The weighted R-factor wR and goodness of fit are based on F^2, conventional R-factors R are based on F, with F set to zero for negative F^2. The threshold expression of $F^2 > 2\sigma(F^2)$ is used only for calculating R-factors.

Table 7: Atomic coordinates [$\times 10^4$] and equivalent isotropic displacement parameters [$Å^2 \times 10^3$] for **19**

U(eq) is defined as one third of the trace of the orthogonalized U_{ij} tensor.

	x	y	z	U(eq)
C(1)	7571(3)	6949(1)	10998(1)	16(1)
C(2)	7234(3)	6400(1)	10297(1)	17(1)
C(3)	9215(3)	6253(1)	9911(1)	15(1)
C(4)	10722(3)	5920(1)	10474(1)	15(1)
C(5)	10903(3)	6518(1)	11139(1)	16(1)
C(6)	8578(3)	5954(1)	8600(1)	17(1)
C(7)	8450(3)	5274(1)	8000(1)	23(1)
C(8)	6288(4)	5053(2)	7911(3)	70(1)
C(9)	9599(4)	4510(1)	8232(1)	31(1)
C(10)	9300(6)	5612(2)	7248(1)	48(1)
C(11)	11255(3)	4460(1)	10508(1)	24(1)
C(12)	10201(3)	3686(1)	10737(1)	23(1)
C(13)	8382(4)	3506(1)	10419(1)	28(1)
C(14)	7383(5)	2797(2)	10630(1)	37(1)
C(15)	8220(6)	2271(2)	11160(2)	46(1)
C(16)	10013(6)	2444(2)	1479(2)	47(1)
C(17)	11011(5)	3152(1)	11270(1)	34(1)
C(18)	12301(3)	6230(1)	11754(1)	20(1)
C(19)	8383(3)	8308(1)	11325(1)	23(1)
O(1)	9004(2)	6625(1)	11497(1)	17(1)
O(2)	10089(2)	5137(1)	10758(1)	18(1)
O(3)	9037(2)	5658(1)	9300(1)	19(1)
O(4)	8296(2)	6668(1)	8476(1)	21(1)
O(5)	8089(2)	7732(1)	10718(1)	18(1)
O(6)	6277(2)	5663(1)	10518(1)	22(1)

All esds (except the esd in the dihedral angle between two l.s. planes) are estimated using the full covariance matrix. The cell esds are taken into account individually in the estimation of esds in distances, angles and torsion angles; correlations between esds in cell parameters are only used when they are defined by crystal

symmetry. An approximate (isotropic) treatment of cell esds is used for estimating esds involving l.s. planes.

Table 8. Bond lengths [Å] and angles [deg] for **19**

C(1)-O(1)	1.412(2)	C(13)-H(13)	0.91(3)
C(1)-O(5)	1.412(2)	C(14)-C(15)	1.385(4)
C(1)-C(2)	1.535(3)	C(14)-H(14)	0.94(3)
C(1)-H(1)	0.95(2)	C(15)-C(16)	1.372(5)
C(2)-O(6)	1.422(2)	C(15)-H(15)	0.94(4)
C(2)-C(3)	1.527(3)	C(16)-C(17)	1.391(4)
C(2)-H(2)	0.94(2)	C(16)-H(16)	0.93(4)
C(3)-O(3)	1.449(2)	C(17)-H(17)	0.99(3)
C(3)-C(4)	1.522(3)	C(18)-H(18A)	0.96(3)
C(3)-H(3)	0.97(2)	C(18)-H(18B)	0.95(3)
C(4)-O(2)	1.437(2)	C(18)-H(18C)	0.95(3)
C(4)-C(5)	1.523(3)	C(19)-O(5)	1.431(2)
C(4)-H(4)	0.96(2)	C(19)-H(19A)	1.01(3)
C(5)-O(1)	1.447(2)	C(19)-H(19B)	0.96(3)
C(5)-C(18)	1.510(3)	C(19)-H(19C)	0.91(3)
C(5)-H(5)	0.93(2)	O(6)-H(6)	0.84(3)
C(6)-O(4)	1.199(2)		
C(6)-O(3)	1.351(2)	O(1)-C(1)-O(5)	112.37(15)
C(6)-C(7)	1.530(3)	O(1)-C(1)-C(2)	112.20(15)
C(7)-C(8)	1.524(4)	O(5)-C(1)-C(2)	106.76(15)
C(7)-C(9)	1.526(3)	O(1)-C(1)-H(1)	105.6(14)
C(7)-C(10)	1.537(3)	O(5)-C(1)-H(1)	109.1(14)
C(8)-H(8A)	0.9800	C(2)-C(1)-H(1)	110.9(14)
C(8)-H(8B)	0.9800	O(6)-C(2)-C(3)	113.11(15)
C(8)-H(8C)	0.9800	O(6)-C(2)-C(1)	110.18(15)
C(9)-H(9A)	0.9800	C(3)-C(2)-C(1)	108.20(15)
C(9)-H(9B)	0.9800	O(6)-C(2)-H(2)	105.9(15)
C(9)-H(9C)	0.9800	C(3)-C(2)-H(2)	110.5(14)
C(10)-H(10A)	0.9800	C(1)-C(2)-H(2)	108.9(14)
C(10)-H(10B)	0.9800	O(3)-C(3)-C(4)	107.06(15)
C(10)-H(10C)	0.9800	O(3)-C(3)-C(2)	110.92(15)
C(11)-O(2)	1.430(2)	C(4)-C(3)-C(2)	111.50(15)
C(11)-C(12)	1.506(3)	O(3)-C(3)-H(3)	109.9(13)
C(11)-H(11A)	0.97(3)	C(4)-C(3)-H(3)	109.1(14)
C(11)-H(11B)	0.96(3)	C(2)-C(3)-H(3)	108.3(13)
C(12)-C(13)	1.389(3)	O(2)-C(4)-C(3)	109.78(15)
C(12)-C(17)	1.390(3)	O(2)-C(4)-C(5)	109.22(15)
C(13)-C(14)	1.392(3)	C(3)-C(4)-C(5)	108.63(15)

O(2)-C(4)-H(4)	111.1(13)	O(2)-C(11)-H(11B)	107.9(18)
C(3)-C(4)-H(4)	110.7(13)	C(12)-C(11)-H(11B)	111.7(18)
C(5)-C(4)-H(4)	107.4(13)	H(11A)-C(11)-H(11B)	108(2)
O(1)-C(5)-C(18)	107.07(15)	C(13)-C(12)-C(17)	119.3(2)
O(1)-C(5)-C(4)	109.60(15)	C(13)-C(12)-C(11)	119.8(2)
C(18)-C(5)-C(4)	113.27(16)	C(17)-C(12)-C(11)	120.9(2)
O(1)-C(5)-H(5)	107.6(15)	C(12)-C(13)-C(14)	120.5(2)
C(18)-C(5)-H(5)	109.9(15)	C(12)-C(13)-H(13)	119(2)
C(4)-C(5)-H(5)	109.2(15)	C(14)-C(13)-H(13)	120(2)
O(4)-C(6)-O(3)	123.27(17)	C(15)-C(14)-C(13)	119.4(3)
O(4)-C(6)-C(7)	124.76(18)	C(15)-C(14)-H(14)	121.1(19)
O(3)-C(6)-C(7)	111.96(16)	C(13)-C(14)-H(14)	119.4(19)
C(8)-C(7)-C(9)	109.2(2)	C(16)-C(15)-C(14)	120.7(2)
C(8)-C(7)-C(6)	107.22(19)	C(16)-C(15)-H(15)	120(3)
C(9)-C(7)-C(6)	112.37(17)	C(14)-C(15)-H(15)	120(3)
C(8)-C(7)-C(10)	111.2(3)	C(15)-C(16)-C(17)	119.9(3)
C(9)-C(7)-C(10)	109.1(2)	C(15)-C(16)-H(16)	119(2)
C(6)-C(7)-C(10)	107.74(18)	C(17)-C(16)-H(16)	121(2)
C(7)-C(8)-H(8A)	109.5	C(12)-C(17)-C(16)	120.3(3)
C(7)-C(8)-H(8B)	109.5	C(12)-C(17)-H(17)	118.4(18)
H(8A)-C(8)-H(8B)	109.5	C(16)-C(17)-H(17)	121.3(18)
C(7)-C(8)-H(8C)	109.5	C(5)-C(18)-H(18A)	109.2(17)
H(8A)-C(8)-H(8C)	109.5	C(5)-C(18)-H(18B)	110.8(15)
H(8B)-C(8)-H(8C)	109.5	H(18A)-C(18)-H(18B)	110(2)
C(7)-C(9)-H(9A)	109.5	C(5)-C(18)-H(18C)	111.8(18)
C(7)-C(9)-H(9B)	109.5	H(18A)-C(18)-H(18C)	110(2)
H(9A)-C(9)-H(9B)	109.5	H(18B)-C(18)-H(18C)	106(2)
C(7)-C(9)-H(9C)	109.5	O(5)-C(19)-H(19A)	110.3(15)
H(9A)-C(9)-H(9C)	109.5	O(5)-C(19)-H(19B)	106.1(19)
H(9B)-C(9)-H(9C)	109.5	H(19A)-C(19)-H(19B)	112(3)
C(7)-C(10)-H(10A)	109.5	O(5)-C(19)-H(19C)	112.5(17)
C(7)-C(10)-H(10B)	109.5	H(19A)-C(19)-H(19C)	107(2)
H(10A)-C(10)-H(10B)	109.5	H(19B)-C(19)-H(19C)	109(3)
C(7)-C(10)-H(10C)	109.5	C(1)-O(1)-C(5)	113.29(13)
H(10A)-C(10)-H(10C)	109.5	C(11)-O(2)-C(4)	114.53(15)
H(10B)-C(10)-H(10C)	109.5	C(6)-O(3)-C(3)	116.52(14)
O(2)-C(11)-C(12)	107.58(17)	C(1)-O(5)-C(19)	111.86(15)
O(2)-C(11)-H(11A)	112.0(15)	C(2)-O(6)-H(6)	105(2)
C(12)-C(11)-H(11A)	109.9(15)	H(17B)-C(17)-H(17C)	109.5

Table 9: Anisotropic displacement parameters [$Å^2 \times 10^3$] for **19**

The anisotropic displacement factor exponent takes the form: $-2\pi^2 [(h\,a^*)^2 U11 + ... + 2\,h\,k\,a^*\,b^*\,U12]$

	U11	U22	U33	U23	U13	U12
C(1)	13(1)	17(1)	19(1)	-1(1)	0(1)	2(1)
C(2)	15(1)	16(1)	18(1)	0(1)	-1(1)	-2(1)
C(3)	19(1)	13(1)	13(1)	-2(1)	0(1)	-3(1)
C(4)	16(1)	13(1)	17(1)	3(1)	3(1)	-2(1)
C(5)	16(1)	15(1)	16(1)	1(1)	0(1)	-1(1)
C(6)	11(1)	22(1)	18(1)	-5(1)	1(1)	0(1)
C(7)	23(1)	23(1)	23(1)	-10(1)	-4(1)	3(1)
C(8)	24(1)	69(2)	115(3)	-73(2)	-13(2)	4(1)
C(9)	46(1)	23(1)	23(1)	-6(1)	5(1)	11(1)
C(10)	95(2)	33(1)	17(1)	-6(1)	1(1)	9(2)
C(11)	24(1)	15(1)	32(1)	2(1)	5(1)	3(1)
C(12)	33(1)	14(1)	21(1)	-2(1)	5(1)	0(1)
C(13)	37(1)	24(1)	22(1)	-2(1)	4(1)	-3(1)
C(14)	45(2)	33(1)	33(1)	-11(1)	5(1)	-16(1)
C(15)	76(2)	23(1)	41(1)	1(1)	12(2)	-21(1)
C(16)	80(2)	23(1)	38(1)	11(1)	-1(2)	-3(1)
C(17)	51(2)	21(1)	30(1)	2(1)	-5(1)	-1(1)
C(18)	16(1)	24(1)	19(1)	2(1)	-3(1)	1(1)
C(19)	22(1)	20(1)	28(1)	-8(1)	-6(1)	3(1)
O(1)	15(1)	21(1)	16(1)	2(1)	1(1)	1(1)
O(2)	21(1)	12(1)	23(1)	3(1)	5(1)	1(1)
O(3)	25(1)	14(1)	17(1)	-3(1)	-1(1)	-1(1)
O(4)	25(1)	20(1)	19(1)	-2(1)	-4(1)	4(1)
O(5)	20(1)	13(1)	21(1)	-2(1)	-2(1)	0(1)
O(6)	18(1)	18(1)	31(1)	1(1)	2(1)	-5(1)

Table 10. Hydrogen coordinates ($\times 10^4$) and isotropic displacement parameters ($Å^2 \times 10^3$) for **19**

	x	y	z	U(eq)
H(1)	6410(40)	6994(14)	11294(13)	12(5)
H(2)	6370(40)	6666(14)	9961(13)	14(5)
H(3)	9680(30)	6769(13)	9708(12)	8(5)
H(4)	11990(40)	5881(13)	10238(12)	9(5)
H(5)	11300(40)	7024(15)	10955(13)	13(5)
H(8A)	5762	4875	8406	104
H(8B)	6153	4608	7538	104
H(8C)	5558	5534	7732	104
H(9A)	10985	4653	8303	46
H(9B)	9480	4094	7831	46
H(9C)	9068	4294	8713	46
H(10A)	8597	6113	7105	72
H(10B)	9147	5202	6843	72
H(10C)	10696	5735	7318	72
H(11A)	12560(40)	4468(15)	10732(14)	23(6)
H(11B)	11400(50)	4500(18)	9963(17)	35(8)
H(13)	7850(50)	3858(18)	10070(16)	35(7)
H(14)	6130(50)	2695(18)	10427(18)	40(8)
H(15)	7550(60)	1790(20)	11310(20)	68(12)
H(16)	10530(60)	2080(20)	11840(20)	59(11)
H(17)	12330(50)	3277(19)	11475(17)	40(8)
H(18A)	12420(50)	6649(17)	12136(16)	32(7)
H(18B)	13560(40)	6110(15)	11542(14)	17(6)
H(18C)	11870(40)	5735(16)	11986(15)	27(7)
H(19A)	7230(40)	8299(16)	11688(15)	24(6)
H(19B)	8550(50)	8830(20)	11083(18)	46(9)
H(19C)	9470(40)	8193(16)	11608(15)	23(6)
H(6)	7180(50)	5348(17)	10665(16)	33

Table 11: Hydrogen bonds for **19** [Å and deg]

D-H...A	d(D-H)	d(H...A)	d(D...A)	<(DHA)
O(6)-H(6)...O(2)	0.84(3)	2.02(3)	2.767(2)	148(3)

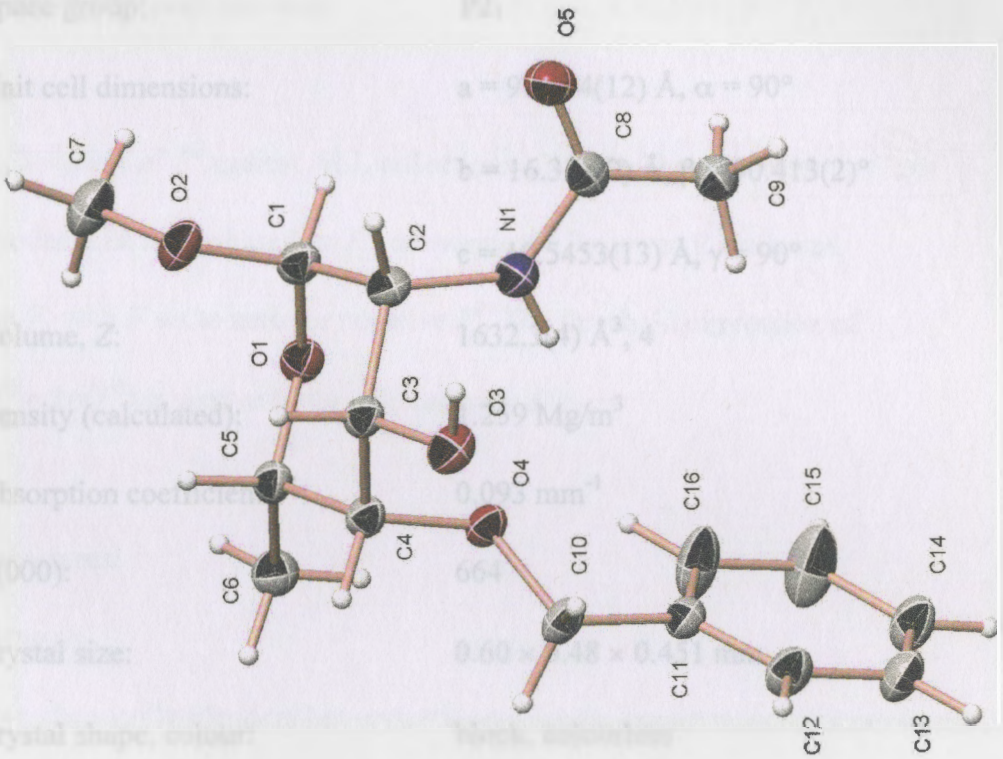

Figure 57: X-Ray crystal structure of **28**

Table 12: Crystal data and structure refinement for **28**.

Empirical formula:	$C_{16}H_{23}NO_5$
Formula weight:	309.35
Temperature:	100(2) K
Wavelength:	0.71073 Å
Crystal system:	Monoclinic
Space group:	$P2_1$
Unit cell dimensions:	a = 9.4804(12) Å, α = 90°
	b = 16.328(2) Å, β = 90.413(2)°
	c = 10.5453(13) Å, γ = 90°
Volume, *Z*:	1632.3(4) $Å^3$, 4
Density (calculated):	1.259 Mg/m^3
Absorption coefficient:	0.093 mm^{-1}
F(000):	664
Crystal size:	0.60 × 0.48 × 0.451 mm
Crystal shape, colour:	block, colourless
θ range for data collection:	1.25 to 28.28°
Limiting indices:	$-12 \le h \le 12$, $-21 \le k \le 21$, $-13 \le l \le 14$
Reflections collected:	16326
Independent reflections:	4148 (R(int) = 0.0305)
Completeness to θ = 28.28°:	99.2 %
Absorption correction:	multi-scan

Max. and min. transmission:	0.959 and 0.7845
Refinement method:	Full-matrix least-squares on F^2
Data / restraints / parameters:	4148 / 1 / 406
Goodness-of-fit on F^2:	1.071
Final R indices [$I>2\sigma(I)$]:	R1 = 0.0410, wR2 = 0.1025
R indices (all data):	R1 = 0.0417, wR2 = 0.1033
Largest diff. peak and hole:	0.379 and -0.183 e × Å^{-3}

Refinement of F^2 against ALL reflections. The weighted R-factor wR and goodness of fit are based on F^2, conventional R-factors R are based on F, with F set to zero for negative F^2. The threshold expression of $F^2 > 2\sigma(F^2)$ is used only for calculating R-factors

Comments:

General:

Two chemically identical but crystallographically unique molecules are found in the unit cell.

Twinning:

The crystal was identified to be pseudo-merohedrally twinned with the unit cell dimensions being very close to an orthorhombic setting. The twin law was found to be 1 0 0 0 -1 0 0 0 -1, and the BASF parameter refined to 0.2580(15). The R values before

applying the twin law had been ca. 0.32 for wR2 and 0.13 for R1.

Treatment of hydrogen atoms:

All hydrogen atoms were placed in calculated positions and were refined with an isotropic displacement parameter 1.5 times (methyl) or 1.2 times (all others) that of the adjacent carbon atom.

Table 13: Atomic coordinates [$\times 10^4$] and equivalent isotropic displacement parameters [$Å^2 \times 10^3$] for **28**

U(eq) is defined as one third of the trace of the orthogonalized U_{ij} tensor.

	x	y	z	U(eq)
O(1)	2345(2)	6523(1)	1773(2)	24(1)
O(2)	3352(2)	7584(1)	584(2)	29(1)
O(3)	5256(2)	5318(1)	-471(2)	28(1)
O(4)	3429(2)	4899(1)	1523(2)	22(1)
O(5)	1648(2)	6071(2)	-2591(2)	31(1)
N(1)	2278(3)	5598(2)	-654(2)	26(1)
C(1)	2532(3)	6867(2)	557(3)	25(1)
C(2)	3248(3)	6265(2)	-350(3)	24(1)
C(3)	4622(3)	5938(2)	263(3)	22(1)
C(4)	4346(3)	5594(2)	1586(3)	21(1)
C(5)	3637(3)	6253(2)	2379(3)	23(1)
C(6)	3244(3)	5938(2)	3685(3)	27(1)
C(7)	2702(4)	8234(2)	1274(4)	37(1)
C(8)	1560(3)	5553(2)	-1756(3)	25(1)
C(9)	561(3)	4831(2)	-1876(3)	29(1)
C(10)	4130(3)	4127(2)	1531(3)	25(1)
C(11)	3023(3)	3467(2)	1457(3)	23(1)
C(12)	3399(3)	2686(2)	1054(3)	28(1)
C(13)	2414(3)	2054(2)	1039(3)	31(1)
C(14)	1048(4)	2200(2)	1405(3)	33(1)
C(15)	656(4)	2978(2)	1766(5)	50(1)
C(16)	1639(4)	3611(2)	1795(4)	41(1)
O(6)	2682(2)	-246(1)	6607(2)	27(1)
O(7)	1642(2)	-1030(1)	4979(2)	33(1)
O(8)	-4(2)	1378(1)	4711(2)	27(1)
O(9)	1693(2)	1402(1)	6929(2)	24(1)
O(10)	4026(3)	660(2)	2873(2)	37(1)
N(2)	2939(3)	1048(2)	4646(2)	26(1)
C(21)	2538(3)	-372(2)	5281(3)	27(1)
C(22)	1919(3)	381(2)	4603(3)	24(1)
C(23)	530(3)	637(2)	5222(3)	22(1)
C(24)	745(3)	739(2)	6662(3)	22(1)
C(25)	1360(3)	-51(2)	7200(3)	25(1)
C(26)	1644(3)	-4(2)	8616(3)	34(1)
C(27)	2238(4)	-1806(2)	5347(4)	40(1)
C(28)	3911(3)	1146(2)	3749(3)	28(1)

C(29)	4829(4)	1894(2)	3876(3)	35(1)
C(30)	1016(3)	2155(2)	7282(3)	30(1)
C(31)	1938(3)	2854(2)	6868(3)	28(1)
C(32)	2879(4)	3220(2)	7720(4)	38(1)
C(33)	3709(4)	3880(2)	7331(5)	49(1)
C(34)	3599(4)	4169(2)	6105(5)	46(1)
C(35)	2696(4)	3797(2)	5249(4)	43(1)
C(36)	1859(4)	3137(2)	5631(3)	36(1)

All esds (except the esd in the dihedral angle between two l.s. planes) are estimated using the full covariance matrix. The cell esds are taken into account individually in the estimation of esds in distances, angles and torsion angles; correlations between esds in cell parameters are only used when they are defined by crystal symmetry. An approximate (isotropic) treatment of cell esds is used for estimating esds involving l.s. planes.

Table 14. Bond lengths [Å] and angles [deg] for **28**

O(1)-C(1)	1.412(4)	C(15)-H(15)	0.9500
O(1)-C(5)	1.447(3)	C(16)-H(16)	0.9500
O(2)-C(1)	1.406(3)	O(6)-C(21)	1.419(4)
O(2)-C(7)	1.429(4)	O(6)-C(25)	1.440(3)
O(3)-C(3)	1.412(3)	O(7)-C(21)	1.406(4)
O(3)-H(3)	0.8400	O(7)-C(27)	1.439(4)
O(4)-C(10)	1.425(3)	O(8)-C(23)	1.418(3)
O(4)-C(4)	1.432(3)	O(8)-H(8)	0.8400
O(5)-C(8)	1.223(4)	O(9)-C(24)	1.433(3)
N(1)-C(8)	1.345(4)	O(9)-C(30)	1.438(4)
N(1)-C(2)	1.458(4)	O(10)-C(28)	1.224(4)
N(1)-H(1A)	0.8800	N(2)-C(28)	1.334(4)
C(1)-C(2)	1.533(4)	N(2)-C(22)	1.457(4)
C(1)-H(1)	1.0000	N(2)-H(2A)	0.8800
C(2)-C(3)	1.545(4)	C(21)-C(22)	1.536(4)
C(2)-H(2)	1.0000	C(21)-H(21)	1.0000
C(3)-C(4)	1.529(4)	C(22)-C(23)	1.532(4)
C(3)-H(3A)	1.0000	C(22)-H(22)	1.0000
C(4)-C(5)	1.521(4)	C(23)-C(24)	1.540(4)
C(4)-H(4)	1.0000	C(23)-H(23)	1.0000
C(5)-C(6)	1.519(4)	C(24)-C(25)	1.524(4)
C(5)-H(5)	1.0000	C(24)-H(24)	1.0000
C(6)-H(6A)	0.9800	C(25)-C(26)	1.517(4)
C(6)-H(6B)	0.9800	C(25)-H(25)	1.0000
C(6)-H(6C)	0.9800	C(26)-H(26A)	0.9800
C(7)-H(7A)	0.9800	C(26)-H(26B)	0.9800
C(7)-H(7B)	0.9800	C(26)-H(26C)	0.9800
C(7)-H(7C)	0.9800	C(27)-H(27A)	0.9800
C(8)-C(9)	1.518(4)	C(27)-H(27B)	0.9800
C(9)-H(9A)	0.9800	C(27)-H(27C)	0.9800
C(9)-H(9B)	0.9800	C(28)-C(29)	1.505(5)
C(9)-H(9C)	0.9800	C(29)-H(29A)	0.9800
C(10)-C(11)	1.506(4)	C(29)-H(29B)	0.9800
C(10)-H(10A)	0.9900	C(29)-H(29C)	0.9800
C(10)-H(10B)	0.9900	C(30)-C(31)	1.504(4)
C(11)-C(16)	1.382(4)	C(30)-H(30A)	0.9900
C(11)-C(12)	1.391(4)	C(30)-H(30B)	0.9900
C(12)-C(13)	1.392(4)	C(31)-C(36)	1.386(5)
C(12)-H(12)	0.9500	C(31)-C(32)	1.395(5)
C(13)-C(14)	1.374(5)	C(32)-C(33)	1.398(6)
C(13)-H(13)	0.9500	C(32)-H(32)	0.9500
C(14)-C(15)	1.378(5)	C(33)-C(34)	1.380(7)
C(14)-H(14)	0.9500	C(33)-H(33)	0.9500
C(15)-C(16)	1.391(5)	C(34)-C(35)	1.381(6)

C(34)-H(34)	0.9500
C(35)-C(36)	1.400(5)
C(35)-H(35)	0.9500
C(36)-H(36)	0.9500
C(1)-O(1)-C(5)	114.3(2)
C(1)-O(2)-C(7)	112.9(2)
C(3)-O(3)-H(3)	109.5
C(10)-O(4)-C(4)	114.72(19)
C(8)-N(1)-C(2)	123.0(2)
C(8)-N(1)-H(1A)	118.5
C(2)-N(1)-H(1A)	118.5
O(2)-C(1)-O(1)	112.7(2)
O(2)-C(1)-C(2)	107.4(2)
O(1)-C(1)-C(2)	111.8(2)
O(2)-C(1)-H(1)	108.3
O(1)-C(1)-H(1)	108.3
C(2)-C(1)-H(1)	108.3
N(1)-C(2)-C(1)	109.5(2)
N(1)-C(2)-C(3)	111.3(2)
C(1)-C(2)-C(3)	109.6(2)
N(1)-C(2)-H(2)	108.8
C(1)-C(2)-H(2)	108.8
C(3)-C(2)-H(2)	108.8
O(3)-C(3)-C(4)	108.2(2)
O(3)-C(3)-C(2)	112.3(2)
C(4)-C(3)-C(2)	111.1(2)
O(3)-C(3)-H(3A)	108.4
C(4)-C(3)-H(3A)	108.4
C(2)-C(3)-H(3A)	108.4
O(4)-C(4)-C(5)	108.4(2)
O(4)-C(4)-C(3)	110.9(2)
C(5)-C(4)-C(3)	108.8(2)
O(4)-C(4)-H(4)	109.6
C(5)-C(4)-H(4)	109.6
C(3)-C(4)-H(4)	109.6
O(1)-C(5)-C(6)	107.0(2)
O(1)-C(5)-C(4)	110.4(2)
C(6)-C(5)-C(4)	111.8(2)
O(1)-C(5)-H(5)	109.2
C(6)-C(5)-H(5)	109.2
C(4)-C(5)-H(5)	109.2
C(5)-C(6)-H(6A)	109.5
C(5)-C(6)-H(6B)	109.5
H(6A)-C(6)-H(6B)	109.5
C(5)-C(6)-H(6C)	109.5
H(6A)-C(6)-H(6C)	109.5
H(6B)-C(6)-H(6C)	109.5
O(2)-C(7)-H(7A)	109.5
O(2)-C(7)-H(7B)	109.5
H(7A)-C(7)-H(7B)	109.5
O(2)-C(7)-H(7C)	109.5
H(7A)-C(7)-H(7C)	109.5
H(7B)-C(7)-H(7C)	109.5
O(5)-C(8)-N(1)	123.2(3)
O(5)-C(8)-C(9)	121.6(3)
N(1)-C(8)-C(9)	115.2(3)
C(8)-C(9)-H(9A)	109.5
C(8)-C(9)-H(9B)	109.5
H(9A)-C(9)-H(9B)	109.5
C(8)-C(9)-H(9C)	109.5
H(9A)-C(9)-H(9C)	109.5
H(9B)-C(9)-H(9C)	109.5
O(4)-C(10)-C(11)	108.0(2)
O(4)-C(10)-H(10A)	110.1
C(11)-C(10)-H(10A)	110.1
O(4)-C(10)-H(10B)	110.1
C(11)-C(10)-H(10B)	110.1
H(10A)-C(10)-H(10B)	108.4
C(16)-C(11)-C(12)	118.7(3)
C(16)-C(11)-C(10)	121.8(3)
C(12)-C(11)-C(10)	119.5(2)
C(11)-C(12)-C(13)	120.6(3)
C(11)-C(12)-H(12)	119.7
C(13)-C(12)-H(12)	119.7
C(14)-C(13)-C(12)	120.1(3)
C(14)-C(13)-H(13)	120.0
C(12)-C(13)-H(13)	120.0
C(13)-C(14)-C(15)	119.6(3)
C(13)-C(14)-H(14)	120.2
C(15)-C(14)-H(14)	120.2
C(14)-C(15)-C(16)	120.5(3)
C(14)-C(15)-H(15)	119.7
C(16)-C(15)-H(15)	119.7
C(11)-C(16)-C(15)	120.4(3)
C(11)-C(16)-H(16)	119.8
C(15)-C(16)-H(16)	119.8
C(21)-O(6)-C(25)	112.4(2)
C(21)-O(7)-C(27)	112.1(2)
C(23)-O(8)-H(8)	109.5
C(24)-O(9)-C(30)	114.6(2)
C(28)-N(2)-C(22)	121.9(3)

C(28)-N(2)-H(2A)	119.0	O(7)-C(27)-H(27B)	109.5
C(22)-N(2)-H(2A)	119.0	H(27A)-C(27)-H(27B)	109.5
O(7)-C(21)-O(6)	112.8(3)	O(7)-C(27)-H(27C)	109.5
O(7)-C(21)-C(22)	106.1(2)	H(27A)-C(27)-H(27C)	109.5
O(6)-C(21)-C(22)	112.2(2)	H(27B)-C(27)-H(27C)	109.5
O(7)-C(21)-H(21)	108.5	O(10)-C(28)-N(2)	121.5(3)
O(6)-C(21)-H(21)	108.5	O(10)-C(28)-C(29)	122.6(3)
C(22)-C(21)-H(21)	108.5	N(2)-C(28)-C(29)	115.8(3)
N(2)-C(22)-C(23)	110.8(2)	C(28)-C(29)-H(29A)	109.5
N(2)-C(22)-C(21)	109.4(2)	C(28)-C(29)-H(29B)	109.5
C(23)-C(22)-C(21)	110.2(2)	H(29A)-C(29)-H(29B)	109.5
N(2)-C(22)-H(22)	108.8	C(28)-C(29)-H(29C)	109.5
C(23)-C(22)-H(22)	108.8	H(29A)-C(29)-H(29C)	109.5
C(21)-C(22)-H(22)	108.8	H(29B)-C(29)-H(29C)	109.5
O(8)-C(23)-C(22)	112.1(2)	O(9)-C(30)-C(31)	108.2(2)
O(8)-C(23)-C(24)	109.1(2)	O(9)-C(30)-H(30A)	110.1
C(22)-C(23)-C(24)	110.0(2)	C(31)-C(30)-H(30A)	110.1
O(8)-C(23)-H(23)	108.5	O(9)-C(30)-H(30B)	110.1
C(22)-C(23)-H(23)	108.5	C(31)-C(30)-H(30B)	110.1
C(24)-C(23)-H(23)	108.5	H(30A)-C(30)-H(30B)	108.4
O(9)-C(24)-C(25)	109.2(2)	C(36)-C(31)-C(32)	119.6(3)
O(9)-C(24)-C(23)	110.7(2)	C(36)-C(31)-C(30)	119.9(3)
C(25)-C(24)-C(23)	108.8(2)	C(32)-C(31)-C(30)	120.6(3)
O(9)-C(24)-H(24)	109.4	C(31)-C(32)-C(33)	120.0(4)
C(25)-C(24)-H(24)	109.4	C(31)-C(32)-H(32)	120.0
C(23)-C(24)-H(24)	109.4	C(33)-C(32)-H(32)	120.0
O(6)-C(25)-C(26)	106.9(2)	C(34)-C(33)-C(32)	120.0(4)
O(6)-C(25)-C(24)	110.9(2)	C(34)-C(33)-H(33)	120.0
C(26)-C(25)-C(24)	112.8(3)	C(32)-C(33)-H(33)	120.0
O(6)-C(25)-H(25)	108.7	C(33)-C(34)-C(35)	120.3(3)
C(26)-C(25)-H(25)	108.7	C(33)-C(34)-H(34)	119.8
C(24)-C(25)-H(25)	108.7	C(35)-C(34)-H(34)	119.8
C(25)-C(26)-H(26A)	109.5	C(34)-C(35)-C(36)	120.0(4)
C(25)-C(26)-H(26B)	109.5	C(34)-C(35)-H(35)	120.0
H(26A)-C(26)-H(26B)	109.5	C(36)-C(35)-H(35)	120.0
C(25)-C(26)-H(26C)	109.5	C(31)-C(36)-C(35)	120.1(3)
H(26A)-C(26)-H(26C)	109.5	C(31)-C(36)-H(36)	120.0
H(26B)-C(26)-H(26C)	109.5	C(35)-C(36)-H(36)	120.0
O(7)-C(27)-H(27A)	109.5		

Table 15: Anisotropic displacement parameters [$Å^2 \times 10^3$] for **28**

The anisotropic displacement factor exponent takes the form: $-2\pi^2 [(h a^*)^2 U11 + ... + 2 h k a^* b^* U12]$

	U11	U22	U33	U23	U13	U12
O(1)	20(1)	23(1)	29(1)	0(1)	1(1)	1(1)
O(2)	29(1)	18(1)	39(1)	2(1)	2(1)	-1(1)
O(3)	32(1)	24(1)	27(1)	0(1)	7(1)	2(1)
O(4)	18(1)	18(1)	31(1)	1(1)	0(1)	1(1)
O(5)	32(1)	33(1)	29(1)	2(1)	-4(1)	4(1)
N(1)	28(1)	24(1)	28(1)	2(1)	-2(1)	-2(1)
C(1)	21(1)	21(1)	33(1)	1(1)	-2(1)	1(1)
C(2)	26(1)	22(1)	25(1)	3(1)	-1(1)	1(1)
C(3)	21(1)	19(1)	26(1)	2(1)	0(1)	-2(1)
C(4)	18(1)	19(1)	27(1)	1(1)	0(1)	-1(1)
C(5)	21(1)	19(1)	28(1)	-1(1)	-2(1)	-1(1)
C(6)	29(1)	27(1)	25(1)	-1(1)	1(1)	3(1)
C(7)	40(2)	21(1)	50(2)	-2(1)	4(2)	1(1)
C(8)	21(1)	25(1)	27(1)	-7(1)	0(1)	6(1)
C(9)	29(1)	28(1)	31(1)	-3(1)	-6(1)	1(1)
C(10)	20(1)	17(1)	38(2)	1(1)	3(1)	2(1)
C(11)	25(1)	19(1)	24(1)	1(1)	0(1)	0(1)
C(12)	23(1)	23(1)	39(2)	-1(1)	3(1)	4(1)
C(13)	33(2)	18(1)	43(2)	0(1)	1(1)	0(1)
C(14)	31(2)	23(1)	47(2)	3(1)	3(1)	-7(1)
C(15)	25(2)	35(2)	92(3)	-14(2)	19(2)	-7(1)
C(16)	29(2)	25(2)	69(2)	-17(2)	14(2)	-2(1)
O(6)	20(1)	25(1)	35(1)	3(1)	1(1)	0(1)
O(7)	29(1)	21(1)	48(1)	-7(1)	-2(1)	1(1)
O(8)	29(1)	23(1)	29(1)	-1(1)	-5(1)	4(1)
O(9)	23(1)	21(1)	28(1)	-3(1)	3(1)	-2(1)
O(10)	44(1)	34(1)	32(1)	4(1)	13(1)	6(1)
N(2)	26(1)	26(1)	26(1)	-1(1)	2(1)	-1(1)
C(21)	21(1)	22(1)	38(2)	-2(1)	3(1)	3(1)
C(22)	23(1)	24(1)	27(1)	-4(1)	1(1)	2(1)
C(23)	20(1)	22(1)	24(1)	-1(1)	-1(1)	-1(1)
C(24)	20(1)	22(1)	23(1)	-1(1)	2(1)	-1(1)
C(25)	19(1)	25(1)	30(1)	3(1)	3(1)	-4(1)
C(26)	30(1)	41(2)	32(1)	10(1)	0(1)	-3(1)
C(27)	39(2)	23(1)	60(2)	-2(2)	2(2)	4(1)
C(28)	26(1)	29(1)	29(1)	11(1)	4(1)	5(1)

C(29)	30(2)	35(2)	41(2)	12(1)	5(1)	-3(1)
C(30)	34(2)	24(1)	31(2)	-4(1)	9(1)	-2(1)
C(31)	25(1)	21(1)	39(2)	-5(1)	4(1)	3(1)
C(32)	38(2)	28(2)	48(2)	-5(2)	-10(1)	2(1)
C(33)	28(2)	34(2)	83(3)	-18(2)	-12(2)	0(1)
C(34)	32(2)	23(2)	83(3)	-2(2)	12(2)	-4(1)
C(35)	55(2)	25(2)	50(2)	4(1)	16(2)	2(2)
C(36)	38(2)	27(2)	42(2)	-4(1)	6(1)	-3(1)

Table 16: Hydrogen coordinates ($\times 10^4$) and isotropic displacement parameters ($Å^2 \times 10^3$) for **28**

	x	y	z	U(eq)
H(3)	5360	5485	-1217	42
H(1A)	2158	5208	-90	32
H(1)	1582	7007	200	30
H(2)	3489	6560	-1150	29
H(3A)	5303	6404	344	27
H(4)	5260	5433	1994	26
H(5)	4291	6730	2474	27
H(6A)	2729	6364	4144	41
H(6B)	4103	5795	4157	41
H(6C)	2646	5451	3596	41
H(7A)	1721	8296	990	55
H(7B)	3216	8745	1123	55
H(7C)	2723	8106	2182	55
H(9A)	-412	5020	-1772	44
H(9B)	786	4426	-1219	44
H(9C)	665	4580	-2715	44
H(10A)	4694	4066	2319	30
H(10B)	4772	4086	798	30
H(12)	4338	2583	787	34
H(13)	2685	1521	775	37
H(14)	379	1767	1410	40
H(15)	-294	3084	1997	60
H(16)	1358	4144	2048	49
H(8)	-374	1286	3999	40
H(2A)	2914	1397	5282	31
H(21)	3492	-487	4924	32
H(22)	1728	236	3696	29
H(23)	-182	195	5073	26
H(24)	-185	851	7069	26
H(25)	680	-508	7033	29
H(26A)	2066	-519	8907	51
H(26B)	755	89	9062	51
H(26C)	2294	449	8794	51
H(27A)	3154	-1877	4935	61
H(27B)	1602	-2249	5085	61
H(27C)	2366	-1820	6269	61
H(29A)	5816	1742	3737	53
H(29B)	4729	2124	4729	53

H(29C)	4540	2303	3245	53
H(30A)	882	2174	8211	36
H(30B)	79	2196	6866	36
H(32)	2955	3020	8564	46
H(33)	4349	4129	7911	58
H(34)	4147	4627	5850	55
H(35)	2643	3990	4399	52
H(36)	1235	2883	5042	43

Table 17: Hydrogen bonds for **28** [Å and deg]

D-H...A	d(D-H)	d(H...A)	d(D...A)	<(DHA)
N(2)-H(2A)...O(9)	0.88	2.09	2.751(3)	130.8
O(8)-H(8)...O(5)#1	0.84	1.94	2.762(3)	166.1
N(1)-H(1A)...O(4)	0.88	2.14	2.779(3)	129.3
O(3)-H(3)...O(10)#2	0.84	1.87	2.686(3)	165.1

Symmetry transformations used to generate equivalent atoms:

#1 -x,y-1/2,-z #2 -x+1,y+1/2,-z